Title

Mechanism of SCRIB-Dependent Regulation of the Hippo Pathway

Author

Colston, Tobey

Publication Date

2024

Peer reviewed|Thesis/dissertation

Mechanism of SCRIB-Dependent Regulation of the Hippo Pathway

By

Tobey J. Colston

A dissertation submitted in partial satisfaction of the

requirements for the degree of

Doctor of Philosophy

in

Molecular and Cell Biology

in the

Graduate Division

of the

University of California, Berkeley

Committee in charge:

Professor Kunxin Luo, Chair
Professor Lin He
Professor David Bilder
Professor Danica Chen

Fall 2024

Abstract

Mechanism of SCRIB-Dependent Regulation of the Hippo Pathway

by

Tobey J. Colston

Doctor of Philosophy in Molecular and Cell Biology

University of California, Berkeley

Professor Kunxin Luo, Chair

The first known documentation of breast cancer comes from an Egyptian transcript that is over 4,000 years old. In this document, the physician Imhotep provided detailed descriptions of breast tumors and stated, "for a treatment, there is none." Today, breast cancer remains incurable and continues to be a major disease affecting women. Cancer stem cells are a subpopulation within solid tumors that drive tumor growth due to their ability to self-renew, initiate tumors, and resist treatment. The characteristics of cancer stem cells are influenced by various signaling pathways, which have significant links to the polarity of epithelial cells.

Polarity is essential for the spatial organization of signaling pathways within cells. Polarity proteins help regulate signal transduction across a diverse range of cellular processes. One critical membrane-bound polarity protein is SCRIB, which maintains the basolateral membrane domain. When SCRIB is mislocalized to the cytosol, it promotes mammary tumor development. SCRIB interacts significantly with the Hippo signaling pathway, which is responsible for regulating tissue growth, organ size, and stem cell fate. The interaction between SCRIB-dependent cell polarity and the Hippo pathway affects the activity of the Hippo effector, TAZ. Oncogenic TAZ is often highly expressed in breast cancer, and its activity—enhanced by disruptions in cell polarity—has been shown to endow breast cancer cells with cancer stem cell characteristics.

The relationship between the pro-oncogene SnoN and the anti-oncogene SCRIB, as well as their connection to the Hippo pathway, is quite fascinating. Current models suggest that the interaction between SCRIB and SnoN is essential for preventing TAZ activity. When this interaction is disrupted, TAZ becomes stabilized. This study aims to gain further insight into the SCRIB-SnoN interaction by examining their binding specificities and identifying additional protein interactions that occur upstream of Hippo kinase activity, with the goal of downregulating TAZ. The SCRIB-SnoN interaction appears to be a promising target for diminishing the TAZ-dependent stemness of breast cancer cells. Understanding the biological function of this interaction is key to unraveling the relationship between SCRIB-dependent cell polarity, Hippo signaling, and the development of cancer stem cell characteristics in breast tumors. Additionally, it may provide valuable insights into mechanisms for controlling cancer cell growth

TABLE OF CONTENTS

ACKNOWLEDGEMENTS

As a nontraditional student, I returned to school more than ten years after earning my bachelor's degree. It had always been my heartfelt prayer to earn a PhD. Twenty years after completing my B.S., I began my doctoral studies in MCB. Throughout this journey, I faced numerous challenges and hardships that made it difficult to complete my dissertation, but I refused to give up. Even when others doubted my abilities, I maintained my faith, believing that what was meant for me would come to pass. I am grateful to God for every blessing and for helping me overcome obstacles. It is through Him that I am able to do all things and that I am more than a conqueror. Now, I am proud to be the first person in my family to earn a doctorate degree.

I want to express my heartfelt gratitude to my husband, son, daughter, and sister for their unwavering belief in me and for always supporting me. I especially thank my husband for being there for me, wiping away my tears as I worked tirelessly to achieve my goals. You have been by my side every step of the way, and you truly understand everything it took to reach this point in my life. Thank you for taking care of the kids and managing the household while I focused on my studies. I appreciate every meal you cooked and every errand you ran while I worked late in the lab. I could not have accomplished this without you. To my children, I hope my achievement teaches you to never give up on your dreams, even in the face of doubt and discouragement. Always remember that God answers prayers.

I am grateful for the support and kindness I received from the MCB department. Thank you for extending the submission deadlines and making a way when I thought none existed. I would like to express my appreciation for the faculty members who played a role in my journey at Berkeley. From David Weisblat and David Bilder, who met with me to discuss the department prior to my application, to David Raulet, who provided me with an outstanding internship opportunity in cancer immunotherapy. Iswar Hariharan and other department chairs, your support is greatly appreciated as well. I also want to acknowledge the department's commitment to diversity, equity, and inclusion, which thrived during my time here. Whether it was through DEI-focused activities during recruitment, the establishment of iMCB, the development of a course on DEI in STEM, or reaching out to underrepresented students for feedback on how to improve, I am proud of the efforts made by the department in these areas.

I am deeply grateful to my graduate advisor, Kunxin Luo. Thank you for teaching me how to be a good scientist, how to conduct research, and how to critically review papers. As a woman in science, you are an inspiration and an excellent role model. I appreciate your mentorship and support in keeping me grounded and focused. You understood the importance of completing this program for me as an African American woman in science. At the same time, you encouraged me not to feel overwhelmed by the responsibility of carrying my community; instead, you emphasized the importance of simply doing my best. Thank you for recognizing my talent for teaching and for valuing teaching equally alongside research. Lastly, I appreciate your belief that failed experiments can still contribute to a meaningful dissertation. I would also like to thank my lab mate, Qingwei, for your friendship and your readiness to help whenever I needed assistance. To Tian Tian and Yi, it was a pleasure working with both of you.

I appreciate my thesis committee for your continued patience as I completed this significant achievement. Thank you for stepping out of the norm and allowing my teaching portfolio to be a chapter in my dissertation.

I want to express my gratitude to everyone who has been in my corner, encouraging me throughout my journey. Thank you to those at Merritt College, CSU East Bay, and Touro

University California for being integral parts of my academic path. Your support means so much to me.

I am incredibly thankful to my family and friends for their love and support. A special thank you goes to my loved ones who are no longer with us. To my mother, who taught me to be a God-fearing woman and whose example I strive to emulate as both a parent and a professor, I am forever grateful—thank you. I am also deeply thankful to my father for his unconditional love and to my grandparents, who always kept me in their prayers. Although they are not here to celebrate my achievements, I know they are proud of me and watching over me with smiles from above.

Chapter 1

Introduction

SUMMARY

The Hippo pathway is a critical regulator of cell proliferation, tissue homeostasis, and organ size. When dysregulated, it is relevant to cancer, leading to tumor development and transformation. Aberrant Hippo signaling is linked to the development of cancer stem cell (CSC) traits in tumor cells, making them capable of seeding tumors and resisting cancer treatments. Apical-basal cell polarity is a major upstream cue that controls Hippo signaling by inhibiting the Hippo effectors. Most studies have focused on the regulation of the Hippo pathway by apical polarity complexes, while the contributions of basolateral complexes have been less understood. In this study, the regulation of the Hippo pathway by basolateral cell polarity was explored, focusing on the role of the protein Scribble (SCRIB) in inhibiting the activity of the Hippo effector, TAZ. The link between SCRIB and the anti- and proto-oncogene, SnoN, was also investigated because their interaction facilitates the mutual regulation between SnoN and the Hippo pathway. An attempt was made to uncover a SCRIB-SnoN-dependent mechanism to prevent TAZ from enabling breast cancer cells to behave like cancer stem cells.

The evolutionarily conserved Hippo pathway

The evolutionarily conserved Hippo pathway, originally identified in *Drosophila melanogaster*, is a critical regulator of tissue growth in multicellular organisms. It maintains tissue homeostasis by controlling cell number through the modulation of proliferation, apoptosis, and differentiation. The pathway responds to intrinsic and extrinsic signals, including mechanical forces, cell polarity, and other signaling pathways. It integrates these upstream cues into a complex signaling network that spans many biological processes, such as development, organ size control, stem cell function, and tissue regeneration. Deregulation of Hippo signaling is implicated in organ overgrowth and tumor formation. Apical-basal cell polarity involves protein complexes that regulate the Hippo pathway. Here, the link between basolateral cell polarity and the mammalian Hippo pathway is highlighted.

Hippo signaling in Drosophila

Regulation of organ size is fundamental for the development and functionality of an organism. Extensive research in *Drosophila* has shown the involvement of several genes and signaling pathways in the control of final organ size (Shingleton, 2010; Gokhale & Shingleton, 2015). The Hippo pathway, identified through studies of tissue overgrowth mutations in flies, is a potent regulator of organ size. Genetic screens identified tumor suppressors as core components of the Hippo pathway, subsequently identified in mammals and other eukaryotes (Mohajan et al., 2021). This pathway, a cascade of kinase activity, regulates the transcriptional control of cell proliferation, survival, mobility, stemness, and differentiation (Ma et al., 2019). In *Drosophila*, the key kinases Hippo (Hpo) and Warts (Wrt), along with additional components Salvador (Sav) and Mob as Tumor Suppressor (Mats), function to inhibit the activity of the downstream effector Yorkie (Yki). Yki is a transcriptional coactivator that interacts with the transcription factor Scalloped (Sd) and induces the expression of Sd target genes that promote tissue growth (Harvey & Hariharan, 2012; Moon et al., 2018). Overexpression of the gene *yki* mimics the effects of mutations in genes *hpo*, *wrt*, and *sav*, which reduce cell death and lead to excessive tissue growth, potentially resulting in tumor formation (Maugeri-Saccà & De Maria, 2018).

Mammalian Hippo Signaling

The core components of mammalian Hippo signaling are similar to those found in fruit flies and are involved in controlling cell proliferation, tissue growth, and organ size (Halder & Johnson, 2011). The protein kinase MST1/2 (Hpo ortholog) is activated by dimerization, including joining with SAV (Sav ortholog) to enhance its kinase activity (Yu & Guan, 2013; Zinatizadeh et al., 2019). This interaction allows MST1/2 to phosphorylate SAV1, MOB1(Wts ortholog), and LATS1/2 (Wts ortholog) (Ma et al., 2019). Activated LATS1/2 and MOB1 kinases negatively regulate the Yki orthologs, YAP and TAZ, which are transcriptional co-activators that influence the expression of genes involved in cell proliferation, survival, and differentiation (Patel et al., 2017). Phosphorylation of YAP/TAZ promotes their interaction with the regulatory 14-3-3 proteins, leading to their retention in the cytoplasm and subsequent degradation through ubiquitination mediated by β-TrCP (Misra & Irvine, 2018). In this scenario, the Hippo pathway is activated, and the exclusion of YAP/TAZ from the nucleus inhibits the expression of target genes that promote cell proliferation and tissue growth (**Fig. 1.1A**).

Disruption of Hippo signaling prevents YAP/TAZ phosphorylation, allowing them to enter the nucleus, where they interact with TEAD (Sd ortholog) family transcription factors and induce the expression of genes that drive tissue growth (**Fig. 1.1B**; Mohajan et al., 2021). This dynamic ON and OFF regulation of the Hippo pathway is crucial for controlling cell number, which is important for development and tissue homeostasis. In abnormal conditions, disrupted Hippo signaling allows uncontrolled cell proliferation, resulting in excessive tissue growth, enlarged organs, and tumor formation.

Upstream Regulators of Hippo Signaling

The microenvironment generates various intrinsic and extrinsic signals that cells detect and convert into the biochemical regulation of cellular processes (Dupont et al., 2011). These signals act upstream of the Hippo pathway and control the phosphorylation-dependent localization and activity of YAP/TAZ. YAP/TAZ connect these signals to the regulation of cell behavior, growth, proliferation, and differentiation (Dupont et al., 2011; Mohajan et al., 2021). Mechanical forces such as extracellular matrix stiffness, cell-cell contact, cell shape, and changes in the cytoskeleton are transmitted through the Hippo pathway. For instance, contact inhibition occurs in densely packed cell cultures, where cell-cell contact deactivates YAP/TAZ and halts cell proliferation (Ma et al., 2019).

Other mediators of Hippo signaling include extracellular soluble factors such as hormones and growth factors that regulate YAP/TAZ through G-protein-coupled receptors (GPCRs) (Meng et al., 2016). The positive or negative regulation of the Hippo pathway through GPCR signaling depends on the G-protein subunits that form the receptors and affect the control of tissue growth and organ size (Ma et al., 2019). The stability and function of YAP/TAZ can be affected by various sources of cellular stress. Signals from conditions such as nutrient starvation, energy stress, and hypoxia are linked to the regulation of YAP/TAZ by factors like glucose metabolism, oxygen availability, and energy-consuming cellular processes (Yu et al., 2015; Kim & Jho, 2018). Additionally, cell polarity, which refers to the asymmetric organization of components and functions within a cell, is a significant upstream regulator of the Hippo pathway, regulating YAP/TAZ activity (Meng et al., 2016; Kim & Jho, 2018). In the following section, cell polarity is discussed with a focus on apical-basal cell polarity and its control of Hippo signaling in epithelial cells.

Cell polarity regulation of Hippo signaling

Cell polarity is the asymmetric organization of components and functions in a cell. It plays a crucial role in various physiological processes, such as cell division, migration, and differentiation, as well as in the development and maintenance of normal tissue integrity (Nelson, 2003; Ellenbroek et al., 2012). For instance, the polarization of an early embryo establishes the axes around which an organism develops (Campanale et al., 2017). Epithelial cell polarity enables the formation of cellular sheets with distinct internal and external surfaces, facilitating cell-cell contacts necessary for tissue function (McCaffrey & Macara, 2011). This polarity also enables epithelial cells to act as selective barriers for transport, absorption, and secretion (Genevet & Tapon, 2011).

The relationship between cell polarity and the Hippo pathway is supported by interactome mapping data, which shows interactions between polarity determinants and Hippo signaling components (Pires & Boxem, 2018). Cell polarity controls Hippo signaling at membrane domains by either increasing the activity of Hippo core kinases to suppress YAP/TAZ activity or by trapping YAP/TAZ at cell junctions, preventing its translocation into the nucleus (Yu & Guan, 2013; Meng et al., 2016). Cell polarity proteins and components of cell junctions are essential for maintaining cell polarity. Loss of polarity is associated with inactivated Hippo signaling, stabilization of YAP/TAZ, and human disease (Misra & Irvine, 2018).

Apical-basal polarity

Epithelial cell polarity is initiated by E-cadherin-mediated cell adhesion to neighboring cells and extracellular substrates (Drubin & Nelson, 1996; Ebnet et al., 2018). This leads to the asymmetrical division of the plasma membrane into apical (free) and basolateral (bounded) domains (**Fig. 1.2**; Nelson, 2003; Ebnet et al., 2018). The boundary between these domains is designated by cell-cell junctions, specifically adherens junctions and tight junctions (**Figure 1.2**), which are defined by highly conserved polarity proteins (Genevet & Tapon, 2011). Polarity proteins, located in complexes at cell junctions, perform mutually antagonistic actions that establish and maintain both membrane domains (Pires & Boxem, 2018). The coordinated actions of proteins at polarity complexes and cell junctions control cell polarity (Yang et al., 2015).

Polarity protein complexes

The main modules for cell polarity in epithelial cells are the Partitioning Defective (PAR), Crumbs (CRB), and Scribble (SCRIB) complexes. These three complexes interact and behave in an antagonistic way to maintain apical-basal polarity and regulate epithelial tissue homeostasis (**Figure 1.2**; Assémat et al., 2008; Yang et al., 2015). The PAR complex (PAR3/PAR6/aPKC) is associated with tight junctions and promotes the initial adhesion cues that establish cell polarity (Ellenbroek et al., 2012; Allam et al., 2018). Although the PAR complex also plays a minor role in the assembly of tight junctions, the CRB complex (CRB/PALS1/PATJ) is essential for their assembly and stabilization (Allam et al., 2018). At the apical membrane domain, the PAR and CRB complexes depend on each other for their distribution, localization, and stabilization (Moreno-Bueno et al., 2008).

Both apical protein complexes act in mutual repression and cooperation with the basolateral SCRIB complex (SCRIB/DLG/LLGL) (Ellenbroek et al., 2012). As a major regulator of apical-basal cell polarity, the SCRIB complex restricts apical proteins from the basolateral domain (Zeitler et al., 2004). The SCRIB complex protein, Lethal Giant Larvae (LLGL), competes with PAR3 for binding to the PAR complex, which excludes the complex from the

apical domain (Moreno-Bueno et al., 2008; Ellenbroek et al., 2012). Conversely, the aPKC-mediated phosphorylation of LLGL dissociates it from PAR complex proteins and promotes its basolateral localization at the SCRIB complex, while also allowing the formation of an active PAR complex (Ellenbroek et al., 2012; Wen & Zhang, 2018; Allam et al., 2018).

Cell junction proteins

The protein components of cell-cell junctions play a crucial role in maintaining cell polarity and regulating the Hippo pathway. Adherens junctions and tight junctions are involved in activating LATS1/2 and inhibiting YAP/TAZ. Disruption of these cell junctions leads to the promotion of YAP/TAZ target gene expression (Yu & Guan, 2013; Meng et al., 2016). E-cadherin and α-catenin, which are proteins of the adherens junction, activate the Hippo pathway by negatively regulating YAP/TAZ activity (Moon et al., 2018; Mohajan et al., 2021). YAP is also negatively regulated by another adherens junction component, protein-tyrosine phosphatase type 14 (Moon et al., 2018; Mohajan et al., 2021). Zonula occludens (ZO) are tight junction scaffolding proteins. ZO-1 inhibits TAZ activity, while ZO-2 downregulates YAP (Yu & Guan, 2013; Moon et al., 2018).

Apical polarity proteins

Many of the proteins that are involved in the upstream regulation of Hippo signaling are in the apical membrane domain, which serves as a crucial organizing and activating site for Hippo pathway components (Genevet & Tapon, 2011; Schroeder & Halder, 2012). The CRB complex blocks the nuclear localization of YAP/TAZ (Schroeder & Halder, 2012). Each protein in the CRB complex activates Hippo signaling by interacting with a family of tight junction-associated adapter proteins called Angiomotins, which bind to YAP/TAZ and keep them in the cytoplasm (Pires & Boxem, 2018). In response to cell polarity, the PAR complex phosphorylates YAP/TAZ and promotes their degradation (Lv et al., 2015). Studies also show that when PAR complex protein PAR3 is not localized to tight junctions, it induces the dephosphorylation of LATS1 by the cytoplasmic phosphatase PP1, allowing TAZ to move into the nucleus (Lv et al., 2015; Meng et al., 2016). Hippo signaling is also influenced by the relationship between the apical polarity complexes and KIBRA, a scaffolding protein and an upstream regulator of the Hippo pathway (Yoshihama et al., 2012). Components of the CRB and PAR complexes interact with KIBRA and positively regulate Hippo signaling to keep YAP/TAZ in the cytoplasm (Swaroop B et al., 2021).

Basolateral polarity proteins

The link between SCRIB-dependent cell polarity and the Hippo pathway suggests that the SCRIB complex is a primary activator of Hippo signaling (Cordenonsi et al., 2011). SCRIB is a basolateral membrane-associated scaffolding protein that serves as an adaptor for the assembly of protein complexes (Bonello & Peifer, 2018). To regulate the Hippo pathway, SCRIB functions as an adaptor for Hippo kinases that facilitate the inhibition of TAZ and likely YAP (Piccolo et al., 2014; Zanconato et al., 2016). Current knowledge indicates that SCRIB recruits MST1/2 to the basolateral membrane to form a complex that includes LATS1/2 and TAZ (Cordenonsi et al., 2011). SCRIB is also necessary for MST1/2 activation, which results in LATS1/2 phosphorylation and the subsequent degradation of TAZ (**Fig. 1.3**; Cordenonsi et al., 2011). The suppression of YAP/TAZ activity via Hippo signaling is associated with the localization of SCRIB at the cell membrane (Piccolo et al., 2014). When SCRIB is mislocalized, and cell

polarity is disrupted, the MST1/2 and LATS1/2 kinase cascade is inactivated, and the nuclear activity of TAZ is stabilized (Piccolo & Cordenonsi, 2013; Bonello & Peifer, 2018).

Basolateral polarity proteins are also linked to the kinase LKB1, which regulates Hippo signaling. LKB1 is a well-characterized tumor suppressor that controls cellular processes, including polarity, through a connection to PAR family proteins (Baas et al., 2004). Studies have demonstrated that LKB1 is crucial for the proper localization and activation of both SCRIB and its polarity partner, Discs Large (DLG), as well as the repression of YAP activity (Mohseni et al., 2014). Findings suggest that the direct regulation of PAR family proteins by LKB1 results in the phosphorylation and targeting of DLG (Zhang et al., 2007) that is required for Hippo signaling. Additionally, knockdown experiments show that SCRIB is necessary for YAP regulation controlled by LKB1 (Mohseni et al., 2014). Overall, the data indicates that the LKB1-mediated regulation of basolateral polarity proteins through PAR family proteins is critical for the regulation of YAP (Mohseni et al., 2014).

The SCRIB polarity complex

Basolateral polarity proteins are not as well understood in mammals compared to apical polarity proteins (Margolis, 2005). Research conducted on *Drosophila* highlights the conserved components of the CRB and PAR modules, with the PAR polarity complex being the most extensively studied to date (Margolis, 2005; Su et al., 2012). This text will focus on the structural features of SCRIB, the intermolecular interactions within the SCRIB polarity complex, and other molecules that work with SCRIB to regulate the Hippo pathway.

An overview of SCRIB

The Scrib gene, initially identified as a tumor suppressor in Drosophila, is essential for cell polarity and organization in embryos (Bilder & Perrimon, 2000). It has also been found to play a key role in maintaining apical-basal cell polarity, ensuring that certain components of the cell membrane are confined to their appropriate regions (Bilder & Perrimon, 2000). The human version of Scrib, known as SCRIB, was identified as a target of ubiquitination and degradation by the human papillomavirus E6 proteins (Nakagawa & Huibregtse, 2000; Assémat et al.). SCRIB, a member of the LAP protein family, contains LRR and PDZ domains and functions as an adaptor protein, mediating protein-protein interactions at the basolateral membrane of epithelial cells (Lim et al., 2017). The protein's LRR domains help target SCRIB to the cell cortex and tether its N-terminus to the membrane, while its PDZ domains enable it to interact with various other proteins, forming large multimolecular complexes (Navarro et al.,2005; Elsum & Humbert, 2013; Bonello & Peifer, 2018).

The SCRIB/DLG/LLGL tripartite

Human SCRIB and its basolateral polarity partners DLG and LLGL regulate apical-basal cell polarity. Although it is not confirmed whether these three proteins interact directly, evidence from their colocalization and loss-of-function phenotypes suggests that they function together to exclude apical determinants from the basolateral domain (Bilder et al., 2000; Assémat et al., 2008). In *Drosophila*, studies found that Dlg helps stabilize Scrib at its cortical location, and Scrib, in turn, recruits Lgl to the membrane (Bilder et al., 2000). While the role of SCRIB in apical-basal polarity is not fully understood, a physical link between SCRIB and DLG was initially reported in *Drosophila*. GUK-holder, an adaptor protein, was reported to connect SCRIB and the GUK domain of DLG (Mathew et al., 2002; Katoh & Katoh, 2004; Su et al., 2012).

Furthermore, research has indicated a partial overlap between SCRIB and LLGL through the LRR domains of SCRIB and the WD40 domains of LLGL (Kallay et al., 2006). The direct interaction between DLG and LLGL requires aPKC-mediated phosphorylation of LLGL to bind the DLG GUK domain (Zhu et al., 2014; Wen & Zhang, 2018).

Crosstalk between SCRIB, SnoN, and the Hippo pathway

The Hippo signaling pathway is regulated through interactions with several major pathways (Misra & Irvine, 2018; Mohajan et al., 2021). Studies have revealed a complex network of molecules, including SCRIB, influencing the Hippo pathway and controlling YAP/TAZ (Bonello & Peifer, 2018). One of these molecules, SnoN, plays a significant role in regulating various signaling pathways crucial for development, physiological processes, and tumorigenesis (Jahchan & Luo, 2010). SnoN, originally classified as part of the Ski family of proto-oncogenes, demonstrates both oncogenic and anti-oncogenic effects. Specifically, SnoN exhibits elevated expression in human carcinoma cells while also being capable of inducing p53-mediated cellular senescence and apoptosis in response to cellular stress (Nomura et al., 1989; Zhu et al., 2007; Jahchan et al., 2013).

Research suggests that the expression level and cellular localization of SnoN are influenced by cell polarity, with SCRIB playing a significant role in the mutual regulation between SnoN and the Hippo pathway (Zhu et al., 2016). The interaction between SnoN and SCRIB results in the downregulation of both SnoN and TAZ. When SnoN and SCRIB dissociate, SnoN stabilizes TAZ, allowing it to translocate into the nucleus and promote cell proliferation (Fig. 1.4; Zhu et al., 2016; Bonello & Peifer, 2018).

SnoN, the proto- and anti-oncogene

SnoN was initially identified as a contributor to mammalian tumorigenesis by facilitating malignant progression during the early stages of tumor growth (Nomura et al., 1989). The cancer-promoting activity of SnoN is reinforced by its role as a critical negative regulator of the transforming growth factor beta (TGF-β) signaling pathway. It directly binds and represses Smad proteins, preventing them from mediating TGF-β-dependent gene expression that would inhibit cell proliferation (Luo, 2004; Lamouille & Derynck, 2009). SnoN also plays a key role in preventing tumorigenesis; losing one allele increases susceptibility to chemical-induced tumor formation in some cells. Additionally, its degradation enhances epithelial-to-mesenchymal transition (EMT) and metastasis (Shinagawa et al., 2000; Zhu et al., 2007; Luo, 2004; Pan et al., 2009). The anti-oncogenic role of SnoN is exemplified by its induction of premature senescence through binding with PML protein in PML nuclear bodies and stabilizing p53 (Pan et al., 2009).

The SnoN-Hippo pathway link

SnoN participates in human cancer and regulates multiple signaling pathways critical to physiological processes (Zhu et al., 2016). It is expressed widely in mammalian tissues and plays a role in accelerating aging, promoting angiogenesis, controlling mammary gland alveologenesis, enhancing lactogenesis, adipocyte differentiation, and white adipose tissue development (Jahchan & Luo, 2010; Pan et al., 2012; Jahchan et al., 2012; Zhu et al., 2013, 2018). In normal mammary epithelial cells, SnoN is located in the cytoplasm but translocates to the nucleus in cancer. The connection to the Hippo signaling pathway was revealed through the cell density influence on the alternate localization of SnoN (Krakowski et al., 2005; Zhu et al., 2016). It was demonstrated that SnoN directly interacts with the Hippo core kinase, LATS, inhibiting its

association with TAZ and the subsequent ubiquitin-mediated proteasomal degradation of TAZ. Consequently, SnoN stabilizes TAZ, promoting the proliferation of mammary epithelial cells (Zhu et al., 2016).

The SCRIB-SnoN interaction

Research has shown that SnoN not only associates with LATS but also co-localizes and interacts with SCRIB. According to the model proposed by Zhu et al. in 2016, under normal conditions of epithelial cell polarity (**Fig. 1.4A**), SCRIB recruits SnoN to the basolateral membrane (**Fig. 1.4B**). At this location, LATS2, activated by SCRIB, phosphorylates both SnoN and TAZ. This phosphorylation promotes their degradation, which in turn inhibits cell proliferation (**Fig. 1.4B**).

In contrast, when cell polarity is disrupted in a cancer context (**Fig. 1.4A**), SCRIB becomes mislocalized, leading to the accumulation of SnoN in the cytosol (**Fig. 1.4A**). In the cytosol, SnoN directly interacts with LATS2 and interferes with its ability to phosphorylate TAZ (**Fig. 1.4B**). This interference allows TAZ to enter the nucleus, resulting in the stabilization of its transcriptional activity (**Fig. 1.4B**; Cordenonsi et al., 2011; Zhu et al., 2016). These findings suggest that the interaction between SCRIB and SnoN is crucial for inhibiting TAZ activity, and any disruption of this interaction leads to the stabilization of TAZ.

Connection to breast cancer cell stemness

Stem cells have attracted significant interest in the field of science and medicine due to their unique abilities in development and disease. These cells can renew themselves and differentiate into various cell types within an organism. For instance, mammary stem cells (MaSCs) play a crucial role in the dynamic development and changes of the mammary gland by giving rise to different cell lineages (Yang et al., 2016). While the capacity for self-renewal and differentiation enables MaSCs to drive mammary gland development, these same traits also make them susceptible to transformation (Yang et al., 2016). When the unique characteristics of stem cells are deregulated, they can turn into cancer stem cells (CSCs) and lead to tumorigenesis (Dontu et al., 2003).

CSCs, having the ability to initiate and sustain tumors, exhibit behaviors similar to both stem cells and cancer cells (**Fig. 1.5**; Yu et al., 2012). The CSC model suggests that tumors originate from a small subset of genetically modified cells within a solid tumor, which can promote tumorigenesis (Charafe-Jauffret et al., 2009). Through their self-renewal capacity, CSCs keep tumors growing by dividing into another CSC and a tumor cell that further differentiates and contributes to tumor heterogeneity (**Fig. 1.5**; Visvader & Lindeman, 2008). One significant aspect of CSCs is their ability to resist cancer treatments (**Fig. 1.5**). Their resistance to chemotherapy is attributed to multidrug resistance proteins that expel anticancer drugs from cells, while their resistance to radiation therapy is credited to the overactivity of DNA damage repair enzymes (Dean et al., 2005; Sodani et al., 2012). These unique features of CSCs make them clinically responsible for therapy resistance, tumor recurrence, and metastasis (Peitzsch et al.,2017; da Silva-Diz et al., 2018).

Cancer stem cells drive breast cancer

There is evidence supporting the existence of a subpopulation of cells with high tumorigenicity in samples of breast cancer. A subset of cells enriched from the MCF-7 breast cancer cell line displayed traits such as anchorage independence and resistance to apoptosis-

promoting agents and were shown to be tumor-inducing (Cariati et al., 2008). These breast tumor cells also exhibited stem cell characteristics and presented the clinically detrimental features of CSC (Cariati et al., 2008). The small population of breast cancer stem cells (BCSCs) in a tumor can be identified by the expression of specific cell surface markers. Exposure of breast tumors to chemotherapy enriches treatment-resistant BCSCs that can initiate mammospheres and tumor growth in mice (Charafe-Jauffret et al., 2009). BCSCs are typically identified and isolated using fluorescence-activated cell sorting (FACS) along with the specific biomarkers, $CD44^{+}/CD24^{-/low}$ and $ALDH1^{+}$. Accumulating data suggests that BCSCs expressing this surface marker signature in breast tumors are responsible for initiating tumors, tumor progression, metastasis, and resistance to treatment (Zhang et al., 2020).

BCSCs, Hippo signaling, and the SRIB-SnoN interaction

The maintenance of breast cancer cell stemness has been linked to different signaling pathways, including the Hippo signaling pathway. The expression level of YAP/TAZ is prominent in BCSCs and correlates with the level of stemness as measured by tumor grade, which increases from low-grade well-differentiated to high-grade anaplastic (Cordenonsi et al., 2011). When TAZ is knocked down in BCSCs, there is significantly less ability to form mammospheres and initiate tumors in mice. Contrarily, TAZ expression in breast cancer cells causes them to behave like BCSCs and become more resistant to chemotherapy. This data shows the necessity of TAZ for BCSCs attributes and links this phenomenon to the Hippo pathway. This is further connected to the SCRIB-dependent stabilization of TAZ by SnoN, which promotes the CSC-dependent propagation of breast cancer cells (Zhu et al., 2016).

Manipulating the SCRIB-SnoN interaction could potentially help inhibit and even reverse cancer stem cell-like traits promoted by TAZ in breast tumor cells. Therefore, it is necessary to understand the mechanism underlying the SCRIB-SnoN interaction and to uncover its biological function. This study aimed to characterize the specific binding domains required for SCRIB and SnoN to interact and to investigate the potential involvement of other components. By uncovering the function of the SCRIB-SnoN interaction, we can further our understanding of how SCRIB regulates the interaction between SnoN and Hippo signaling. If this interaction is essential for inhibiting TAZ, it could be utilized as a therapeutic strategy to prevent the stem-like characteristics of breast cancer cells.

FIGURES

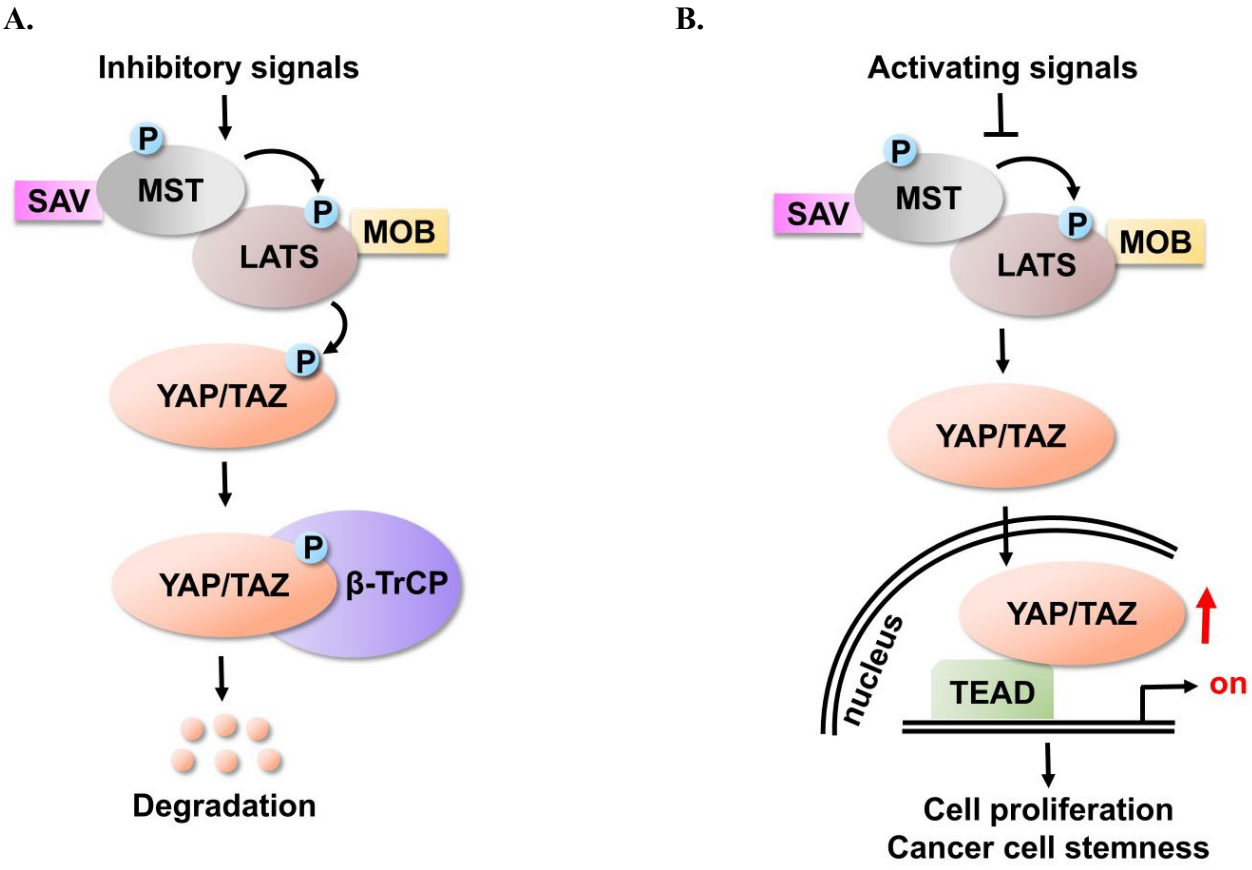

Figure 1.1. The dynamics of the mammalian Hippo pathway.
(A) Hippo ON. (B) Hippo OFF. The red arrow indicates accumulated protein. The circled Ps indicate phosphorylation.

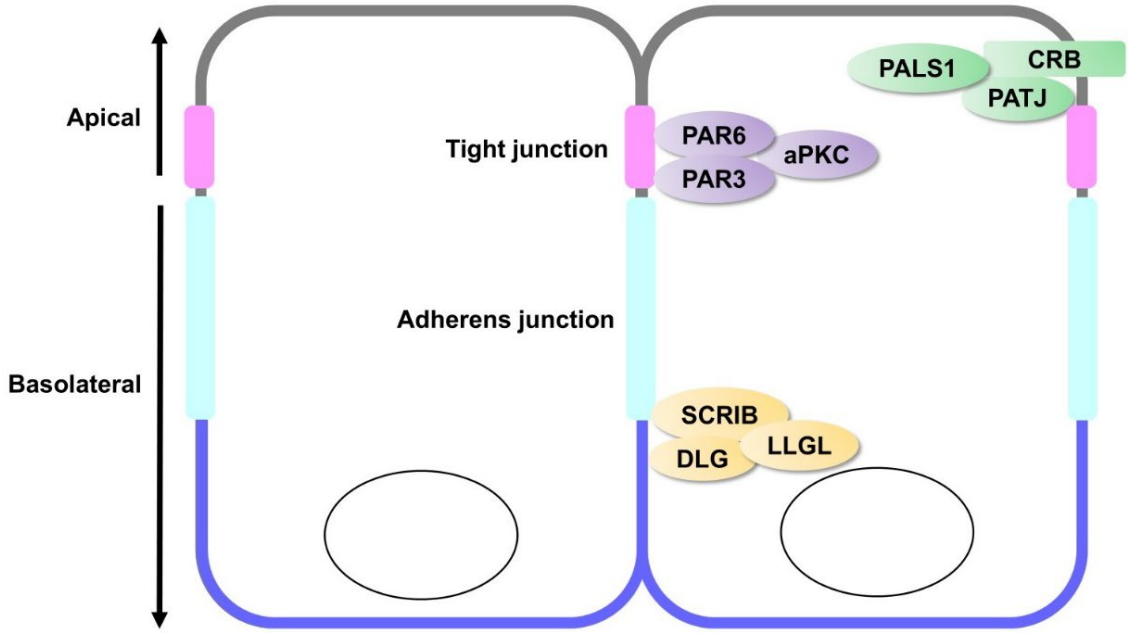

Figure 1.2. Components of the apical and basolateral polarity complexes in polarized epithelial cells.
Abbreviations: CRB, Crumbs; PALS1, protein-associated with Lin- 7; PATJ, Pals1 associated tight junction protein; PAR, partitioning-defective proteins 3 and 6; aPKC, atypical protein kinase C; SCRIB, Scribble; DLG, Discs large; LLGL, Lethal giant larvae.

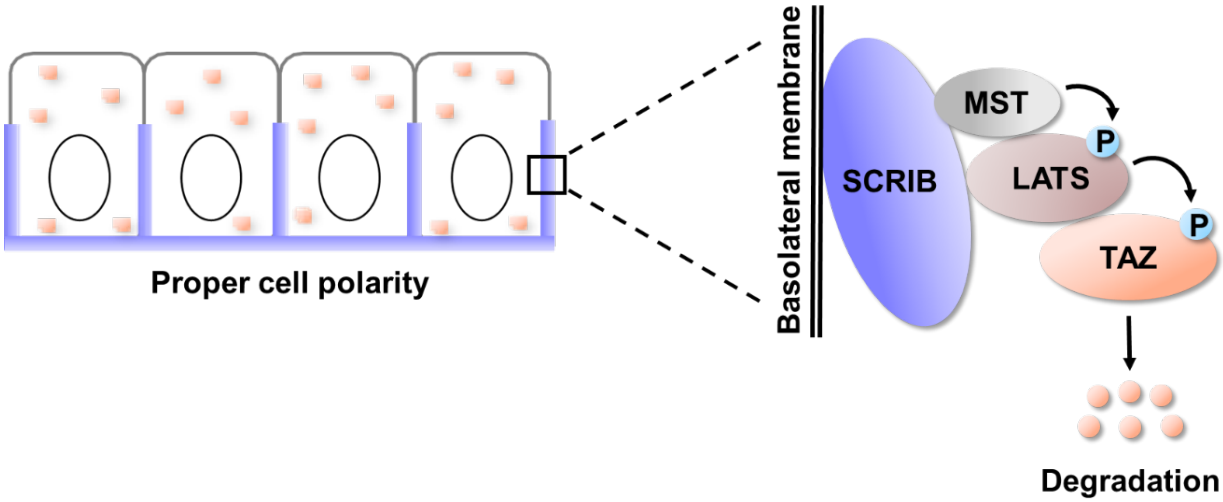

Figure 1.3. A model depicting the proposed mechanism for SCRIB-dependent TAZ degradation by the Hippo pathway.
SCRIB (blue) localized to the basolateral membrane, and TAZ (orange) in the cytosol. SCRIB activates MST1/2, which results in LATS1/2 phosphorylation and the subsequent degradation of TAZ. The circled Ps indicate phosphorylation.

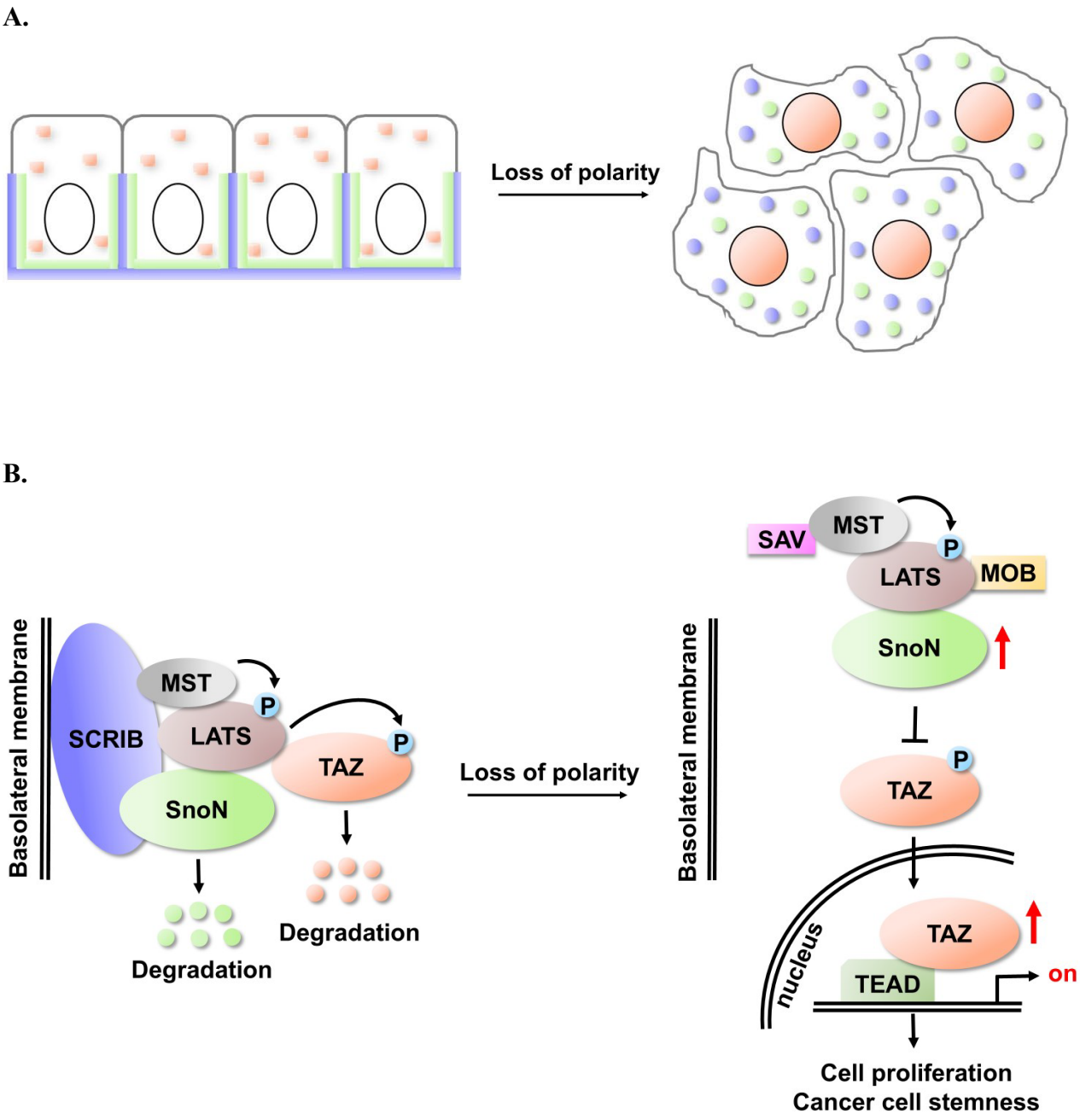

Figure 1.4. A model of SCRIB-dependent mutual regulatory interaction between SnoN and the Hippo pathway during proper polarity conditions and loss of polarity.
(A & B, left) Proper polarity conditions with SCRIB (blue) and SnoN (green) localized to the basolateral membrane and TAZ (orange) in the cytosol. (A & B, right) Loss of polarity with SCRIB mislocalized to the cytosol, SnoN upregulated in the cytosol, and TAZ translocated into the nucleus. The red arrows indicate accumulated proteins. The circled Ps indicate phosphorylation.

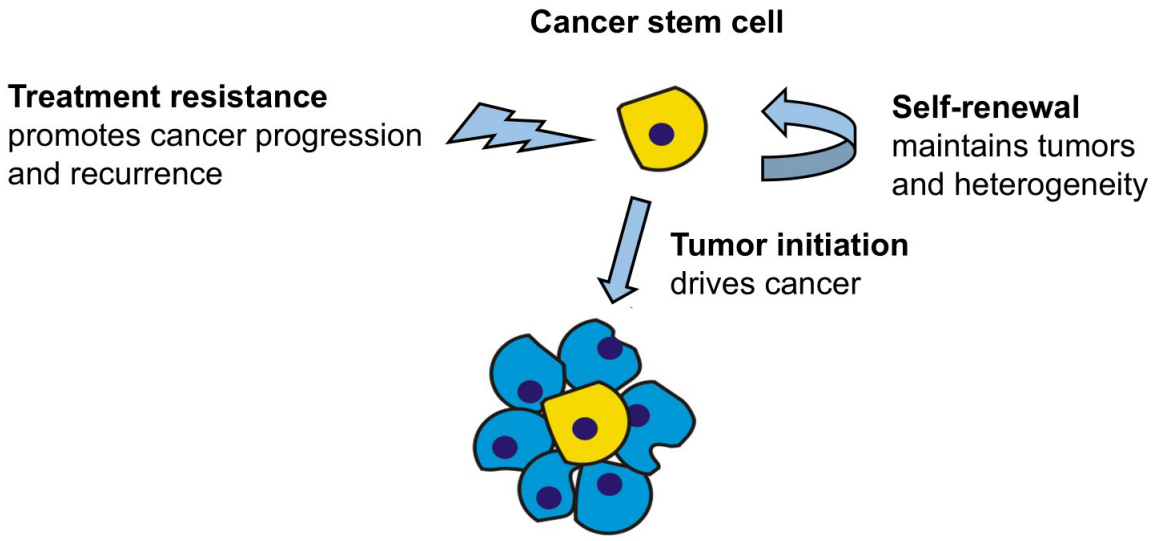

Figure 1.5. Cancer stem cells drive tumorigenesis.
Cancer stem cells are a subpopulation of cells in solid tumors that drive tumorigenesis through their capacity for self-renewal, tumor initiation, and drug resistance

Chapter 2

Characterization of the SCRIB-SnoN Interaction

SUMMARY

It is essential to understand the roles of known protein-protein interactions involved in the process of inhibiting the TAZ-dependent stemness of breast cancer cells. One promising candidate for targeting TAZ is the interaction between SCRIB and SnoN. Investigating the biological function of the SCRIB-SnoN interaction is crucial for understanding how SCRIB-dependent cell polarity, Hippo signaling, and the development of cancer stem cell-related traits in breast tumor cells are interconnected.

This study aims to identify the specific amino acid sequences in SnoN and SCRIB that are necessary for their interaction. These binding domains enable both proteins to engage in SCRIB-dependent, mutually regulating interactions that involve SnoN and Hippo signaling. While current co-immunoprecipitation data confirm the interaction between SCRIB and SnoN, this research seeks to characterize how this interaction regulates Hippo signaling.

EXPERIMENTAL PROCEDURES

Cells, antibodies, and constructs

293T cells were cultured in complete medium composed of Dulbecco's Modified Eagle's Medium (DMEM) supplemented with 10% fetal bovine serum (FBS),100 U/mL penicillin, and 100 μg/mL streptomycin. The normal human mammary epithelial cell line MCF10A was maintained in DMEM/F-12 containing 5% horse serum, epidermal growth factor (EGF) at 20 ng/mL, hydrocortisone at 0.5 μg/mL, insulin at 10 μg/mL, cholera toxin at 100 ng/mL, along with penicillin and streptomycin. MCF10A-m cells, which express full-length SnoN containing a Smad binding site mutation that prevents rapid degradation, were maintained under the same conditions as MCF10A cells.

Antibodies specific for the following proteins were utilized at the indicated concentrations: SCRIB (1:4000), FLAG (1:5000), HA (1:2000), Smad4 (1:4000), and GAPDH (1:4000).

Full-length SnoN, NDR1, NDR2, and Smad4 were expressed in pCMV5b-FLAG or pCMV5b-HA vectors. The following truncated SnoN mutants were expressed using pCMV5b-FLAG: SnoN(1-366), which lacks residues 367-684, and SnoN(367-684), which lacks residues 1-366. Full-length SCRIB was expressed using pTagBFP-N. MSCV-Puro-SCRIB and pRK5m-FLAG served as tools for molecular biology techniques to generate FLAG-tagged SCRIB.

Mammalian cell transfection

Plasmid DNA was delivered to cells through the process of transfection, with a total of 5 μg of DNA introduced to each sample. For co-transfection, the concentrations of two distinct plasmid DNAs were tested to determine optimal expression levels. Cells were seeded on p60 cell culture plates at a density that would achieve 50-80% confluency after 24 hours. Transient transfection was conducted using either Lipofectamine or polyethyleneimine-based protocols.

Lipofectamine 3000 (Invitrogen) or Lipofectamine LTX & PLUS (Invitrogen) were utilized according to the manufacturer's instructions. For transfection with Lipofectamine 3000, the lipofectamine reagent was diluted 1:30 in serum-free medium. Plasmid DNA was diluted 1:50 (w/v) in a serum-free medium, along with the P3000 transfection-enhancing reagent at a ratio of 1:2 (DNA:P3000, w/v). This was then combined with the lipofectamine dilution at a 1:1 ratio.

For transfections using Lipofectamine LTX & PLUS, a 1:10 dilution of the lipofectamine reagent was prepared in serum-free medium, and the plasmid DNA was diluted 1:50 (w/v) in serum-free medium, with the PLUS reagent at a 1:1 ratio (DNA:PLUS, w/v). The diluted plasmid DNA was then mixed with the diluted Lipofectamine LTX reagent at a 1:1 ratio.

In the case of transient transfection using polyethyleneimine (PEI), the plasmid DNA was diluted 1:30 (w/v) in a serum-free medium. A 1:10 dilution of PEI in serum-free medium was combined with the diluted plasmid DNA at a 1:10 ratio (1:4, DNA:PEI, w/v). For each transfection protocol, the DNA-lipid complex was transferred to the cells, and the cells were incubated at 37°C for 48-72 hours.

Cell lysis and immunoprecipitation

Proteins were isolated from transfected cells using immunoprecipitation. The cells were lysed in either a low-salt (150 mM NaCl) or high-salt (420 mM NaCl) lysis buffer, which contained 50 mM HEPES-KOH (pH 7.8), 5 mM EDTA, 0.1% NP-40, 3 mM dithiothreitol (DTT), and 0.5 mM phenylmethylsulfonyl fluoride (PMSF).

Cell lysates were precleared to minimize non-specific binding by incubating them with 30 µL of protein A-Sepharose beads for 30 minutes at 4°C. After this, the lysates were transferred to agarose beads that were conjugated with the appropriate antibody for immunoprecipitation. To isolate FLAG- or HA-tagged proteins, beads coupled with a polyclonal antibody specific to the respective tag were utilized. Co-immunoprecipitation experiments were performed to investigate direct interactions between proteins, where one protein, bound to the agarose beads, served as the bait, while the other protein of interest acted as the prey.

Tagged proteins were eluted using either the FLAG or HA peptide in buffer D, which contains 250 mM KCl, 20 mM HEPES-KOH (pH 7.8), 0.2 mM EDTA, 0.1% NP-40, 15% glycerol, and 1 mM DTT. Alternatively, they could be eluted with 0.1 M glycine (pH 2-3). After elution, the fractions were separated and analyzed by immunoblotting.

Immunoblotting

Protein expression was analyzed using Western blotting. Total cell lysate was prepared with 4X Laemmli sample buffer and boiled at 95°C for 5 minutes. SDS-polyacrylamide gel electrophoresis (SDS-PAGE) was then employed to separate the purified proteins. Samples were loaded into a gradient gel and run at 90 V through the 4% stacking gel (comprising 30% acrylamide, 2% bisacrylamide, 2 M Tris-Cl at pH 6.8, 10% SDS, 10% ammonium persulfate, 1% TEMED, and Milli-Q H_2O) before being run at 325 V through the 10% resolving gel (comprising 30% acrylamide, 2% bisacrylamide, 2 M Tris-Cl at pH 8.8, 10% SDS, 10% ammonium persulfate, 1% TEMED, and Milli-Q H_2O) until the dye front reached the bottom.

After separation, proteins were transferred from the gel to a PVDF membrane using semi-dry electrophoretic transfer. Before blocking, protein lanes were visualized using Ponceaus S staining to evaluate transfer efficiency. The membrane was then blocked with 1% non-fat dry milk in TBST and probed with appropriate concentrations of primary antibodies specific to the proteins of interest. Following a washing step, the membrane was incubated with an HRP-conjugated secondary antibody that reacted with the primary antibody. The proteins of interest were detected via a luminol-based chemiluminescent reaction catalyzed by the HRP enzyme. The resulting light signal was captured using X-ray film.

Polymerase chain reaction (PCR)

PCR was utilized to amplify DNA samples for experiments involving specific sequences.

Primer design

Primers were designed with restriction enzyme digestion sites at their ends to allow for the cloning of the sequence of interest into a plasmid vector that encodes a protein tag. The coding sequence (CDS) of the target gene was retrieved from the NCBI Nucleotide database.

For protein fusion with an N-terminal protein tag, the forward primer was designed to start with the codon directly following the ATG start codon of the CDS and to end with a G or C at the 3' end. The reverse primer was constructed to start with a G or C at the 5' end and to end with a STOP codon. For fusion with a C-terminal protein tag, the forward primer began with the ATG start codon of the CDS, while the reverse primer excluded the STOP codon.

The length of each primer depended on the GC content, as indicated by the theoretical annealing temperature. The following formula was used to calculate the annealing temperature: T_a = [4(no. of GC base pairs) + 2(no. of AT base pairs)] - 5. Primers were designed to have an ideal annealing temperature between 51°C and 57°C.

The CDS and plasmid vector sequence were analyzed using A Plasmid Editor (APE). Two different restriction sites were identified that were absent in the CDS but present in the multiple cloning site (MCS) of the vector. To ensure the proper addition of the protein tag, the sequences of the tag and the gene of interest were aligned in the same reading frame. The forward primer was adjusted with the necessary number of nucleotides to maintain the correct reading frame between the tag incorporated in the vector and the sequence to be inserted into the MCS.

For the restriction sites, the cut sequence of one enzyme was added to the 5' end of the forward primer, upstream of any nucleotides included for maintaining the reading frame. The cut sequence for the other enzyme was added after the STOP codon at the end of the reverse primer. The restriction sites were carefully positioned to ensure that the final orientation of the CDS within the plasmid vector was correct. Extra nucleotides were added to the ends of the primers to improve cleavage efficiency. The New England Biolabs (NEB) usage guideline, "Cleavage Close to End of DNA Fragments," was referenced for the required number of extra nucleotides to facilitate effective enzyme digestion. For PCR amplification, the reverse complement was utilized in the final design of the reverse primer.

Oligonucleotides (50 nmol) were purchased from Thermo Fisher Scientific. Lyophilized primers were briefly spun down to ensure the powder was at the bottom of the tube. The primers were reconstituted in nuclease-free H_2O at a concentration of 50 pmol/mL and stored at -20°C.

PCR procedure

PCR was performed to amplify the target sequence, incorporating selected restriction sites at both ends. The PCR reactions were carried out in a final volume of 100 µL, which included the following components: 1X Pfu buffer, 5 mM dNTPs, 60 ng of template DNA, 50 pmol of forward primer, 50 pmol of reverse primer, 1.25 U of Pfu polymerase, and 1.5 µL of DMSO in water.

The thermocycler was programmed with the following conditions: 5 cycles of 94°C for 1 minute and 30 seconds; 48°C for 1 minute and 30 seconds; 72°C for 1 minute and 30 seconds. Followed by 20 cycles of 94°C for 1 minute; the appropriate primer annealing temperature (°C) for 1 minute; 72°C for 1 minute. Finally, 1 cycle at 72°C for 5 minutes and hold at 4°C.

Phenol-chloroform extraction and ethanol precipitation

The PCR product was transferred to a 1.5 mL microcentrifuge tube for extraction. To the amplicons, 100 µL of phenol/chloroform was added and mixed by vortexing for 1 minute. The tube was then centrifuged at maximum speed for 2 minutes. The top layer was carefully transferred to a new tube, avoiding the white interface where proteins were located.

To precipitate the DNA, 10 µL of 3M sodium acetate (pH 5.2) and 300 µL of ice-cold ethanol were added, and the tube was incubated at -20°C for at least 5 minutes. After centrifuging at 4°C for 15 minutes, the liquid was carefully decanted without disturbing the pellet. Next, 500 µL of 70% ethanol was added to the tube without disturbing the pellet. The ethanol was then poured out, and the pellet was allowed to air dry. Finally, the DNA was resuspended in 20 µL of water.

DNA gel electrophoresis and purification

A standard 1% agarose gel was prepared in 1X TAE buffer, with GelRed added to achieve a final concentration of 1X. The resuspended PCR product was mixed with 6X loading dye and then loaded onto the gel for electrophoresis. After running the gel, the DNA bands were extracted using the Qiaex II Gel Extraction Kit. The purified DNA was eluted in 20 µl of 10 mM Tris·Cl (pH 8.5). The concentration of the final PCR product was measured using a NanoDrop spectrophotometer.

Restriction digest

To prepare for cloning, the purified PCR fragment and the expression vector were subjected to double digestion using the appropriate restriction enzymes. The NEB online tools, NEBcloner and Double Digest Finder, were utilized to design the following double digest reaction: 1X NEBuffer that maximizes the activity of both enzymes, 30 U of each restriction enzyme, the total volume of the PCR product, or 5 µg of the plasmid vector, and enough nuclease-free H_2O to achieve a final volume of 30 µl. The digestion reactions were incubated for 2 hours at 37°C.

To prevent the reclosure of the linearized plasmid, 1 U of calf intestinal alkaline phosphatase (CIP) was added to the vector digest reaction for every 1 µg of a 3 kb plasmid. This CIP reaction was incubated for 45 minutes at 37°C and was subsequently stopped by heat inactivation at 80°C for 2 minutes.

The digested PCR fragment was purified using phenol/chloroform extraction followed by ethanol precipitation, then resuspended in 20 µl of nuclease-free H_2O. The digested and CIP-treated vector DNA was purified through gel electrophoresis, extracted with the Qiaex II Gel Extraction Kit, and eluted in 20 µl of nuclease-free H_2O.

Ligation

The PCR fragment was ligated into an expression vector to create a plasmid that encodes a tagged protein. For the ligation reaction, a molar ratio of the vector to the insert between 1:1 and 1:3 was desired. To evaluate this, 1 µL of the vector and 1 µL of the insert were run on an electrophoresis gel. The gel was imaged, and the band intensities were analyzed using Image J, with the intensity of the weaker band set to 1 for normalization.

The sizes of the vector (Sv) and the insert (Si), the relative band intensities of the vector (Iv) and the insert (Ii), along with the volumes of the vector (Vv) and the insert (Vi) used in the gel, were utilized in the following formula to calculate the volume of the insert (Li) needed for

ligation, relative to the volume of the vector (Lv), which was set to 2 µL:

$$Li = 3 * Lv * (Si/Sv) * (Iv/Ii) * (Vi/Vv).$$

A typical ligation reaction was prepared as follows: 1X ligation buffer, 2 µL of vector, x µL of insert (Li), 1 µL of T4 ligase, and nuclease-free H_2O to reach a final volume of 10 to 15 µL. The ligation reaction was incubated at 37°C for 30 minutes. As a control, ligation of the vector alone was performed to verify that the vector was fully digested and that the CIP treatment was effective.

Bacterial transformation

DH5α *E. coli* cells were transformed with the ligation product to amplify the plasmid. Competent DH5α cells were thawed on ice. Then, 60 µL of the competent cells were transferred to the ligation reaction and mixed by gently tapping the tube. The mixture was incubated on ice for 20 minutes. Following this, the cells underwent heat shock at 42°C for 45 seconds and were immediately placed back on ice.

Next, 900 µL of Luria broth (LB) was added, and the cells were incubated on a shaker at 37°C for 45 minutes. The bacterial cells were then centrifuged for 30 seconds in a microcentrifuge. The medium was carefully aspirated, leaving approximately 50 µL to resuspend the pellet by pipetting. The cells were spread onto an LB agar plate containing 100 µg/mL ampicillin (Amp) to select for transformants. Finally, the plate was incubated upside down for 16-20 hours at 37°C.

Plasmid purification

Single colonies of transformants were selected from the selective plate. Starter cultures were inoculated in 2 mL of LB medium supplemented with 100 mg/mL ampicillin and incubated overnight on a shaker at 37°C. The plasmid was initially isolated using the mini-prep method explained below.

The culture was transferred into a 1.5 mL microcentrifuge tube and centrifuged at maximum speed for 1 minute. The supernatant was discarded, and the pellet was resuspended in 100 µL of Solution I (25 mM Tris, pH 8, 50 mM glucose, and 10 mM EDTA). Next, 200 µL of fresh Solution II (0.2 M NaOH, 1% SDS) was added to the suspension, which was mixed by inverting the tube three times.

Following this, 150 µL of Solution III (composed of 6 mL of 5M KOAc, 1.15 mL of acetic acid, and 2.85 mL of H2O) was added to the tube, and the mixture was inverted gently before being placed on ice for 5 minutes. Afterward, the tube was centrifuged for 3 minutes at 4°C, and 800 µL of the supernatant was transferred to a clean tube.

To this supernatant, 480 µL of isopropanol was added and mixed thoroughly. After allowing it to sit at room temperature for 5 minutes, the tube was centrifuged for 5 minutes. The supernatant was discarded, and the pellet was washed with 250 µL of 100% ethanol and then air-dried. Finally, the pellet was resuspended in 50 µL of TE buffer containing RNase.

The mini-prepped plasmid DNA was subjected to diagnostic digestion to confirm the presence of the expected insert size, which was analyzed by examining the fragment pattern on a gel. Cultures that contained the correct construct were then used to inoculate 100 mL overnight cultures for plasmid maxi-preps, following the Qiagen Plasmid Purification protocol.

Site-directed mutagenesis

The QuikChange II XL Site-Directed Mutagenesis Kit (Agilent Technologies) was used to insert a C-terminal protein tag into a double-stranded plasmid containing the sequence of interest. In this protocol, *PfuUltra* high-fidelity (HF) DNA polymerase (Agilent Technologies) facilitated mutagenic primer-directed replication of both strands of the plasmid, starting with the double-stranded DNA (dsDNA) template vector and two oligonucleotide primers. Alternatively, the KAPA HiFi PCR Kit (KAPA Biosystems) was used to generate the plasmid containing the sequence of interest fused to the protein tag sequence.

The mutagenic primers were designed to include the protein tag sequence (the desired mutation) and were complementary to opposite strands of the vector. During temperature cycling, *PfuUltra* HF DNA polymerase or KAPA HiFi DNA polymerase extended these primers to generate the mutated plasmid. After the temperature cycling, the product was treated with *Dpn* I endonuclease, which specifically targets methylated DNA, to digest the parental DNA template and enrich for the synthesized plasmid DNA containing the mutation.

Finally, the vector DNA was transformed into XL10-Gold ultracompetent cells (Agilent Technologies).

Primer design

Mutagenic primers were designed using the web-based QuikChange Primer Design Program available online at www.agilent.com/genomics/qcpd. The primers were 25 to 45 bases in length, with a melting temperature (T_m) of at least 78°C. To estimate the Tm for primers intended to introduce insertions, the following formula was used: $T_m = 81.5 + 0.41(\%GC) - (675/N)$, where N does not include the bases being inserted. The desired insertion sequence (protein tag) was placed in the center of the primer, flanked by approximately 10-15 bases of unmodified nucleotide sequence on both sides. The primers had a minimum GC content of 40% and ended with one or more C or G bases. 50 nmol of lyophilized oligonucleotides from Thermo Fisher Scientific were reconstituted in H_2O at a concentration of 50 pmol/mL.

Mutant strand synthesis reaction

Sample reactions were prepared with a final volume of 50 µL, which included the following components: 10 µL of 10X reaction buffer, 10 ng of double-stranded DNA (dsDNA) template, 125 ng of forward primer, 125 ng of reverse primer, 1 µL of dNTP mix, 3 µL of QuikSolution (known to enhance linear amplification), and nuclease-free water to bring the total volume to 50 µL. After mixing these components, 1 µL of *PfuUltra* HF DNA polymerase (2.5 U/µL) was added to each reaction.

The reactions were cycled using the following parameters on a thermocycler: 1 cycle at 95°C for 1 minute. Then, 18 cycles of 95°C for 50 seconds; the appropriate primer annealing temperature (°C) for 50 seconds; 68°C for 1 minute per kilobase of plasmid length. Finally, 1 cycle at 68°C for 7 minutes and hold at 4°C.

Alternative mutant strand synthesis reaction

Sample reactions were also prepared using the KAPA HiFi PCR Kit. A final volume of 50 µL included 10 µL of 5X KAPA HiFi Buffer, 100 ng of double-stranded DNA (dsDNA) template, 125 ng of forward primer, 125 ng of reverse primer, 1.5 µL of 10 mM of KAPA dNTP mix, 1 µL of 1 U/µL KAPA HiFi DNA polymerase, and nuclease-free water to bring the total volume to 50 µL.

The reactions were cycled using the following parameters on a thermocycler: 1 cycle at 95°C for 2 minutes. 18 cycles of 98°C for 20 seconds; the appropriate primer annealing temperature (°C) for 15 seconds, 72°C for 1 minute per kilobase of plasmid length. Finally, 1 cycle at 72°C for 5 minutes and hold at 4°C

Dpn I digestion

To digest the parental (non-mutated) dsDNA template, 1 µl of the Dpn I restriction enzyme (10 U/µl) was added directly to each amplification reaction. The reaction mixtures were mixed gently and thoroughly by pipetting up and down several times. After mixing, the samples were spun down in a microcentrifuge for 1 minute and then incubated at 37°C for 1 hour.

Transformation of E. coli cells

For the QuikChange II XL Site-Directed Mutagenesis protocol, XL10-Gold ultracompetent *E. coli* cells were gently thawed on ice. For each transformation reaction, 45 µl of the ultracompetent cells were aliquoted into a pre-chilled 14-mL polypropylene round-bottom tube. Then, 2 µl of the β-ME mix provided with the kit was added to the cells. The tube was gently swirled and incubated on ice for 10 minutes, with swirling every 2 minutes. For mutagenic vectors derived using the KAPA HiFi PCR method, DH5α *E. coli* cells were prepared for transformation without the use of β-ME.

Next, 2 µl of the *Dpn* I-treated DNA was transferred from each reaction into separate aliquots of the ultracompetent cells. The transformation reactions were gently swirled to mix and then incubated on ice for 30 minutes. To heat shock the cells, the tubes were transferred to a 42°C water bath for 30 seconds and then placed back on ice for 2 minutes.

After that, 0.5 mL of preheated (42°C) LB broth was added to each tube, which was then incubated at 37°C for 1 hour while shaking. Finally, the appropriate volume from each transformation reaction was plated on agar plates containing the appropriate antibiotic for the plasmid vector, and the plates were incubated at 37°C for more than 16 hours. Plasmids were subsequently purified according to a maxiprep protocol.

Gibson Assembly

The NEB Gibson Assembly protocol was used to combine multiple DNA fragments into a sealed DNA molecule, resulting in an expression vector that contains the desired sequence and a protein tag. The master mix includes exonuclease, which generates single-stranded 3' overhangs to facilitate the annealing of fragments that have complementary ends at the overlap region. DNA polymerase then fills in any gaps within the annealed fragments, while DNA ligase seals any nicks in the assembled DNA.

Primer design and PCR

PCR primers were designed to amplify fragments of the sequence of interest along with the vector containing the protein tag. This design ensured that there was appropriate complementary overlap for assembling a fully sealed double-stranded DNA construct. Both forward and reverse primers were created to facilitate overlapping between the sequence fragments and the vector. They included restriction enzyme digestion sites and extra nucleotides for cleavage efficiency. Additionally, the necessary nucleotides were incorporated into the primers to maintain the correct reading frame between the tag in the vector and the sequence of interest. The primers were designed to have optimal GC content and length, which allowed for

an ideal annealing temperature. A total of 50 nmol of lyophilized oligonucleotide primers (Thermo Fisher Scientific) were reconstituted in nuclease-free H_2O to achieve a concentration of 50 pmol/mL.

The PCR reactions were set up with a final volume of 50 µL, which included the following components: 10X reaction buffer, 10 mM dNTPs, 10 µM forward primer, 10 µM reverse primer, 5 U/µL Taq polymerase, 0.5 µg/µL template DNA, and nuclease-free H_2O to reach the total volume of 50 µL. The PCR machine was programmed with the following settings: 1 cycle at 95°C for 5 minutes; 30 cycles consisting of 98°C for 30 seconds; the appropriate primer annealing temperature (°C) for 1 minute; 68°C for 5 minutes; 1 cycle at 68°C for 10 minutes and hold at 4°C.

Reaction procedure

The concentration of DNA fragments was measured using a Nanodrop spectrophotometer. For an assembly of 4 to 6 fragments, a 1:1 molar ratio of each DNA fragment to the linearized vector was combined with 10 µL of 2X Gibson Assembly Master Mix (NEB) and nuclease-free water to achieve a total volume of 20 µL. The total amount of DNA fragments used varied from 0.2 to 1.0 pmol and constituted no more than 20% of the total assembly reaction volume. The reactions were incubated in a thermocycler at 50°C for 1 hour.

Bacterial transformation

After incubation, 60 µL of competent DH5α *E. coli* cells were transformed with 2 µL of the assembly reaction. The appropriate volume from each transformation reaction was plated on agar plates containing the appropriate antibiotic for the plasmid vector, and the plates were incubated at 37°C for more than 16 hours. Plasmids were subsequently purified from colonies of transformants.

DNA sequencing

Sequencing was conducted to determine the order of bases in DNA samples, which were sequenced by the UC Berkeley DNA Sequencing Facility.

Primer design

The complete CDS of the gene of interest was analyzed using APE. Sequencing primers were designed to be between 18 and 22 bases in length, to end with either G or C, and to have an annealing temperature ranging from 51°C to 57°C. Oligonucleotides (50 nmol) were purchased from Thermo Fisher Scientific.

Sequencing protocol

To sequence the plasmid DNA, 1 µg of DNA was combined with 8 pmols of primer and nuclease-free H_2O was added to achieve a total volume of 13 µL. The samples were sequenced at the UC Berkeley DNA Sequencing Facility. Sequences of interest were verified using the NCBI Nucleotide BLAST tool (https://blast.ncbi.nlm.nih.gov/Blast.cgi). Additionally, a diagnostic restriction digest was performed to confirm the presence of the insert by analyzing its size.

RESULTS

Reproducing the SCRIB-SnoN interaction

We previously determined that SnoN and SCRIB colocalize at the basolateral membrane using MCF10A cells (Zhu et al., 2016). Co-immunoprecipitation experiments were conducted to reproduce the SCRIB-SnoN interaction. In these experiments, FLAG-tagged SnoN was overexpressed in cells and served as bait to pull down SCRIB.

Verification of gene inserts

The experiments commenced with the identification of genes of interest within expression vectors using Sanger sequencing. Genes were sequenced from the plasmid pCMV5b-FLAG with the primer 5'-CGCAAATGGGCGGTAGGCGTG-3'. The resulting sequences of SnoN (**Fig. 2.1A**) and the truncated SnoN mutants (**Figs. S2.1A** and **S2.1B**) were compared to sequences in the NCBI database using the Nucleotide BLAST tool to identify sequences with nearly 100% identity. Each sequence of interest consistently aligned with the same top match: the Homo sapiens SKI-like proto-oncogene (**Fig. 2.1B**). The Ski oncogene, which was crucial in the initial discovery of the Sno gene (Ski novel gene), was identified due to their close homology. The next best alignment hit was the human Sno oncogene mRNA, which corresponds to the SnoN protein and is ski-related.

The presence of the target genes in the vectors was confirmed by analyzing the sizes of the DNA fragments. Virtual digests, performed using APE, revealed the expected fragment sizes after digestion with SalI and XbaI. The vector pCMV5b-FLAG-SnoN produced a fragment measuring 2058 bp (**Fig. 2.2A**). The vector pCMV5b-FLAG-SnoN(1-366) resulted in a fragment of 1104 bp, while pCMV5b-FLAG-SnoN(367-684) yielded a fragment of 966 bp (**Fig. 2.2A**). Actual double restriction digests with SalI and XbaI further validated that the expression vectors contained the desired sequences (**Fig. 2.2B**). These vectors were subsequently used in transfection experiments.

A.

NNNNNNNNNNNNGCNGANCTCGTTTAGTGAACCGTCAGAATTGATCTGGTACCAC
GCGTATCGATACCATGGACTACAAGGACGACGATGACAAGGGTCGACAAGAAAACC
TCCAGACAAATTTCTCCTTGGTTCAGGGCTCAACTAAAAAACTGAATGGGATGGGAG
ATGATGGCAGCCCCCCAGCGAAAAAAATGATAACGGACATTCATGCAAATGGAAAA
ACGATAAACAAGGTGCCAACAGTTAAGAAGGAACACTTGGATGACTATGGAGAAGC
ACCAGTGGAAACTGATGGAGAGCATGTTAAGCGAACCTGTACTTCTGTTCCTGAAAC
TTTGCATTTAAATCCCAGTTTGAAACACACATTGGCACAATTCCATTTAAGTAGTCA
GAGCTCGCTGGGTGGACCAGCAGCATTTTCTGCTCGGCATTCCCAAGAAAGCATGTC
GCCTACTGTATTTCTGCCTCTTCCATCACCTCAGGTTCTTCCTGGCCCATTGCTCATC
CCTTCAGATAGCTCCACAGAACTCACTCAGACTGTGTTGGAAGGGGAATCTATTTCT
TGTTTTCAAGTTGGAGGAGAAAAGAGACTCTGTTTGCCCCAAGTCTTAAATTCTGTT
CTCCGAGAATTTACACTCCAGCAAATAAATACAGTGTGTGATGAACTGTACATATAT
TGTTCAAGGTGTACTTCAGACCAGCTTCATATCTTAAAGGTACTGGGCATACTTCCA
TTCAATGCCCCATCCTGTGGGCTGATTACATTAACTGATGCACAAAGATTATGTAAT
GCTTTATTGCGGCCACGAACTTTTCCTCAAAATGGTAGCGTACTTCCTGCTAAAAGC
TCATTGGCCCAGTTAAAGGAAACTGGCAGTGCCTTTGAAGTGGAGCATGAATGCCTA

GGCAAATGTCAGGGTTTATTTGCACCCCAGTTTTATGTTCAGCCTGATGCTCCGTGTA
TTCAATGTCTGGAGTGTTGTGGAATGTTTGCACCCCAGACGTTTGTGATGCATTCTCA
CAGATCACCTGACAAAAGAACTTGCCACTGGGGCTTTGAATCAGCTAAATGGCATTG
CTATCTTCATGTGAACCAAAAATACTTAGGAANACCTGAANAAANNAACTGAANAN
AATTTTANNAAAATGAGGGANAANTTTAGCATGANAANNGGAANNNNAAATCAAT
CCANNNNNNATGCCCCNNCNGGAANGGAATTNNNNNCCNGGNNNCCNGTNTNNAA
NNNGGAAGGTGANNNNNTTNNNAAANNNNNNNNTTTTNNNCCCCNNNNNCCNNNN
NAANNGGGGGNAA

B.

Homo sapiens SKI like proto-oncogene (SKIL), transcript variant 1, mRNA

Sequence ID: **NM_005414.5** Length: 7155 Number of Matches: 1

Range 1: 686 to 1778

Score	Expect	Identities	Gaps	Strand	Frame
1938 bits(1049)	0.0()	1073/1093(98%)	2/1093(0%)	Plus/Plus	

```
Query  106   GAAAACCTCCAGACAAATTTCTCCTTGGTTCAGGGCTCAACTAAAAAACTGAATGGGATG  165
             ||||||||||||||||||||||||||||||||||||||||||||||||||||||||||||
Sbjct  686   GAAAACCTCCAGACAAATTTCTCCTTGGTTCAGGGCTCAACTAAAAAACTGAATGGGATG  745

Query  166   GGAGATGATGGCAGCCCCCCAGCGaaaaaaaTGATAACGGACATTCATGCAAATGGAAAA  225
             ||||||||||||||||||||||||||||||||||||||||||||||||||||||||||||
Sbjct  746   GGAGATGATGGCAGCCCCCCAGCGAAAAAAATGATAACGGACATTCATGCAAATGGAAAA  805

Query  226   ACGATAAACAAGGTGCCAACAGTTAAGAAGGAACACTTGGATGACTATGGAGAAGCACCA  285
             ||||||||||||||||||||||||||||||||||||||||||||||||||||||||||||
Sbjct  806   ACGATAAACAAGGTGCCAACAGTTAAGAAGGAACACTTGGATGACTATGGAGAAGCACCA  865

Query  286   GTGGAAACTGATGGAGAGCATGTTAAGCGAACCTGTACTTCTGTTCCTGAAACTTTGCAT  345
             ||||||||||||||||||||||||||||||||||||||||||||||||||||||||||||
Sbjct  866   GTGGAAACTGATGGAGAGCATGTTAAGCGAACCTGTACTTCTGTTCCTGAAACTTTGCAT  925

Query  346   TTAAATCCCAGTTTGAAACACACATTGGCACAATTCCATTTAAGTAGTCAGAGCTCGCTG  405
             ||||||||||||||||||||||||||||||||||||||||||||||||||||||||||||
Sbjct  926   TTAAATCCCAGTTTGAAACACACATTGGCACAATTCCATTTAAGTAGTCAGAGCTCGCTG  985

Query  406   GGTGGACCAGCAGCATTTTCTGCTCGGCATTCCCAAGAAAGCATGTCGCCTACTGTATTT  465
             ||||||||||||||||||||||||||||||||||||||||||||||||||||||||||||
Sbjct  986   GGTGGACCAGCAGCATTTTCTGCTCGGCATTCCCAAGAAAGCATGTCGCCTACTGTATTT  1045

Query  466   CTGCCTCTTCCATCACCTCAGGTTCTTCCTGGCCCATTGCTCATCCCTTCAGATAGCTCC  525
             ||||||||||||||||||||||||||||||||||||||||||||||||||||||||||||
Sbjct  1046  CTGCCTCTTCCATCACCTCAGGTTCTTCCTGGCCCATTGCTCATCCCTTCAGATAGCTCC  1105

Query  526   ACAGAACTCACTCAGACTGTGTTGGAAGGGGAATCTATTTCTTGTTTTCAAGTTGGAGGA  585
             ||||||||||||||||||||||||||||||||||||||||||||||||||||||||||||
Sbjct  1106  ACAGAACTCACTCAGACTGTGTTGGAAGGGGAATCTATTTCTTGTTTTCAAGTTGGAGGA  1165

Query  586   GAAAAGAGACTCTGTTTGCCCCAAGTCTTAAATTCTGTTCTCCGAGAATTTACACTCCAG  645
             ||||||||||||||||||||||||||||||||||||||||||||||||||||||||||||
Sbjct  1166  GAAAAGAGACTCTGTTTGCCCCAAGTCTTAAATTCTGTTCTCCGAGAATTTACACTCCAG  1225

Query  646   CAAATAAATACAGTGTGTGATGAACTGTACATATATTGTTCAAGGTGTACTTCAGACCAG  705
             ||||||||||||||||||||||||||||||||||||||||||||||||||||||||||||
Sbjct  1226  CAAATAAATACAGTGTGTGATGAACTGTACATATATTGTTCAAGGTGTACTTCAGACCAG  1285

Query  706   CTTCATATCTTAAAGGTACTGGGCATACTTCCATTCAATGCCCCATCCTGTGGGCTGATT  765
             ||||||||||||||||||||||||||||||||||||||||||||||||||||||||||||
Sbjct  1286  CTTCATATCTTAAAGGTACTGGGCATACTTCCATTCAATGCCCCATCCTGTGGGCTGATT  1345
```

```
Query   766   ACATTAACTGATGCACAAAGATTATGTAATGCTTTATTGCGGCCACGAACTTTTCCTCAA  825
              ||||||||||||||||||||||||||||||||||||||||||||||||||||||||||||
Sbjct   1346  ACATTAACTGATGCACAAAGATTATGTAATGCTTTATTGCGGCCACGAACTTTTCCTCAA  1405

Query   826   AATGGTAGCGTACTTCCTGCTAAAAGCTCATTGGCCCAGTTAAAGGAAACTGGCAGTGCC  885
              ||||||||||||||||||||||||||||||||||||||||||||||||||||||||||||
Sbjct   1406  AATGGTAGCGTACTTCCTGCTAAAAGCTCATTGGCCCAGTTAAAGGAAACTGGCAGTGCC  1465

Query   886   TTTGAAGTGGAGCATGAATGCCTAGGCAAATGTCAGGGTTTATTTGCACCCCAGTTTTAT  945
              ||||||||||||||||||||||||||||||||||||||||||||||||||||||||||||
Sbjct   1466  TTTGAAGTGGAGCATGAATGCCTAGGCAAATGTCAGGGTTTATTTGCACCCCAGTTTTAT  1525

Query   946   GTTCAGCCTGATGCTCCGTGTATTCAATGTCTGGAGTGTTGTGGAATGTTTGCACCCCAG  1005
              ||||||||||||||||||||||||||||||||||||||||||||||||||||||||||||
Sbjct   1526  GTTCAGCCTGATGCTCCGTGTATTCAATGTCTGGAGTGTTGTGGAATGTTTGCACCCCAG  1585

Query   1006  ACGTTTGTGATGCATTCTCACAGATCACCTGACAAAAGAACTTGCCACTGGGGCTTTGAA  1065
              ||||||||||||||||||||||||||||||||||||||||||||||||||||||||||||
Sbjct   1586  ACGTTTGTGATGCATTCTCACAGATCACCTGACAAAAGAACTTGCCACTGGGGCTTTGAA  1645

Query   1066  TCAGCTAAATGGCATTGCTATCTTCATGTGAACCAAAAATACTTAGGAANACCTGAANaa  1125
              |||||||||||||||||||||||||||||||||||||||||||||||| |||||||  ||
Sbjct   1646  TCAGCTAAATGGCATTGCTATCTTCATGTGAACCAAAAATACTTAGGAACACCTGAAGAA  1705

Query   1126  ann-aactgaananaattttanna-aaatgaggganaantttagcatganaannggaann  1183
              |   |||||||  |  |||||||   |  |||||| ||| || |||||||||| ||   ||||
Sbjct   1706  AAGAAACTGAAGATAATTTTAGAAGAAATGAAGGAGAAGTTTAGCATGAGAAGTGGAAAG  1765

Query   1184  nnaaaTCAATCCA  1196
                |||||||||||
Sbjct   1766  AGAAATCAATCCA  1778
```

Figure 2.1. Verification of the sequence for the SnoN gene insert in the pCMV5b-FLAG vector.
(A) The sequence of the SnoN gene fragment is presented, with unidentified bases designated as "N." (B) The alignment of the predicted SnoN nucleotide sequence (query) with the Ski homolog (subject) was performed using the NCBI Nucleotide BLAST online tool. Nucleotide numbers are shown at the right and left of each line. Matching characters in the nucleotide sequences are aligned vertically, while gaps are represented by dashes. Lowercase letters indicate low-confidence calls or masked bases, which include interspersed repeats. The GenBank/EMBL accession number for the Homo sapiens SKI-like proto-oncogene (SKIL) is NM_005414.5.

A.

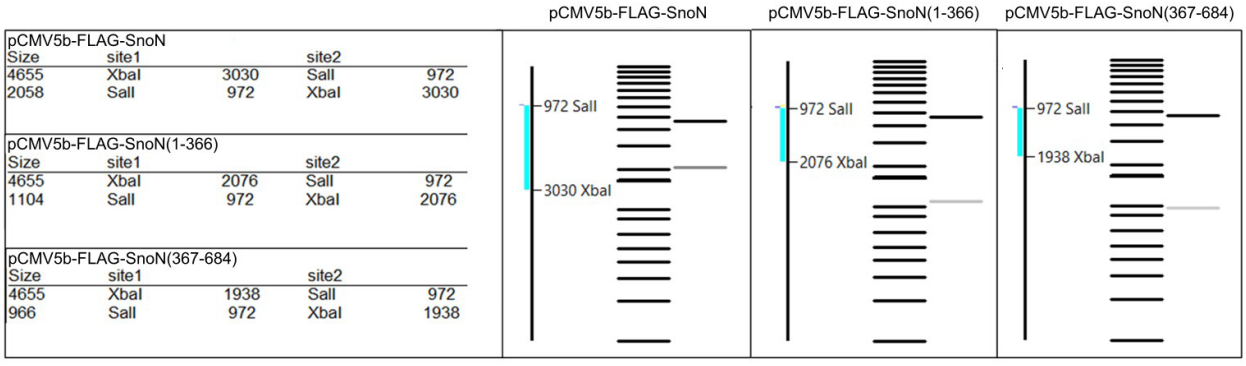

B.

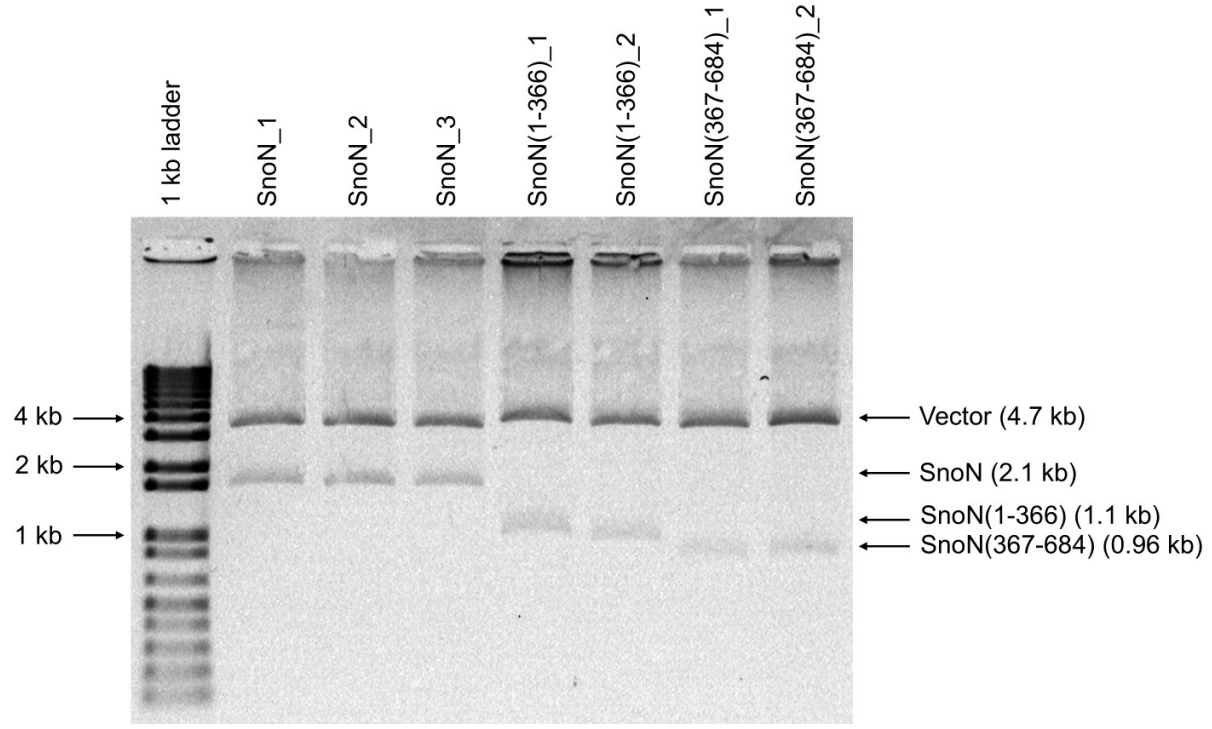

Figure 2.2. Verification of the sizes of SnoN and mutant SnoN sequences in the pCMV5b-FLAG vector. (A) Virtual digests using the enzymes SalI and XbaI produced the expected fragment sizes: SnoN = 2058 bp; SnoN(1-366) = 1104 bp; SnoN(367-684) = 957 bp; and linearized vector pCMV5b-FLAG = 4655 bp. (B) Gel electrophoresis of restriction digest products (1 kb Plus DNA Ladder from New England Biolabs). Double digests with SalI and XbaI confirmed expected fragment sizes, validating that the expression vectors contained the correct sequences.

Co-immunoprecipitation of SnoN and endogenous SCRIB

MCF10A cells were transiently transfected with FLAG-tagged SnoN (F-SnoN), and co-immunoprecipitation experiments were conducted. However, attempts to pull down endogenous SCRIB bound to SnoN were unsuccessful, as no transfection of F-SnoN was observed in any of the experiments (data not shown). This led to the conclusion that the MCF10A cells are difficult to transfect. Additionally, SnoN has a Smad binding site that, when bound by Smad3, leads to its rapid ubiquitin-dependent proteasomal degradation (Stroschein et al., 2001). Due to these challenges, the transfection experiments were conducted in 293T cells instead.

Transient transfection was performed in 293T cells using F-SnoN. Western blot analysis detected SCRIB (175 kDa), F-SnoN (77 kDa), and the loading control GAPDH (36 kDa) in both the input and pre-cleared lysates (**Fig. 2.3A**). However, immunoprecipitation yielded only minimal isolation of F-SnoN from a single lysate sample, and there was no evidence of binding between SCRIB and SnoN (**Fig. 2.3A**). This suggests that the procedures for transfecting the cells and capturing F-SnoN with associated proteins were not successful.

Interestingly, a nonspecific protein smaller than F-SnoN remained in the lysate after pre-clearing (**Fig. 2.3A**). This observation indicated that the buffer conditions were preventing the binding of proteins to the Sepharose A beads. Since this nonspecific protein was visible in every sample, including the negative control (FLAG alone), it was evident that the anti-FLAG antibody

(αFLAG) was able to bind to it.

Incubation with αFLAG-conjugated agarose beads effectively removed the nonspecific protein from the lysates while F-SnoN remained in solution (**Fig. 2.3B**). This outcome suggested that the nonspecific proteins were outcompeting F-SnoN for binding to the beads. Additionally, significant quantities of both F-SnoN and SCRIB were detected in the lysates following incubation with the αFLAG beads (**Fig. 2.3B**). Both proteins were also identified in the wash solution used to remove unbound proteins before the elution process. Since F-SnoN did not bind to the beads, co-immunoprecipitation with SCRIB was unsuccessful.

A.

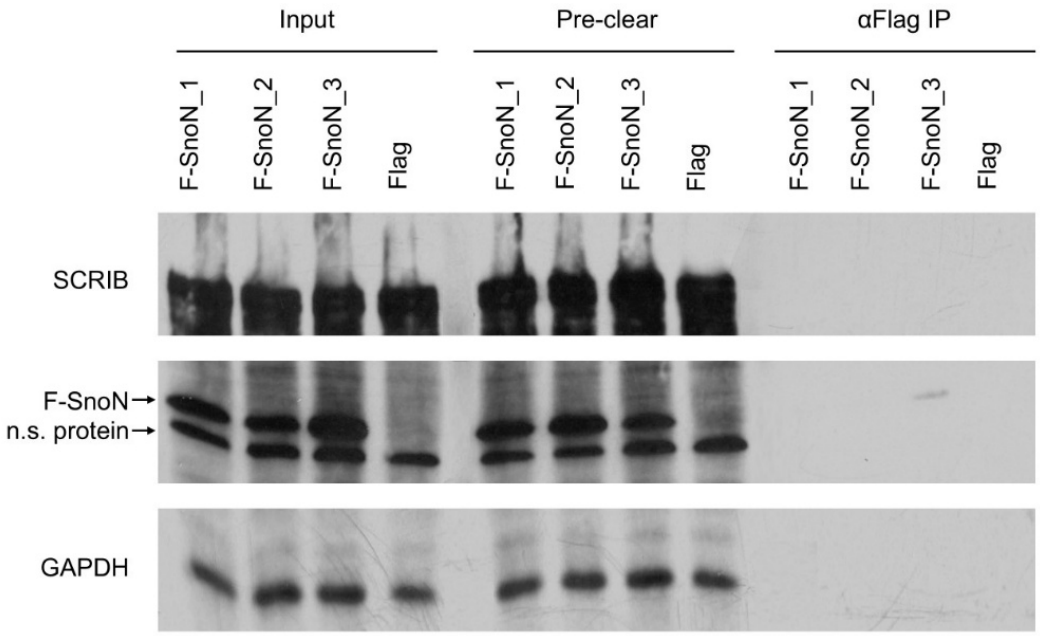

B.

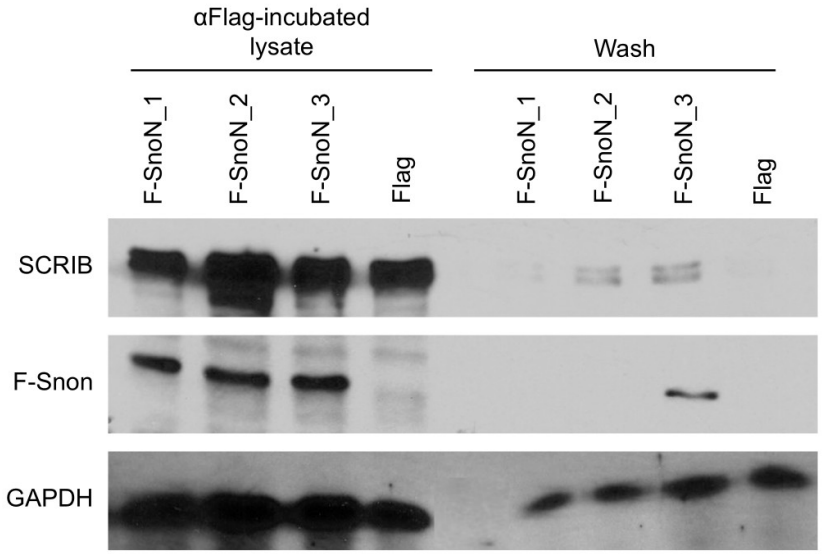

Figure 2.3. Binding competition hindered co-immunoprecipitation of SnoN and endogenous SCRIB. (A) Attempt to isolate F-SnoN by immunoprecipitation (IP) with αFLAG from 293T cells transfected with F-SnoN. Proteins were assessed through Western blotting. GAPDH was used as a loading control. A nonspecific (n.s.) protein is indicated below F-SnoN. F-SnoN was not immunoprecipitated, and SCRIB was not pulled down. (B) Both F-SnoN and SCRIB remained in the lysate following incubation with the α-FLAG beads. They were also detected in the wash solution used to eliminate unbound proteins from beads prior to elution.

Optimization of co-immunoprecipitation

In immunoprecipitation experiments, it is expected that the diluted lysate (input) will show a lower concentration of the protein of interest compared to the eluted sample, which contains a concentrated amount of that protein extracted from the lysate. This difference is visually evident, as the band representing the eluted protein appears much more intense than the band for the input sample. However, further attempts to co-immunoprecipitate SCRIB and SnoN from 293T cells consistently resulted in weak elution bands for F-SnoN, even without any evidence of binding competition from nonspecific proteins (**Fig. 2.4**). Moreover, SCRIB was not successfully pulled down in these experiments. These findings suggest that the lysis buffer may not be suitable for maintaining protein integrity or facilitating protein interactions.

For immunoprecipitation, the lysis buffer is essential for providing the appropriate ionic strength needed to disrupt cells while also maintaining optimal conditions for protein integrity. The salt concentration in the lysis buffer is crucial for the success of immunoprecipitation, as it helps maintain protein solubility and enables specific protein interactions. Low salt buffers are recommended for proteins that have weak interactions to prevent their disruption. Conversely, higher salt concentrations can help reduce nonspecific protein binding during the immunoprecipitation process.

Using freshly prepared lysis buffer creates an optimal environment for co-immunoprecipitation of proteins. The lysis buffer contains protease inhibitors that prevent protein degradation, which is crucial during cell lysis to maintain protein integrity and promote proper protein-protein interactions. It is important to avoid using old lysis buffer, as it can lead to poor affinity purification, increase background noise due to nonspecific proteins, and cause degradation of the proteins of interest due to inactive protease inhibitors.

To optimize the conditions for co-immunoprecipitation of proteins, lysis buffers with different sodium chloride (NaCl) concentrations were tested and compared: 150 mM (lysis-150) and 420 mM (lysis-420). Only freshly prepared buffer solutions were used. As shown in **Figure 2.5A**, lysis-150 resulted in less SnoN being immunoprecipitated compared to lysis-420, which is illustrated in **Figure 2.5B**. At both NaCl concentrations, the expected band intensities were observed, with eluted F-SnoN appearing strong, while F-SnoN in the lysate was faint. It is important to note that SCRIB was not captured by SnoN and remained present in the lysates after the incubation with αFLAG beads. Although F-SnoN was better purified using fresh lysis-420, these conditions did not enhance the interaction between SCRIB and SnoN.

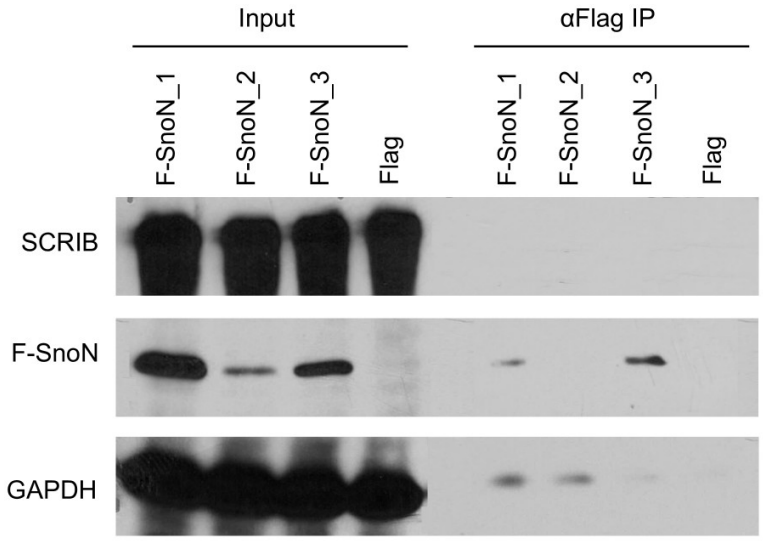

Figure 2.4. Unexpected concentrations of eluted proteins during co-immunoprecipitation of F-SnoN and endogenous SCRIB.
A representative co-immunoprecipitation of F-SnoN and endogenous SCRIB from 293T cells transfected with F-SnoN. Western blotting was conducted to detect SCRIB associated with F-SnoN, with GAPDH included as a loading control. The use of an αFLAG antibody to label F-SnoN resulted in less intense bands for eluted concentrated F-SnoN compared to the diluted protein in the lysate, which is unexpected.

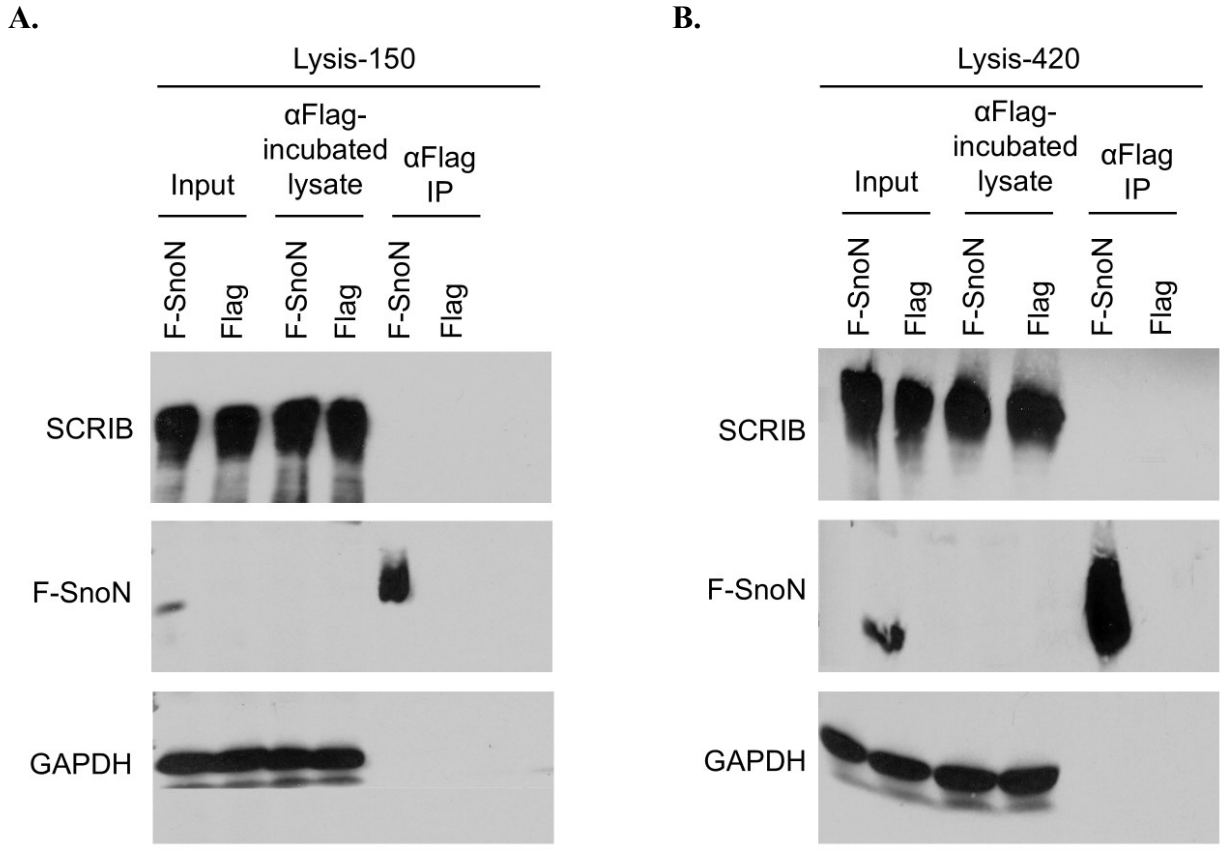

Figure 2.5. Optimization of the lysis buffer enhanced the immunoprecipitation of F-SnoN.
(A) Immunoprecipitation of F-SnoN, using αFLAG, from 293T cells that were transfected with F-SnoN to detect SCRIB associated with F-SnoN through Western blotting. A freshly prepared lysis buffer containing 150 mM NaCl was used. (B) Immunoprecipitation was also conducted with fresh lysis buffer containing 420 mM NaCl. GAPDH served as a loading control for the experiments.

Identifying the region of SnoN that interacts with SCRIB

To identify the specific region of SnoN that binds to SCRIB, co-immunoprecipitation experiments were performed using the truncated mutants: SnoN(1-366) and SnoN(367-684). HA-tagged Smad4, which is known to bind SnoN, was used as a positive control in experiments, while the FLAG tag alone served as a negative control.

Co-immunoprecipitation of truncated SnoN and endogenous SCRIB

293T cells were transiently transfected with FLAG-tagged full-length SnoN or its truncation mutants, SnoN(1-366) and SnoN(367-684), both also FLAG-tagged, to assess their interaction with endogenous SCRIB through co-immunoprecipitation. Western blot analysis showed the presence of SCRIB (175 kDa), F-SnoN (77 kDa), F-SnoN(1-366) (41 kDa), F-SnoN(367-684) (36 kDa), and the loading control GAPDH (36 kDa) in the lysates (**Fig. 2.6**). However, similar to previous experiments, attempts to pull down endogenous SCRIB were unsuccessful, even after multiple optimization efforts.

Co-immunoprecipitation after co-transfection

Due to difficulties in co-immunoprecipitating SnoN and its truncation mutants with endogenous SCRIB, co-transfections were performed to overexpress the SnoN variants and SCRIB. 293T cells were co-transfected with the pCMV5b-FLAG containing SnoN or a truncation mutant, along with the pTagBFP-N-SCRIB vector. After verifying the sequence and fragment size of the Smad4 gene insert in pCMV5b-FLAG (**Fig. S2.2**), it was co-transfected with SnoN to serve as a positive control for SnoN binding. The pCMV5b-FLAG vector was included as a negative control.

Prior to co-immunoprecipitation experiments, the SCRIB gene was sequenced from the pTagBFP-N-SCRIB plasmid with the primer, 5'-ATGCTCAAGTGCATCCCG SCRIB-3'. The SCRIB sequence (**Fig. S2.3A**) matched the Homo sapiens scribble (SCRIB) mRNA, complete CDS (**Fig. S2.3B**). To further verify the SCRIB gene insert, a double restriction digest was performed using EcoRI and BamHI. The expected fragment sizes of SCRIB (4897 bp) and linearized pTagBFP-N- (4700 bp) were determined using a virtual digest and confirmed with actual digestion (**Fig. 2.7**). Due to the similarity in size, one band appears between 4 and 5 kb.

The successful co-immunoprecipitation of the positive control, Smad4 (60 kDa), along with SnoN, confirmed that the experimental conditions were effective for pulling down SnoN-bound proteins (**Fig. 2.8A**). However, despite overexpressing the relevant genes and using an improved lysis buffer, SCRIB could not be co-immunoprecipitated with SnoN or its truncation mutants (**Fig. 2.8B**). This raised concerns regarding the integrity of the pTagBFP-N-SCRIB vector, as the αSCRIB antibody detected nonspecific proteins during Western blotting. The labeling with the αSCRIB consistently produced bands that were not only extremely intense but also extended unusually far below the 180 kDa protein size marker used to identify SCRIB. For these reasons, it was decided to construct new SCRIB expression vectors.

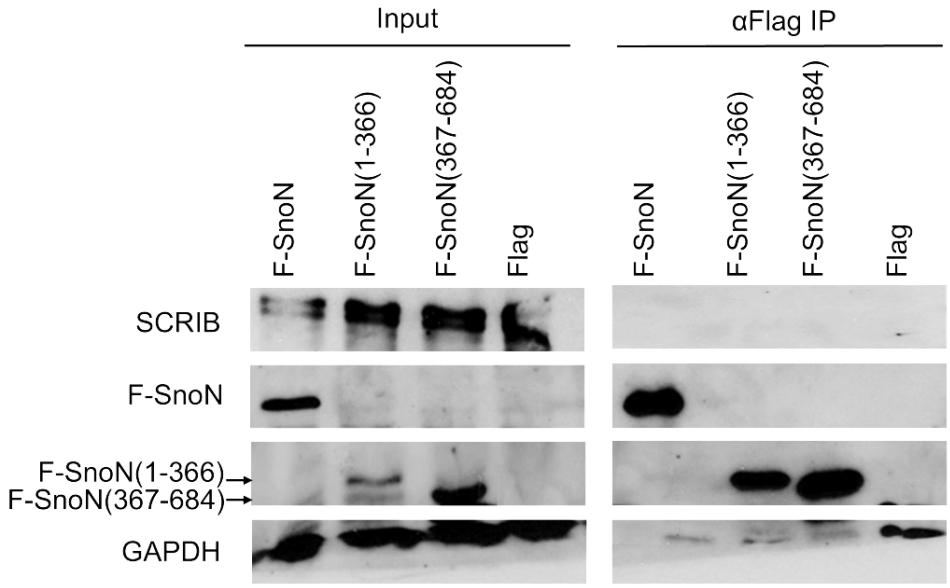

Figure 2.6. Efforts to co-immunoprecipitate truncation mutants of SnoN with endogenous SCRIB.
Immunoprecipitation of F-SnoN, F-SnoN(1-366), and F-SnoN(367-684) was conducted using αFLAG with 293T cells transfected with the appropriate constructs. Full-length SnoN and its truncation mutants were successfully immunoprecipitated and detected by Western blotting. Endogenous SCRIB was not pulled down.

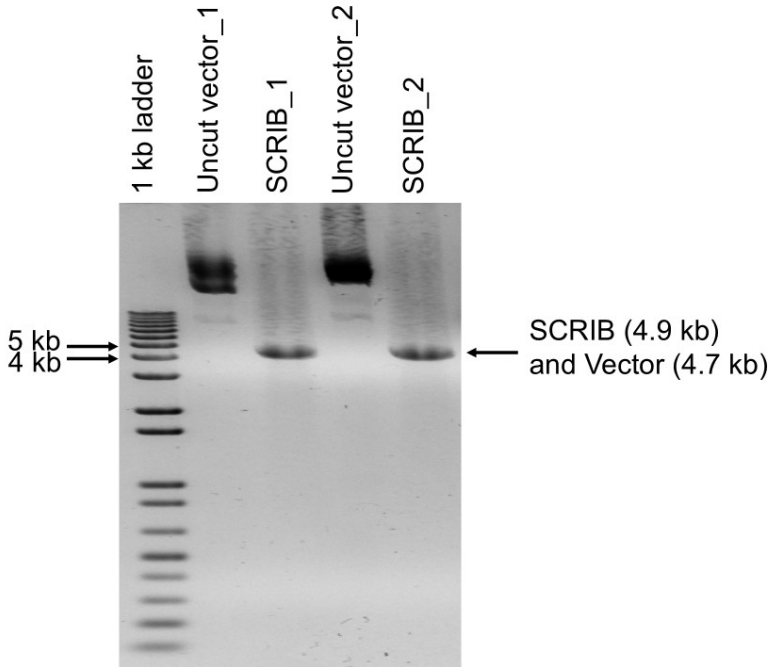

Figure 2.7. Verification of the size of SCRIB in the pTagBFP-N-SCRIB vector.
Gel electrophoresis of restriction digest products (1Kb Plus DNA Ladder from New England Biolabs). Double digests with EcoRI and BamHI confirmed the expected fragment sizes: SCRIB = 4897 bp and linearized vector pTagBFP-N- = 4700 bp, validating that the expression vector contained the correct sequence for SCRIB.

A.

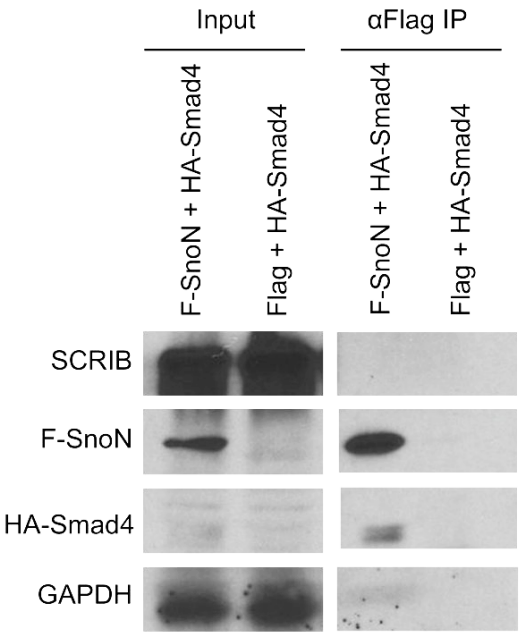
Input
αFlag IP
F-SnoN + HA-Smad4
Flag + HA-Smad4
F-SnoN + HA-Smad4
Flag + HA-Smad4
SCRIB
F-SnoN
HA-Smad4
GAPDH

B.

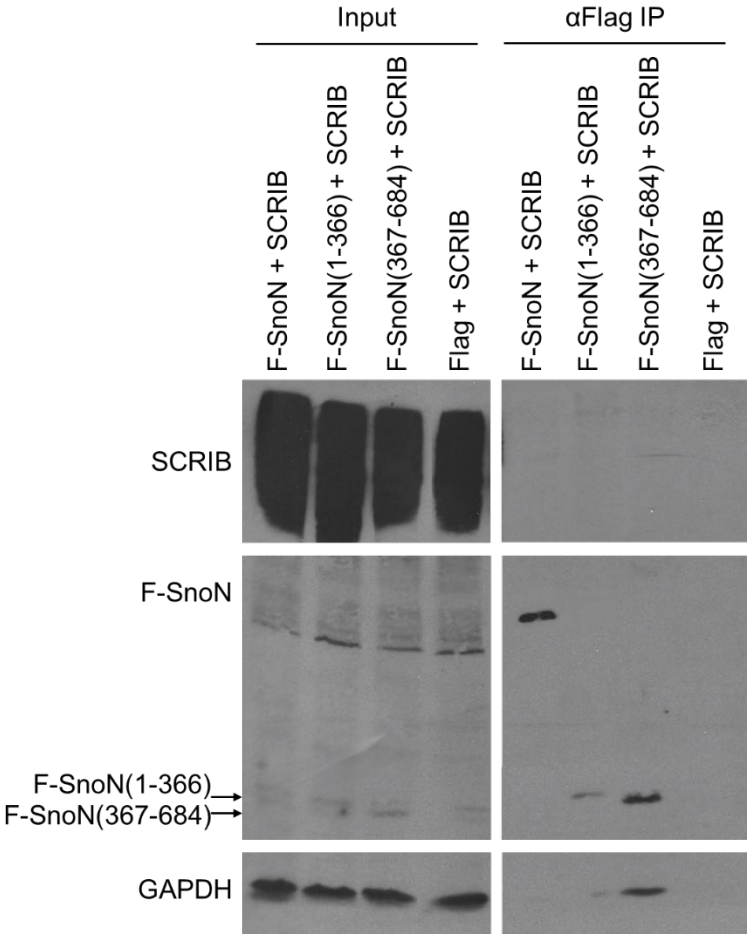
Input
αFlag IP
F-SnoN + SCRIB
F-SnoN(1-366) + SCRIB
F-SnoN(367-684) + SCRIB
Flag + SCRIB
F-SnoN + SCRIB
F-SnoN(1-366) + SCRIB
F-SnoN(367-684) + SCRIB
Flag + SCRIB
SCRIB
F-SnoN
F-SnoN(1-366)
F-SnoN(367-684)
GAPDH

Figure 2.8. Efforts to co-immunoprecipitate F-SnoN and SCRIB from co-transfected cells.
(A) Co-immunoprecipitation was conducted on 293T cells that were transiently co-transfected with F-SnoN or a truncation mutant of F-SnoN alongside SCRIB. Western blotting was used to analyze the proteins, with GAPDH serving as a loading control. HA-Smad4 was co-transfected with F-SnoN as a positive control for SnoN binding, while FLAG served as a negative control. The results showed that SnoN was successfully immunoprecipitated in association with Smad4. (B) From the same cell lysate, each SnoN variant was immunoprecipitated successfully, but SCRIB was not detected as an associated protein.

Constructing SCRIB expression vectors

Plans were developed to use various techniques for constructing a functional vector that expresses SCRIB linked to either the FLAG or HA protein tag. Since the SCRIB coding sequence is quite large, consisting of 4,897 bp, the cloning process involved dividing the gene into smaller segments. PCR-based mutagenesis was utilized to clone SCRIB in two segments, while Gibson Assembly was employed to clone it in three parts into vectors containing a protein tag. Additionally, site-directed mutagenesis was attempted to insert a FLAG tag at the C-terminus of SCRIB.

To prepare for the cloning experiments, the sequence of the SCRIB insert in the MCSV-puro-SCRIB vector was verified using the sequencing primer 5'- AAAGCAGGCTTAATGCTC AAG-3'. This verification was necessary to ensure that the vector could be used as a template for different cloning techniques.

PCR-Based Mutagenesis

The goal of PCR-based mutagenesis was to create a pCMV5b-HA-SCRIB vector with the HA tag positioned at the N-terminus of SCRIB. To achieve this, the SCRIB gene was amplified in two segments from the plasmid MCSV-puro-SCRIB. The first primer set included 5' SalI and 3' SrfI cut sites, while the second primer set contained 5' SrfI and 3' XbaI cut sites to facilitate subcloning into the pCMV5b-HA vector. The primer sets designed for both segments of the SCRIB sequence were as follows:

- Forward primer 1: 5'-TCGAGTCGACTCCTCAAGTGCATCCCGCTG-3'
- Reverse primer 1: 5'-GAAGCTGCCCGGGCCGCAGGGCCTTCC-3'
- Forward primer 2: 5'-AGCTTCGCCCGGGCTGGAGTCCGTGTGG-3'
- Reverse primer 2: 5'-CTAGTCTAGACTAGGAGGGCACAGGGCC-3'

Amplicons of the SCRIB halves were verified by sequence and size. SCRIB part 1 amplicons were sequenced using sequencing primer. Expected amplicon sizes were determined through virtual analyses (**Figure 2.9A**). The first half of SCRIB, flanked by SalI and SrfI cut sites, was estimated to be 2586 bp, while the second half, flanked by SrfI and XbaI, was estimated to be 2311 bp. After performing PCR to generate the SCRIB halves, the expected amplicon sizes were confirmed using gel electrophoresis (**Figure 2.9B**). The amplicons were then gel-purified prior to cleavage of SCRIB part 1 with SalI and SrfI, and part 2 with SrfI and XbaI. Both sets of cleaved amplicons were subsequently ligated together with the pCMV5b-HA vector, which had also been cut with SalI and XbaI. This process resulted in the production of the pCMV5b-HA-SCRIB vector.

After transforming bacteria with the ligation product, no colonies were found on the selective plates. This indicated that the ligation product was not successfully generated. It was

concluded that the ligation process may have been hindered because SrfI produces blunt ends. Blunt ends are more difficult to ligate compared to sticky ends, as they lack complementary base pairs to hold the DNA fragments together. This results in a less efficient ligation process and increases the likelihood of failure. To address this issue, other restriction enzymes were examined; however, the only alternative that can generate SCRIB halves of similar lengths is Tth111I, which produces only a one-base pair overhang. Consequently, alternative cloning techniques were developed.

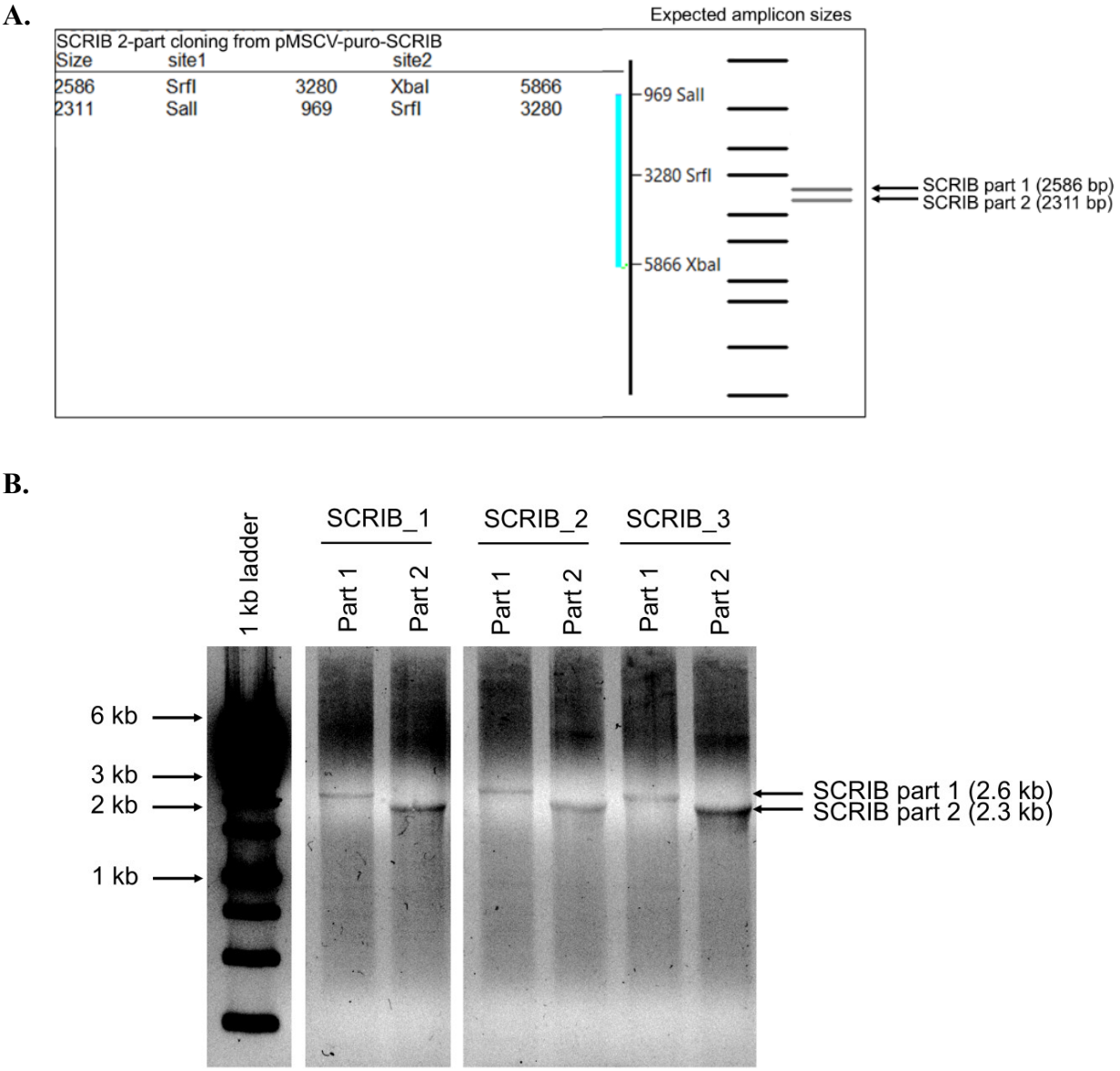

Figure 2.9. Verification of the sizes of SCRIB amplicons for two-part cloning using PCR-based mutagenesis.
(A) Virtual analysis of the amplicons of SCRIB halves using SalI and SrfI for the first half, and SrfI and XbaI for the second half, resulted in the following fragment sizes: SCRIB part 1 = 2586 bp; SCRIB part 2 = 2311 bp. (B) The fragment sizes were confirmed through gel electrophoresis of the restriction digest products. A 1

kb Plus DNA Ladder from New England Biolabs was used for size reference.

Gibson Assembly

Gibson Assembly (GA) was chosen as a cloning technique because it enables the joining of multiple DNA fragments, ranging from relatively short sequences to hundreds of kilobases, in a single, isothermal *in vitro* reaction. This method is particularly effective for creating large molecular clones from PCR products.

The objective of the GA experiments was to clone SCRIB into the pRK5m-FLAG vector, which would facilitate the attachment of a FLAG tag to the C-terminus of SCRIB. SCRIB was amplified from the MSCV-puro-SCRIB construct, incorporating BamHI and NotI restriction sites at both ends of the amplicons, along with bases that are complementary to the pRK5m-FLAG vector. This was accomplished using the forward primer 5'-TCGAGGATCCATGCT CAAGTGCATCCCGCTGTGGCGCTGC-3' and the reverse primer 5'-CTAGGCGGCCGC AGGAGGGCACAGGGCCCAGGCCACGGCG-3'. This process yielded a 5 kb SCRIB fragment, which was subsequently utilized in assembly reactions with the linearized vector (**Fig. 2.10**).

To create the linearized pRK5m-FLAG vector, the nsp7 gene sequence was cut from the pRK5m-nsp7-FLAG vector using BamHI and NotI restriction enzymes. A virtual digestion analysis predicted an expected fragment size of 4691 bp (**Fig. 2.11A**), which was later confirmed through actual digestion with BamHI and NotI (**Fig. 2.11B**). GA reactions were performed using the SCRIB fragments and the linearized pRK5m-FLAG vector to generate assemblies. These assemblies were then subjected to restriction digests to verify the fragment sizes.

Restriction digests were conducted using various enzymes on several SCRIB/pRK5m-FLAG assemblies. The results showed that many of the assemblies did not work as expected. Furthermore, reactions that produced results were not validated by digestion because the sizes of the actual digested fragments did not align with the expected sizes from virtual digestion (**Figs. 2.12** and **S2.4**). Modifications were made to the GA procedure to achieve successful assembly.

Although GA is a technique suitable for large constructs, the next attempt to build a pRK5m-FLAG-SCRIB vector involved dividing SCRIB into three fragments, close in length, for assembly with linearized pRK5m-FLAG. To amplify these three parts of SCRIB, three primer sets were designed. Primer set 1 included a BamHI restriction site for subcloning, along with nucleotides that are complementary to one end of the linearized pRK5m-FLAG vector. Primer set 2 facilitated the assembly of all three parts of SCRIB, with part 2 acting as a link between parts 1 and 3. Finally, primer set 3 had a NotI cut site and nucleotides for the assembly of SCRIB part 3 with the opposite end of the vector. The three parts of SCRIB were amplified using the following primer sets:

- Forward primer 1 : 5'-TATCGATTGAATTAAGCTTGGTGGATCCTCATGCTCAAG TGCATCCCGCTG-3'
- Reverse primer 1: 5'-CCTGTGCCTCAGCCGACGG-3'
- Forward primer 2: 5'-CCGTCGGCTGAGGCACAGG-3'
- Reverse primer 2: 5'-GGTCCCTCCGCACCAGCAG-3'
- Forward primer 3: 5'- CTGCTGGTGCGGAGGGACC -3'
- Reverse primer 3: 5'-CGTCATCGTCTTTGTAGTCCATGCGGCCGCAGGAGGGCA CAGGGCCCAGG -3'

From virtual analyses, the expected sizes of the SCRIB fragments were determined to be as follows: part 1 = 1663 bp, part 2 = 1663 bp, and part 3 = 1738 bp. Gel electrophoresis of each part yielded bands corresponding to these lengths, confirming that the correct SCRIB fragments were generated (**Fig. 12.13** and **Fig. S2.5**). Sequence alignment of each SCRIB part matched the Homo sapiens scribble (SCRIB) mRNA, complete CDS, further verifying the successful amplification of each part (**Fig. S2.6**).

GA reactions were conducted using three SCRIB fragments along with the linearized pRK5m-FLAG vector to create assemblies. Band intensities were examined on electrophoresis gels to visually assess the relative amounts and identify the optimal ratios of insert-to-vector fragments for these reactions. *E. coli* cells were directly transformed with the assembly reactions and then plated on selective media. The resulting colonies were used to initiate cultures, which were subsequently subjected to plasmid preparation. However, restriction digests performed to confirm the successful purification of a pRK5m-SCRIB-FLAG vector yielded negative results. This could be attributed to the presence of a significant number of satellite colonies on the culture plates (**Fig. 12.14**). These satellite colonies, which did not incorporate the SCRIB/pRK5m-FLAG assembly, may have been mistakenly selected. This issue, combined with low transformation efficiency, likely contributed to missed transformants and the negative results observed.

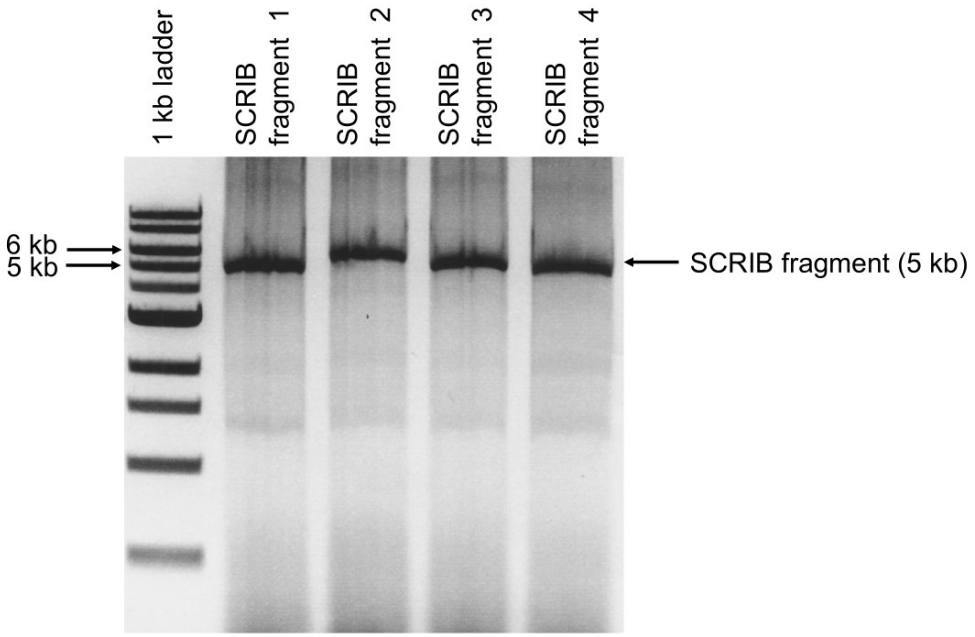

Figure 2.10. SCRIB fragment amplified for Gibson assembly.
Gel electrophoresis confirmed the successful production of 5 kb SCRIB fragments for assembly. The fragments contained BamHI and NotI cut sites, as well as nucleotides complementary to the linearized pRK5m-FLAG vector at their ends. The 1 kb Plus DNA Ladder used in this process was obtained from New England Biolabs.

A.

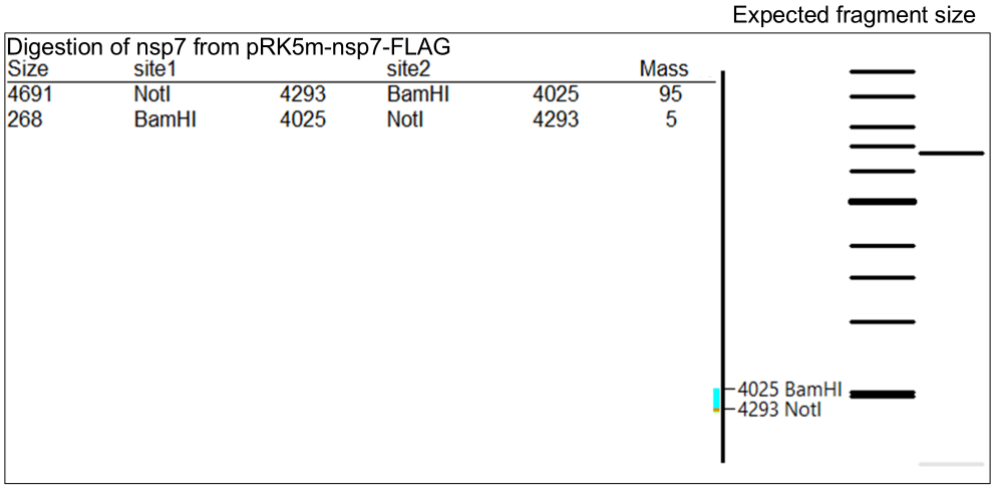

B.

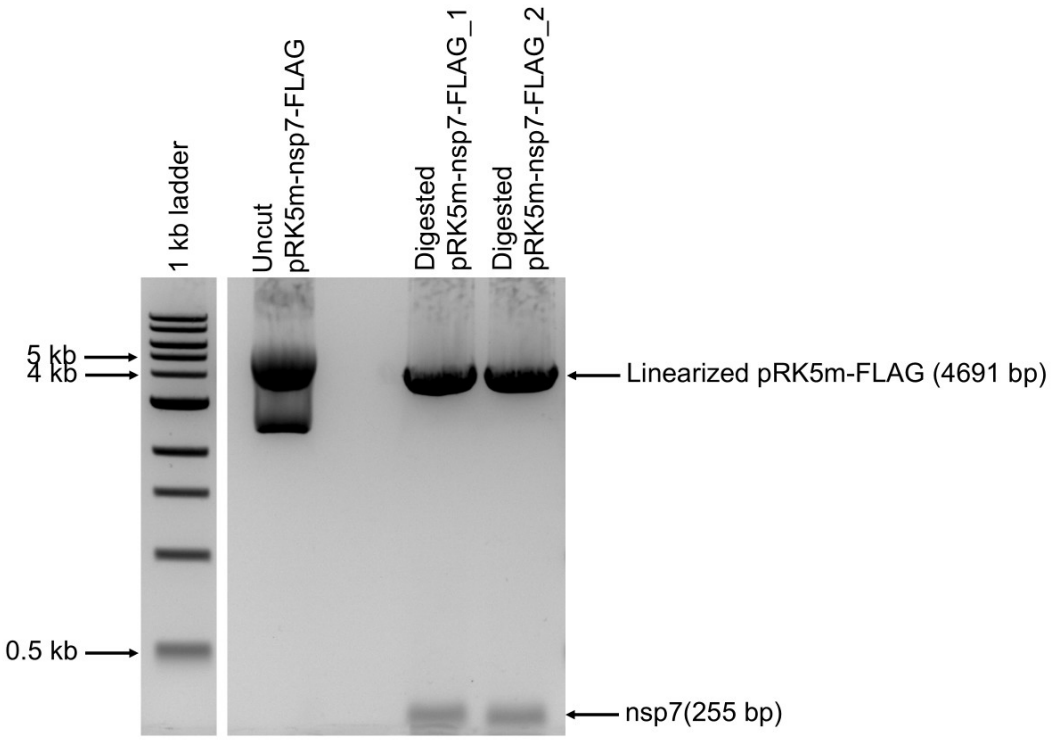

Figure 2.11. pRK5m-nsp7-FLAG digested to produce linearized pRK5m-FLAG for Gibson assembly. (A) A virtual digest with the enzymes BamHI and NotI provided the expected fragment size of 4691 bp for the linearized pRK5m-FLAG vector. (B) The pRK5m-nsp7-FLAG vector was double-digested with BamHI and NotI to remove the nsp7 gene sequence, thereby linearizing the vector for assembly with the SCRIB fragment. Gel electrophoresis of the restriction digest products confirmed that the expected fragment sizes were obtained, indicating the successful removal of the nsp7 gene. The 1 kb DNA Ladder used in this process was sourced from New England Biolabs.

A.

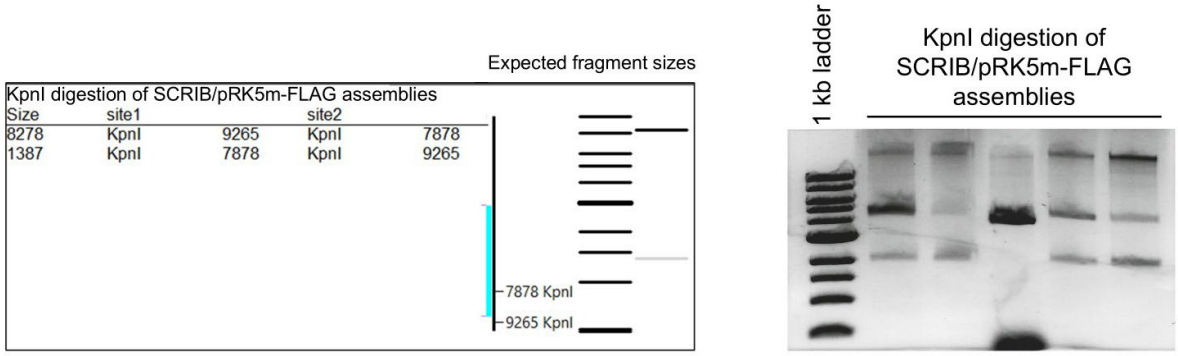

B.

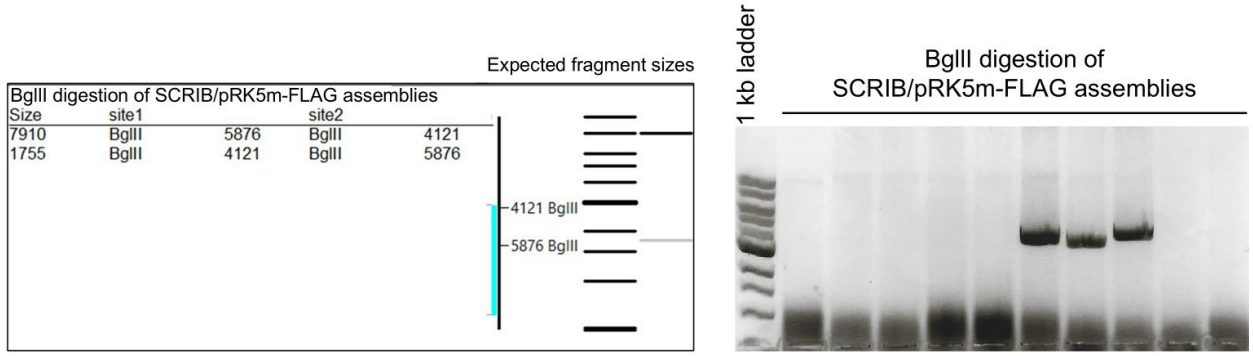

Figure 2.12. Restriction digests of SCRIB/pRK5m-FLAG assemblies to verify fragments by size. Several SCRIB/pRK5m-FLAG assemblies were digested using various restriction enzymes (digested with KpnI in 2.12A; digested with BgllI 2.12B). Gel electrophoresis of the digestion products revealed that many of the assemblies did not perform as anticipated. Additionally, reactions that yielded results were not validated through digestion, as the sizes of the actual digested fragments did not correspond with the expected sizes from virtual digestion.

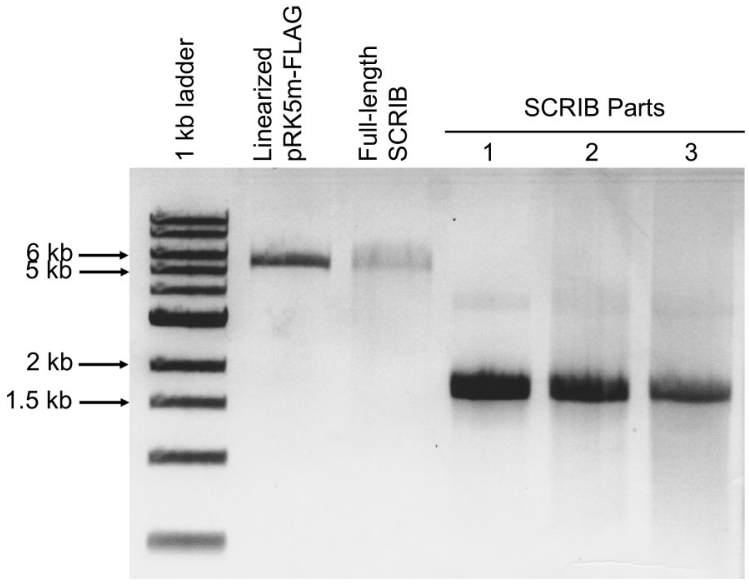

Figure 2.13. Verification of the sizes of the three SCRIB amplicons for 3-part cloning using Gibson Assembly.
Virtual analysis of the amplicons of SCRIB parts resulted in the following expected fragment sizes: SCRIB part 1 = 1663 bp; SCRIB part 2 = 1663 bp; SCRIB part 3 = 1738 bp. These fragment sizes were confirmed through gel electrophoresis of the amplicons. Full-length SCRIB and linearized pRK5m-FLAG appear as bands near 5 kb. Band intensities were analyzed to evaluate the relative amounts of fragments, which helped determine the appropriate ratios of insert to vector for assembly reactions. A 1 kb DNA Ladder from New England Biolabs was used for size reference.

Figure 2.14. Bacterial colonies were acquired after transformation with the SCRIB / pRK5m-FLAG assembly.
E. coli cells transformed with confirmed GA assemblies formed colonies. The abundance of satellite colonies may have interfered with the results, as the final restriction digest check for the pRK5m-FLAG-SCRIB produced negative results.

Site-directed mutagenesis

Site-directed mutagenesis (SDM) was performed to insert a FLAG tag at the C-terminus of SCRIB within the MCSV-puro-SCRIB vector. The following mutagenic primers were designed to include the FLAG tag sequence, a BamHI restriction site, and bases complementary to the vector: Forward primer 5'-TGGGCCCTGTGCCCTCCGACTACAAGGACGACGATGACAAGGGATCCTAGTACCCAGCTTTCTTGTAC-3' and reverse primer 5'-GTACAAGAAAGCTGGGTACTAGGATCCCTTGTCATCGTCGTCCCTTGTAGTCGGAGGGCACAGGGCCCA-3'

Although SDM was attempted multiple times, none of the experiments successfully yielded a vector containing SCRIB-FLAG.

DISCUSSION

The significant impact of basolateral polarity proteins on Hippo signaling prompted this research to investigate the relationship between the Hippo pathway and the basolateral polarity module by examining specific protein-protein interactions. SCRIB, a scaffolding protein that can assemble various multiprotein complexes, influences Hippo signaling through multiple interactions with Hippo kinases. Furthermore, at the basolateral membrane, SCRIB is crucial for regulating the activity of the Hippo effector, TAZ. SCRIB also interacts with SnoN, a protein

involved in the mutual regulation of the Hippo pathway, and that helps stabilize TAZ. Understanding the SCRIB-SnoN interaction is essential for exploring its potential as a mechanism to prevent the TAZ-induced development of cancer stem cell traits in breast tumor cells.

The research described here faced several technical challenges that impeded the experimental evaluations necessary to address the proposed questions. The procedures for transfection, co-immunoprecipitation, and cloning require optimization. Minimal yield of immunoprecipitated proteins from cell lysates suggested very low transfection efficiencies of plasmid DNA. This low efficiency may be due to several factors, including the health and viability of the cell line, the number of passages, the degree of confluency, and the quality and quantity of the nucleic acid used. To achieve long-term and consistent gene expression in mammalian cells, stable transfection is more effective than transient transfection. The best way to achieve stable gene expression in mammalian cells is through viral transduction, as this method is particularly effective for cells that are difficult to transfect using non-viral techniques.

Low transfection efficiency may have contributed to the limited quantities of immunoprecipitated bait protein observed in co-immunoprecipitation experiments. However, the quality of the lysis buffer appeared to play a significant role in affinity purification. Increasing the salt concentration improved the amount of protein extracted from lysates, but it did not enhance the co-immunoprecipitation of binding partners. Therefore, optimizing the composition of the lysis buffer is crucial for effectively purifying both the proteins of interest and their binding partners.

In addition to these technical issues, molecular obstacles may have also contributed to unsuccessful experiments. Characterizing the activity of polarity proteins in epithelial cells is challenging due to the significant impact that cell culture system organization has on gene expression and cellular behavior. The traditional two-dimensional (2D) culture system, which consists of a monolayer of cells adhered to a flat plastic dish, has been widely used for *in vitro* studies of cellular responses. However, in 2D systems, cellular processes such as proliferation, differentiation, and migration often differ from *in vivo* responses (Duval et al., 2017).

To address the limitations of traditional culture methods, three-dimensional (3D) culture environments more accurately mimic the natural in vivo requirements of cells (Duval et al., 2017). 3D systems, such as Matrigel, allow epithelial cells to demonstrate classical apical-basal polarity. In these systems, a cyst forms from a monolayer of cells that creates an inward-facing apical surface, which encloses a lumen (McCaffrey & Macara, 2011). The geometric differences between 2D and 3D cultures influence the localization and function of proteins involved in signaling pathways, resulting in greater accuracy and biological relevance in 3D cultures (McCaffrey & Macara, 2011). For example, in a 2D culture of MCF10A cells, knockdown of SCRIB does not exhibit any noticeable phenotype; however, in a 3D culture, cell polarity becomes deregulated as expected (McCaffrey & Macara, 2011). Thus, in vitro studies examining polarity proteins would benefit from being conducted in 3D culture systems, enhancing both accuracy and reproducibility.

SUPPLEMENTAL FIGURES

Figure S2.1

A.

AGCTCGTTTAGTGNNNGTCAGAATTGATCTGGTACCACGCGTATCGATACCATGGAC
TACAAGGACGACGATGACAAGGGTCGACAAGAAAACCTCCAGACAAATTTCTCCTT
GGTTCAGGGCTCAACTAAAAAACTGAATGGGATGGGAGATGATGGCAGCCCCCCAG
CGAAAAAAATGATAACGGACATTCATGCAAATGGAAAAACGATAAACAAGGTGCC
AACAGTTAAGAAGGAACACTTGGATGACTATGGAGAAGCACCAGTGGAAACTGATG
GAGAGCATGTTAAGCGAACCTGTACTTCTGTTCCTGAAACTTTGCATTTAAATCCCA
GTTTGAAACACACATTGGCACAATTCCATTTAAGTAGTCAGAGCTCGCTGGGTGGAC
CAGCAGCATTTTCTGCTCGGCATTCCCAAGAAAGCATGTCGCCTACTGTATTTCTGCC
TCTTCCATCACCTCAGGTTCTTCCTGGCCCATTGCTCATCCCTTCAGATAGCTCCACA
GAACTCACTCAGACTGTGTTGGAAGGGGAATCTATTTCTTGTTTTCAAGTTGGAGGA
GAAAAGAGACTCTGTTTGCCCCAAGTCTTAAATTCTGTTCTCCGAGAATTTACACTC
CAGCAAATAAATACAGTGTGTGATGAACTGTACATATATTGTTCAAGGTGTACTTCA
GACCAGCTTCATATCTTAAAGGTACTGGGCATACTTCCATTCAATGCCCCATCCTGT
GGGCTGATTACATTAACTGATGCACAAAGATTATGTAATGCTTTATTGCGGCCACGA
ACTTTTCCTCAAAATGGTAGCGTACTTCCTGCTAAAAGCTCATTGGCCCAGTTAAAG
GAAACTGGCAGTGCCTTTGAAGTGGAGCATGAATGCCTAGGCAAATGTCAGGGTTT
ATTTGCACCCCAGTTTTATGTTCAGCCTGATGCTCCGTGTATTCAATGTCTGGAGTGT
TGTGGAATGTTTGCACCCCAGACGTTTGTGATGCATTCTCACAGATCACCTGACAAA
AGAACTTGCCACTGGGGCTTTGAATCAGCTAAATGGCATTGCTATCTTCATGTGAAC
CAAAAATACTTAGGAACACCTGANNAAAAAAAACTGAANANAATTTTANAANAAA
NGAGGGANAANTTTAGCATGANAANNGGAAANNNAAATCAATCCAAGTAAAAACT
TNNNAACCCGGGNGGNANCCNNNNNACCCNNCCCCANNGCNNNNCNGGGCCNNGA
AATTGCNNNNCCNNNGCCCNNNNCCCTNNCCAAA

B

NNNNNNNNNNNNNNNNAGNNNAANNNNNNNTNNGNGNNNGTCNGAATTGNNNN
NGGTACCACGCGTATCGATACCATGGACTACAAGGACGACGATGACAAGGGTCGAC
AAACAGATGCACCATCAGGAATGGAATTACAGTCATGGTATCCTGTTATAAAGCAG
GAAGGTGACCATGTTTCTCAGACACATTCATTTTTACACCCCAGCTACTACTTATACA
TGTGTGATAAAGTGGTTGCCCCAAATGTGTCACTTACTTCTGCAGTATCCCAGTCTA
AAGAGCTCACAAAGACAGAGGCAAGTAAGTCCATATCAAGACAGTCGGAAAAAGC
TCACAGTAGTGGTAAACTTCAAAAAACAGTGTCTTATCCAGATGTCTCACTTGAGGA
ACAGGAGAAAATGGATTTAAAAACAAGTAGAGAATTATGTAGCCGTTTAGATGCAT
CAATCTCAAATAATTCTACAAGTAAAAGGAAATCTGAGTCTGCCACTTGCAACTTAG
TCAGAGACATAAACAAAGTGGGAATTGGCCTTGTTGCTGCCGCTTCATCTCCGCTTC
TTGTGAAAGATGTCATTTGTGAGGATGATAAGGGAAAAATCATGGAAGAAGTAATG
AGAACTTATTTAAAACAACAGGAAAAACTAAACTTGATTTTGCAAAAGAAGCAACA
ACTTCAGATGGAAGTAAAAATGTTGAGTAGTTCAAAATCTATGAAGGAACTCACTG
AAGAACAGCAGAATTTACAGAAAGAGCTTGAATCTTTGCAGAATGAACATGCTCAA

AGAATGGAAGAATTTTATGTTGAACAGAAAGACTTAGAGAAAAAATTGGAGCAGAT
AATGAAGCAAAAATGTACCTGTGACTCAAATTTAGAAAAAGACAAAGAGGCTGAAT
ATGCAGGACAGTTGGCAGAACTGAGGCAGAGATTGGACCATGCTGAGGCCGATAGG
CAAGAACTCCAAGATGAACTCAGACAGGAACGGGAAGCAAGACAGAAGTTAGAGA
TGATGATAAAAGAGCTAAAGCTGCAAATTCTGAAATCATCAAAGACTGCTAAAGAA
TAGTCTAGACCCGGGTGGCATCCCTGTGACCCCTCCCCAGTGCCTCTCCTGGCNCTG
GAAGTTGCCACTCCAGTGCCCACCAGCCTTGTCCTAANAAAATTAAGTTGCATCATT
TTGTNTGACTAGGNNCTNNNNAAANNNGGGGGGGGGGGGNGGGGNNNNNNNNNNN
NNNNNNGGGNNNNTTTGGNAAAAANNNNNNNNNNGGCNGGGGGGNNNNNNGGGA
ANNNNNNNGNNNNNNNANGGGNNAATNNNNNGNNNNNNGAANTTCC

Figure. S2.1, related to Figure 2.1. The sequences of the mutant SnoN gene inserts in the pCMV5b-FLAG vector.
(A) Sequence of the mutant SnoN(1-366) gene fragment. (B) Sequence of the mutant SnoN(367-684) gene fragment. In both sequences, unidentified bases are designated N.

Figure S2.2

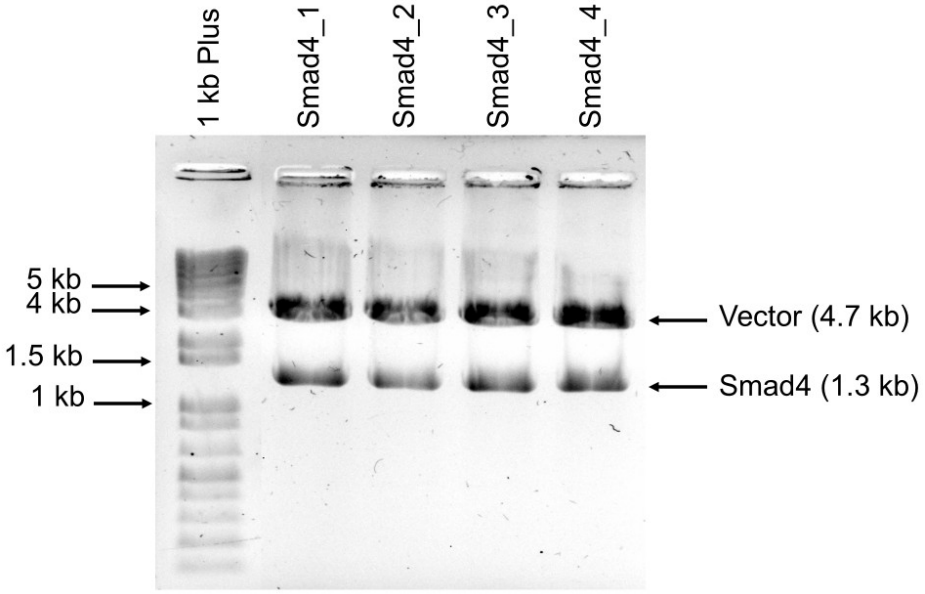

Figure S2.2, related to Figure 2.8. Verification of the size of the Smad4 sequence in the pCMV5b-FLAG vector.
Gel electrophoresis of restriction digest products (1 kb Plus DNA Ladder from New England Biolabs). Double digests with SalI and XbaI confirmed expected fragment sizes: Smad4 = 1300 bp and pCMV5b-FLAG = 4655 bp, validating that expression vectors contained the correct sequences.

Figure S2.3

A.

NNNNNNNNNNNNNNNAGNNNANCTGGTTTAGTGAACCGTCAGATCCGCTAGCGCT
ACCGGACTCAGATCTCGAGCTCAAGCTTCGAATTCATGCTCAAGTGCATCCCGCTGTG
GCGCTGCAACCGGCACGTGGAGTCGGTGGACAAGCGGCACTGTTCGCTGCAGGCCG
TGCCGGAGGAGATCTACCGCTACAGCCGCAGCCTGGAGGAGCTGCTGCTCGACGCCA
ACCAGCTGCGCGAGCTGCCCAAGCCTTTTTTCCGGCTGCTGAACTTGCGCAAGCTGG
GCCTGAGCGACAACGAGATCCAGCGGTTGCCTCCCGAGGTGGCCAACTTCATGCAGC
TGGTGGAGCTGGACGTGTCCCGGAACGATATCCCTGAGATCCCGGAGAGCATCAAGT
TCTGCAAGGCTCTGGAGATCGCGGACTTCAGTGGGAACCCCCTCTCCAGGCTCCCTG
ATGGCTTCACTCAGCTGCGCAGCCTGGCTCACCTGGCCCTGAATGATGTGTCTCTGCA
GGCACTGCCCGGGGACGTGGGCAACCTCGCCAACCTGGTGACCCTGGAGCTCCGGG
AGAACCTGCTCAAGTCCCTGCCAGCGTCCCTGTCATTTCTGGTCAAGCTGGAACAGC
TGGATCTGGGAGGCAACGATCTGGAAGTGCTGCCAGACACTCTGGGGGCTCTGCCCA
ATCTTCGGGAGCTGTGGCTTGACCGGAACCAGCTGTCAGCACTGCCCCCGGAGCTCG
GGAACCTGCGGCGCCTGGTGTGCCTGGACGTGTCGGAAAACCGGCTGGAGGAGCTG
CCTGCTGAGCTCGGCGGGCTGGTGCTGCTCACTGACCTGCTGCTGTCCCAGAACCTG
CTGCGGAGGCTGCCCGACGGCATCGGTCAGCTGAAGCAGCTATCCATCCTAAAGGTA
GACCAGAATCGGCTGTGCGAGGTGACTGAGGCCATCGGGGACTGTGAGAACCTCTCT
GAGCTGATCCTCACGGANAACCTGCTGATGGCCCTGCCCCGCTCCCTGGGAAAGCTG
ACTAAGCTGACCAACCTCAACGTGGACCGGAACCNCCTCGAGGCGCTGCCNCCCGN
NATCGGGGGCTGNNTGGCACTCNGCGTCCTNNNCTTGAGGGANAACCGCCTGGCCG
TCTGNCACANNNCTGGCCNNNCGANAAANCTGNNNGTGCTGGANNNGGCGGGGAA
CCCCTGCAANTNNGCGTTCNNNNNNCCNNCTCAATNNAAGGCCNNNNNCNGGNNAA
AACAGGCCACCCNNNNNNGGTTCAAAAG

B.

Homo sapiens scribble (SCRIB) mRNA, complete cds

Sequence ID: **AY062238.1** Length: 5153 Number of Matches: 1

Range 1: 9 to 1121

Score	Expect	Identities	Gaps	Strand	Frame
1919 bits(1039)	0.0()	1080/1113(97%)	4/1113(0%)	Plus/Plus	

```
Query  91   CATGCTCAAGTGCATCCCGCTGTGGCGCTGCAACCGGCACGTGGAGTCGGTGGACAAGCG  150
            ||||||||||||||||||||||||||||||||||||||||||||||||||||||||||||
Sbjct  9    CATGCTCAAGTGCATCCCGCTGTGGCGCTGCAACCGGCACGTGGAGTCGGTGGACAAGCG  68

Query  151  GCACTGTTCGCTGCAGGCCGTGCCGGAGGAGATCTACCGCTACAGCCGCAGCCTGGAGGA  210
            ||||||||||||||||||||||||||||||||||||||||||||||||||||||||||||
Sbjct  69   GCACTGTTCGCTGCAGGCCGTGCCGGAGGAGATCTACCGCTACAGCCGCAGCCTGGAGGA  128
```

```
Query  211   GCTGCTGCTCGACGCCAACCAGCTGCGCGAGCTGCCCAAGCCTTTTTTCCGGCTGCTGAA  270
             ||||||||||||||||||||||||||||||||||||||||||||||||||||||||||||
Sbjct  129   GCTGCTGCTCGACGCCAACCAGCTGCGCGAGCTGCCCAAGCCTTTTTTCCGGCTGCTGAA  188

Query  271   CTTGCGCAAGCTGGGCCTGAGCGACAACGAGATCCAGCGGTTGCCTCCCGAGGTGGCCAA  330
             ||||||||||||||||||||||||||||||||||||||||||||||||||||||||||||
Sbjct  189   CTTGCGCAAGCTGGGCCTGAGCGACAACGAGATCCAGCGGTTGCCTCCCGAGGTGGCCAA  248

Query  331   CTTCATGCAGCTGGTGGAGCTGGACGTGTCCCGGAACGATATCCCTGAGATCCCGGAGAG  390
             ||||||||||||||||||||||||||||||||||||||||||||||||||||||||||||
Sbjct  249   CTTCATGCAGCTGGTGGAGCTGGACGTGTCCCGGAACGATATCCCTGAGATCCCGGAGAG  308

Query  391   CATCAAGTTCTGCAAGGCTCTGGAGATCGCGGACTTCAGTGGGAACCCCCTCTCCAGGCT  450
             |||||||||||||||||||||||||||||||||||| ||||||||||||||||||||||
Sbjct  309   CATCAAGTTCTGCAAGGCTCTGGAGATCGCGGACTTCAGCGGGAACCCCCTCTCCAGGCT  368

Query  451   CCCTGATGGCTTCACTCAGCTGCGCAGCCTGGCTCACCTGGCCCTGAATGATGTGTCTCT  510
             ||||||||||||||||||||||||||||||||||||||||||||||||||||||||||||
Sbjct  369   CCCTGATGGCTTCACTCAGCTGCGCAGCCTGGCTCACCTGGCCCTGAATGATGTGTCTCT  428

Query  511   GCAGGCACTGCCCGGGGACGTGGGCAACCTCGCCAACCTGGTGACCCTGGAGCTCCGGGA  570
             ||||||||||||||||||||||||||||||||||||||||||||||||||||||||||||
Sbjct  429   GCAGGCACTGCCCGGGGACGTGGGCAACCTCGCCAACCTGGTGACCCTGGAGCTCCGGGA  488

Query  571   GAACCTGCTCAAGTCCCTGCCAGCGTCCCTGTCATTTCTGGTCAAGCTGGAACAGCTGGA  630
             ||||||||||||||||||||||||||||||||||||||||||||||||||||||||||||
Sbjct  489   GAACCTGCTCAAGTCCCTGCCAGCGTCCCTGTCATTTCTGGTCAAGCTGGAACAGCTGGA  548

Query  631   TCTGGGAGGCAACGATCTGGAAGTGCTGCCAGACACTCTGGGGGCTCTGCCCAATCTTCG  690
             ||||||||||||||||||||||||||||||||||||||||||||||||||||||||||||
Sbjct  549   TCTGGGAGGCAACGATCTGGAAGTGCTGCCAGACACTCTGGGGGCTCTGCCCAATCTTCG  608

Query  691   GGAGCTGTGGCTTGACCGGAACCAGCTGTCAGCACTGCCCCCGGAGCTCGGGAACCTGCG  750
             ||||||||||||||||||||||||||||||||||||||||||||||||||||||||||||
Sbjct  609   GGAGCTGTGGCTTGACCGGAACCAGCTGTCAGCACTGCCCCCGGAGCTCGGGAACCTGCG  668

Query  751   GCGCCTGGTGTGCCTGGACGTGTCGGAAAACCGGCTGGAGGAGCTGCCTGCTGAGCTCGG  810
             ||||||||||||||||||||||||||||||||||||||||||||||||||||||||||||
Sbjct  669   GCGCCTGGTGTGCCTGGACGTGTCGGAAAACCGGCTGGAGGAGCTGCCTGCTGAGCTCGG  728

Query  811   CGGGCTGGTGCTGCTCACTGACCTGCTGCTGTCCCAGAACCTGCTGCGGAGGCTGCCCGA  870
             ||||||||||||||||||||||||||||||||||||||||||||||||||||||||||||
Sbjct  729   CGGGCTGGTGCTGCTCACTGACCTGCTGCTGTCCCAGAACCTGCTGCGGAGGCTGCCCGA  788

Query  871   CGGCATCGGTCAGCTGAAGCAGCTATCCATCCTAAAGGTAGACCAGAATCGGCTGTGCGA  930
             ||||||||||||||||||||||||||||||||||||||||||||||||||||||||||||
Sbjct  789   CGGCATCGGTCAGCTGAAGCAGCTATCCATCCTAAAGGTAGACCAGAATCGGCTGTGCGA  848

Query  931   GGTGACTGAGGCCATCGGGGACTGTGAGAACCTCTCTGAGCTGATCCTCACGGANAACCT  990
             ||||||||||||||||||||||||||||||||||||||||||||||||||||| ||||||
Sbjct  849   GGTGACTGAGGCCATCGGGGACTGTGAGAACCTCTCTGAGCTGATCCTCACGGAGAACCT  908

Query  991   GCTGATGGCCCTGCCCCGCTCCCTGGGAAAGCTGACTAAGCTGACCAACCTCAACGTGGA  1050
             ||||||||||||||||||||||||||||||||||||||||||||||||||||||||||||
Sbjct  909   GCTGATGGCCCTGCCCCGCTCCCTGGGAAAGCTGACTAAGCTGACCAACCTCAACGTGGA  968

Query  1051  CCGGAACCNCCTCGAGGCGCTGCCNCCCGNNATCGGGGGCTGNNTGGCACTCNGCGTCCT  1110
             |||||||| |||||||||||||||| ||||  |||||||||||  |||||||| ||||||||
Sbjct  969   CCGGAACCACCTCGAGGCGCTGCCGCCCGAGATCGGGGGCTGTGTGGCACTCAGCGTCCT  1028

Query  1111  NNNCTTGAGGGANAACCGCCTGGCCGTC-TGNCA-CANNNCTGGCCNNN-CGANAAANCT  1167
               |||||||| |||||||||||||||| || || ||   ||||||    ||| | | ||
Sbjct  1029  CTCCTTGAGGGACAACCGCCTGGCCGTCCTGCCACCAGAGCTGGCCCACACGACAGAGCT  1088

Query  1168  GNNNGTGCTGGANNNGGCGGGGAACC-CCTGCA  1199
              |   ||||||||   |||||||||| |||||||
Sbjct  1089  GCACGTGCTGGACGTGGCGGGGAACCGCCTGCA  1121
```

Figure S2.3, related to Figure 2.7. Verification of the sequence for the SCRIB gene insert in the pTagBFP-N-SCRIB vector.
(A) The sequence of the SCRIB gene fragment, with unidentified bases designated as "N." (B) The alignment of the predicted SCRIB nucleotide sequence (query) with the Homo sapiens scribble (SCRIB) mRNA, complete CDS (subject) was performed using the NCBI Nucleotide BLAST online tool. Nucleotide numbers are shown at the right and left of each line. Matching characters in the nucleotide sequences are aligned vertically, while gaps are represented by dashes. Lowercase letters indicate low-confidence calls or masked bases, which include interspersed repeats. The sequence ID for the Homo sapiens scribble (SCRIB) mRNA, complete CDS is AY062238.1.

Figure S2.4

A.

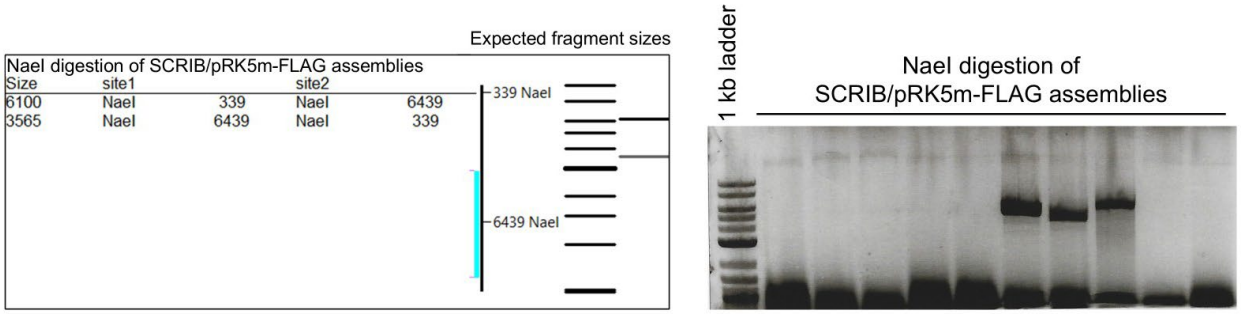

B.

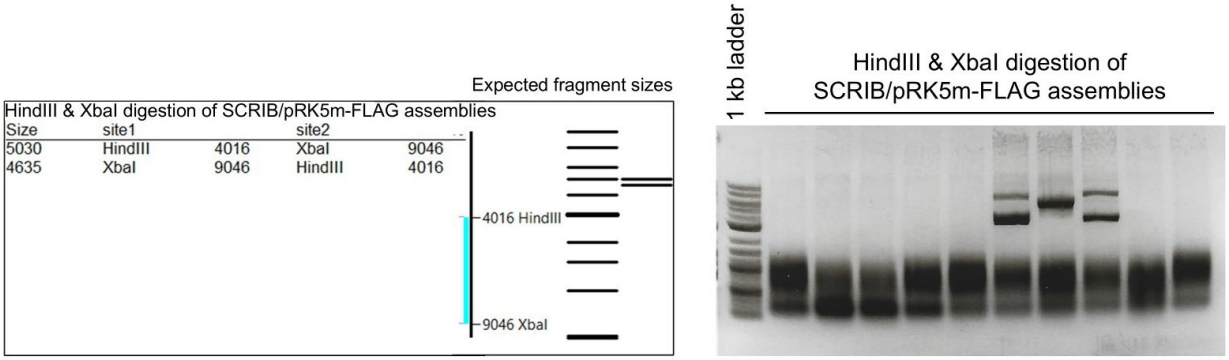

Figure S2.4, related to figure 2.12. Restriction digests of SCRIB/pRK5m-FLAG assemblies to verify fragments by size.
Several SCRIB/pRK5m-FLAG assemblies were digested using various restriction enzymes (digested with NaeI in S2.4A; digested with HindIII and XbaI in S2.4B). Gel electrophoresis of the digestion products revealed that many of the assemblies did not perform as anticipated. Additionally, reactions that yielded results were not validated through digestion, as the sizes of the actual digested fragments did not correspond with the expected sizes from virtual digestion.

Figure S2.5

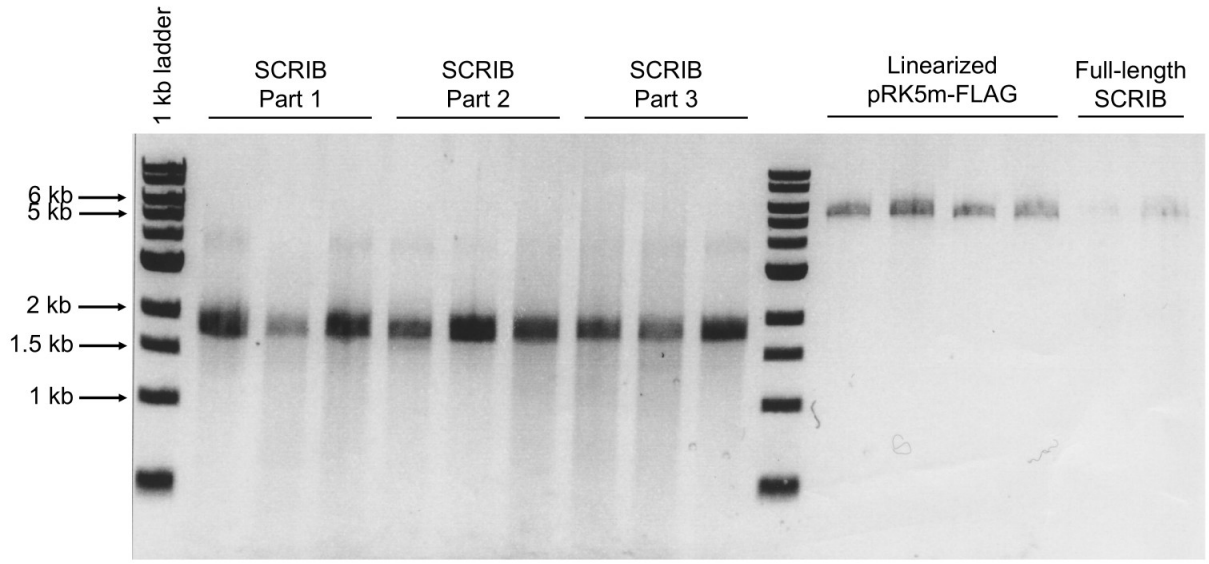

Figure S2.5, related to Figure 12.13. Verification of the sizes of the three SCRIB amplicons for 3-part cloning using Gibson Assembly.
Virtual analysis of the amplicons of SCRIB parts resulted in the following expected fragment sizes: SCRIB part 1 = 1663 bp; SCRIB part 2 = 1663 bp; SCRIB part 3 = 1738 bp. Linearized pRK5m-FLAG (4691 bp) and full-length SCRIB (4897 bp) are also shown. The fragment sizes were confirmed through gel electrophoresis of the amplicons. A 1 kb DNA Ladder from New England Biolabs was used for size reference.

Figure S2.6

A.

TTTGGCGCTGCAACCGGCACGTGGGAGTCGGTGGACAAGCGGCACTGTTCGCTGCA
GGCCGTGCCGGAGGAGATCTACCGCTACAGCCGCAGCCTGGAGGAGCTGCTGCTCG
ACGCCAACCAGCTGCGCGAGCTGCCCAAGCCTTTTTTCCGGCTGCTGAACTTGCGCA
AGCTGGGCCTGAGCGACAACGAGATCCAGCGGTTGCCTCCCGAGGTGGCCAACTTC
ATGCAGCTGGTGGAGCTGGACGTGTCCCGGAACGATATCCCTGAGATCCCGGAGAGC
ATCAAGTTCTGCAAGGCTCTGGAGNTTGCGGACTTCAGTGGGAACCCCCTCTCCAGG
CCCNNTGATGGCTGCACTCATATNNGCAGTCNNNNNNCAGCTGCCCCTNNATGCTCT
GGTATTCCNNGTACNNNNCGGCNNNNNNNGNNNNCTGCANNNNNNNGNTNNCTCGN
NNGCNNCNNNNGACGCGCTTCTTCNNTCNGAGTNNTCNNNNNGNNNGNNNGATCTN
ANNCGNNCTNCTGNNGNNNNNNNCGNNGNNNNTNNTNCNTNANNN

B.

NNNNNNNNNNNNNNNNNNNNTGANNNNGGNNNNACNNGACCTCGNNCNGGNNN
NAGCTTGGNNATCTTGAAGTGCTTTTTATAATGAGGTGTGTCCTTGCGAATNAGCCGC
TNCCTCCCGCCTGGCAGGGNCCAGGGGGCCTCAGGCTGCCCCTCCTCGATCTCCCTG
TCATCCCCGGGCAGCAGTGCGTCCTCAGAGAAATGCANNNTNNGCTCCTGGTAGTCC
TCTTCGGCGTCTTCCTCCCCGCCAGCAGTCGTGGCTTCCGNCTGGNNNCCACCCGGG
GCCCCACCCAACGNN

C.

NNNNNNNNNNNNNNNNTNNNNNNNNCCACGGCCGGCCCAAGGCCTTACGGGGCG
GCGGCTGCTGCACAGTGCCACATCTTCAGGGCCCACAGCGCCGGGTGAGGGCCTGN
NNAGANNNACCAGAGCCACTTCTCCATCCTCCTCCTGCGGGCCAGGGCTGGGAGATG
GTTCCAGGGACCTCAACTCCTCAGCAAAGTCCGGTGACAGGCGTCNCGAGGANGGT
GCATGNNCTNGGGGCCAATNTNTCTTCCACAGGGTNNCCCGGACGCTGTGGGCGCN
AGAAGANAGGGGACTNTGCCAGNTACGCTCCAGGGGCGCAAGCGTGCCCGGCCTTC
CTGGGCCCNNNNNCCNNCNNG

Figure S2.6. Verification of the sequences for the three parts of SCRIB to be assembled with the linearized pRK5m-FLAG vector.
Sequences of each SCRIB part (part 1 in S2.6A, part 2 in S2.6B, part 3 in S2.6C) matched the Homo sapiens scribble (SCRIB) mRNA, complete CDS (Sequence ID: AY062238.1), further confirming the successful amplification of each part.

Chapter 3

Identifying proteins involved in the SCRIB-SnoN interaction

SUMMARY

To inhibit the TAZ-dependent stemness of breast cancer cells, it is essential to identify any unknown proteins that may be involved in this process. The interaction between SCRIB and SnoN plays a significant role in inhibiting TAZ. Understanding how other proteins might promote or inhibit the biological functions of the SCRIB-SnoN interaction is crucial. Findings from this research could enhance our understanding of the relationship between SCRIB-dependent cell polarity, Hippo signaling, and the development of cancer stem cell-related traits in breast tumor cells.

This study aims to investigate whether specific proteins—particularly members of protein kinase families involved in Hippo signaling or those known to interact with SCRIB—contribute to the degradation of SnoN and TAZ in a SCRIB-dependent manner. This process may impact tumorigenesis. The results could identify potential targets for inhibiting the initiation and progression of TAZ-dependent mammary carcinogenesis and provide insights into the mechanisms regulating the expansion of breast cancer stem cells.

EXPERIMENTAL PROCEDURES

Cells, antibodies, and constructs

293T cells were cultured in complete medium composed of Dulbecco's Modified Eagle's Medium (DMEM) supplemented with 10% fetal bovine serum (FBS),100 U/mL penicillin, and 100 µg/mL streptomycin. The normal human mammary epithelial cell line MCF10A was maintained in DMEM/F-12 containing 5% horse serum, epidermal growth factor (EGF) at 20 ng/mL, hydrocortisone at 0.5 µg/mL, insulin at 10 µg/mL, cholera toxin at 100 ng/mL, along with penicillin and streptomycin. MCF10A-m cells, which express full-length SnoN containing a Smad binding site mutation that prevents rapid degradation, were maintained under the same conditions as MCF10A cells.

Antibodies specific for the following proteins were utilized at the indicated concentrations: SCRIB (1:4000), FLAG (1:5000), HA (1:2000), Smad4 (1:4000), and GAPDH (1:4000).

Full-length SnoN, TAZ, NDR1, NDR2, and Smad3 were expressed in pCMV5b-FLAG or pCMV5b-HA vectors. SCRIB, LGL1, LGL2, and DLG1, expressed in pcDNA3.1+/C-(K)DYK (FLAG) (GenScript), were generously provided by G. Giorgi from the Biosciences Department at Merritt College in Oakland, CA.

Transfection

Plasmid DNA was delivered to cells through the process of transfection, with a total of 5 µg of DNA introduced to each sample. For co-transfection, the concentrations of two distinct plasmid DNAs were tested to determine optimal expression levels. Cells were seeded on p60 cell culture plates at a density that would achieve 50-80% confluency after 24 hours. Transient transfection was conducted using either Lipofectamine or polyethyleneimine-based protocols.

Lipofectamine 3000 (Invitrogen) or Lipofectamine LTX & PLUS (Invitrogen) were utilized according to the manufacturer's instructions. For transfection with Lipofectamine 3000, the lipofectamine reagent was diluted 1:30 in serum-free medium. Plasmid DNA was diluted 1:50 (w/v) in a serum-free medium, along with the P3000 transfection-enhancing reagent at a ratio of 1:2 (DNA:P3000, w/v). This was then combined with the lipofectamine dilution at a 1:1

ratio.

For transfections using Lipofectamine LTX & PLUS, a 1:10 dilution of the lipofectamine reagent was prepared in serum-free medium, and the plasmid DNA was diluted 1:50 (w/v) in serum-free medium, with the PLUS reagent at a 1:1 ratio (DNA:PLUS, w/v). The diluted plasmid DNA was then mixed with the diluted Lipofectamine LTX reagent at a 1:1 ratio.

In the case of transient transfection using polyethyleneimine (PEI), the plasmid DNA was diluted 1:30 (w/v) in a serum-free medium. A 1:10 dilution of PEI in serum-free medium was combined with the diluted plasmid DNA at a 1:10 ratio (1:4, DNA:PEI, w/v). For each transfection protocol, the DNA-lipid complex was transferred to the cells, and the cells were incubated at 37°C for 48-72 hours.

Cell lysis and immunoprecipitation

Proteins were isolated from transfected cells using immunoprecipitation. The cells were lysed in either a low-salt (150 mM NaCl) or high-salt (420 mM NaCl) lysis buffer, which contained 50 mM HEPES-KOH (pH 7.8), 5 mM EDTA, 0.1% NP-40, 3 mM dithiothreitol (DTT), and 0.5 mM phenylmethylsulfonyl fluoride (PMSF).

Cell lysates were precleared to minimize non-specific binding by incubating them with 30 µL of protein A-Sepharose beads for 30 minutes at 4°C. After this, the lysates were transferred to agarose beads that were conjugated with the appropriate antibody for immunoprecipitation. To isolate FLAG- or HA-tagged proteins, beads coupled with a polyclonal antibody specific to the respective tag were utilized. Co-immunoprecipitation experiments were performed to investigate direct interactions between proteins, where one protein, bound to the agarose beads, served as the bait, while the other protein of interest acted as the prey.

Tagged proteins were eluted using either the FLAG or HA peptide in buffer D, which contains 250 mM KCl, 20 mM HEPES-KOH (pH 7.8), 0.2 mM EDTA, 0.1% NP-40, 15% glycerol, and 1 mM DTT. Alternatively, they could be eluted with 0.1 M glycine (pH 2-3). After elution, the fractions were separated and analyzed by immunoblotting.

Immunoblotting

Protein expression was analyzed using Western blotting. Total cell lysate was prepared with 4X Laemmli sample buffer and boiled at 95°C for 5 minutes. SDS-polyacrylamide gel electrophoresis (SDS-PAGE) was then employed to separate the purified proteins. Samples were loaded into a gradient gel and run at 90 V through the 4% stacking gel (comprising 30% acrylamide, 2% bisacrylamide, 2 M Tris-Cl at pH 6.8, 10% SDS, 10% ammonium persulfate, 1% TEMED, and Milli-Q H_2O) before being run at 325 V through the 10% resolving gel (comprising 30% acrylamide, 2% bisacrylamide, 2 M Tris-Cl at pH 8.8, 10% SDS, 10% ammonium persulfate, 1% TEMED, and Milli-Q H_2O) until the dye front reached the bottom.

After separation, proteins were transferred from the gel to a PVDF membrane using semi-dry electrophoretic transfer. Before blocking, protein lanes were visualized using Ponceaus S staining to evaluate transfer efficiency. The membrane was then blocked with 1% non-fat dry milk in TBST and probed with appropriate concentrations of primary antibodies specific to the proteins of interest. Following a washing step, the membrane was incubated with an HRP-conjugated secondary antibody that reacted with the primary antibody. The proteins of interest were detected via a luminol-based chemiluminescent reaction catalyzed by the HRP enzyme. The resulting light signal was captured using X-ray film.

Polymerase chain reaction (PCR)

PCR was utilized to amplify DNA samples for experiments involving specific sequences.

Primer design

Primers were designed to amplify target sequences. The length of each primer depended on the GC content, as indicated by the theoretical annealing temperature. The following formula was used to calculate the annealing temperature: T_a = [4(no. of GC base pairs) + 2(no. of AT base pairs)] - 5. Primers were designed to have an ideal annealing temperature between 51°C and 57°C. Oligonucleotides (50 nmol) were purchased from Thermo Fisher Scientific. Lyophilized primers were briefly spun down to ensure the powder was at the bottom of the tube. The primers were reconstituted in nuclease-free H_2O at a concentration of 50 pmol/mL and stored at -20°C.

PCR reaction

The PCR reactions were carried out in a final volume of 100 µL, which included the following components: 1X Pfu buffer, 5 mM dNTPs, 60 ng of template DNA, 50 pmol of forward primer, 50 pmol of reverse primer, 1.25 U of Pfu polymerase, and 1.5 µL of DMSO in water.

Thermocycler parameters

The thermocycler was programmed with the following conditions: 5 cycles of 94°C for 1 minute and 30 seconds; 48°C for 1 minute and 30 seconds; 72°C for 1 minute and 30 seconds. Followed by 20 cycles of 94°C for 1 minute; the appropriate primer annealing temperature (°C) for 1 minute; 72°C for 1 minute. Finally, 1 cycle at 72°C for 5 minutes and hold at 4°C. Additionally, these parameters were optimized to enhance amplification.

Phenol-chloroform extraction and ethanol precipitation

The PCR product was transferred to a 1.5 mL microcentrifuge tube for extraction. To the amplicons, 100 µL of phenol/chloroform was added and mixed by vortexing for 1 minute. The tube was then centrifuged at maximum speed for 2 minutes. The top layer was carefully transferred to a new tube, avoiding the white interface where proteins were located.

To precipitate the DNA, 10 µL of 3M sodium acetate (pH 5.2) and 300 µL of ice-cold ethanol were added, and the tube was incubated at -20°C for at least 5 minutes. After centrifuging at 4°C for 15 minutes, the liquid was carefully decanted without disturbing the pellet. Next, 500 µL of 70% ethanol was added to the tube without disturbing the pellet. The ethanol was then poured out, and the pellet was allowed to air dry. Finally, the DNA was resuspended in 20 µL of water.

DNA gel electrophoresis and purification

A standard 1% agarose gel was prepared in 1X TAE buffer, with GelRed added to achieve a final concentration of 1X. DNA samples were mixed with 6X loading dye and then loaded onto the gel for electrophoresis. After running the gel, the DNA bands were extracted using the Qiaex II Gel Extraction Kit. The purified DNA was eluted in 20 µl of 10 mM Tris·Cl (pH 8.5). The concentration of the final product was measured using a NanoDrop spectrophotometer.

Restriction digest

To prepare for cloning, the purified PCR fragment and the expression vector were subjected to double digestion using the appropriate restriction enzymes. The NEB online tools, NEBcloner and Double Digest Finder, were utilized to design the following double digest reaction: 1X NEBuffer that maximizes the activity of both enzymes, 30 U of each restriction enzyme, the total volume of the PCR product, or 5 µg of the plasmid vector, and enough nuclease-free H_2O to achieve a final volume of 30 µl. The digestion reactions were incubated for 2 hours at 37°C.

To prevent the reclosure of the linearized plasmid, 1 U of calf intestinal alkaline phosphatase (CIP) was added to the vector digest reaction for every 1 µg of a 3 kb plasmid. This CIP reaction was incubated for 45 minutes at 37°C and was subsequently stopped by heat inactivation at 80°C for 2 minutes.

The digested PCR fragment was purified using phenol/chloroform extraction followed by ethanol precipitation, then resuspended in 20 µl of nuclease-free H_2O. The digested and CIP-treated vector DNA was purified through gel electrophoresis, extracted with the Qiaex II Gel Extraction Kit, and eluted in 20 µl of nuclease-free H_2O.

Bacterial transformation

DH5α *E. coli* cells were transformed with the ligation product to amplify the plasmid. Competent DH5α cells were thawed on ice. Then, 60 µL of the competent cells were transferred to the ligation reaction and mixed by gently tapping the tube. The mixture was incubated on ice for 20 minutes. Following this, the cells underwent heat shock at 42°C for 45 seconds and were immediately placed back on ice.

Next, 900 µL of Luria broth (LB) was added, and the cells were incubated on a shaker at 37°C for 45 minutes. The bacterial cells were then centrifuged for 30 seconds in a microcentrifuge. The medium was carefully aspirated, leaving approximately 50 µL to resuspend the pellet by pipetting. The cells were spread onto an LB agar plate containing 100 µg/mL ampicillin (Amp) to select for transformants. Finally, the plate was incubated upside down for 16-20 hours at 37°C.

Plasmid purification

Single colonies of transformants were selected from the selective plate. Starter cultures were inoculated in 2 mL of LB medium supplemented with 100 mg/mL ampicillin and incubated overnight on a shaker at 37°C. The plasmid was initially isolated using the following mini-prep method:

The culture was transferred into a 1.5 mL microcentrifuge tube and centrifuged at maximum speed for 1 minute. The supernatant was discarded, and the pellet was resuspended in 100 µL of Solution I (25 mM Tris, pH 8, 50 mM glucose, and 10 mM EDTA). Next, 200 µL of fresh Solution II (0.2 M NaOH, 1% SDS) was added to the suspension, which was mixed by inverting the tube three times.

Following this, 150 µL of Solution III (composed of 6 mL of 5M KOAc, 1.15 mL of acetic acid, and 2.85 mL of H2O) was added to the tube, and the mixture was inverted gently before being placed on ice for 5 minutes. Afterward, the tube was centrifuged for 3 minutes at 4°C, and 800 µL of the supernatant was transferred to a clean tube.

To this supernatant, 480 µL of isopropanol was added and mixed thoroughly. After allowing it to sit at room temperature for 5 minutes, the tube was centrifuged for 5 minutes. The

supernatant was discarded, and the pellet was washed with 250 µL of 100% ethanol and then air-dried. Finally, the pellet was resuspended in 50 µL of TE buffer containing RNase.

The mini-prepped plasmid DNA was subjected to diagnostic digestion to confirm the presence of the expected insert size, which was analyzed by examining the fragment pattern on a gel. Cultures that contained the correct construct were then used to inoculate 100 mL overnight cultures for plasmid maxi-preps, following the Qiagen Plasmid Purification protocol.

Cycloheximide chase assay

The cycloheximide chase assay was conducted to evaluate the degradation of the target protein over time. Cycloheximide (CHX) is a small molecule that functions as a ribosome inhibitor, which helps to halt the translation of eukaryotic proteins. By inhibiting protein synthesis with CHX, the levels of intracellular protein degradation facilitated by the ubiquitin-proteasome pathway can be more clearly observed.

Cell culture and transfection

293T cells were seeded in 6-well plates at a density of 4.5×10^5 cells per well. The cells were cultured in complete medium for 24 hours prior to transient transfection using the previously described PEI protocol. The 293T cells were transfected with either FLAG-SnoN alone, FLAG-TAZ alone, or these constructs in combination with HA-NDR1, HA-NDR2, or HA-LATS2.

CHX treatment

After transfecting the cells for 48 hours, they were treated with CHX for specific time points. A 100 mg/mL stock solution of CHX was prepared by dissolving 100 mg of CHX in 1 mL of dimethyl sulfoxide (DMSO). This stock solution was then diluted in complete medium to achieve a final concentration of 100 µg/mL.

The cell medium was removed, and 1 mL of the 100 µg/mL CHX solution in the medium was added to the cells. The cells were either left untreated (0-hour time point) or treated with CHX for 4 or 8 hours.

Extracting cellular proteins

Proteins were isolated from cells that were singly transfected by using immunoprecipitation with anti-FLAG. For cells that were co-transfected, lysates were treated with anti-FLAG agarose to isolate the bait with the associated. The half-lives of the populations of proteins were evaluated using gel electrophoresis.

DNA sequencing

Sequencing was conducted to determine the order of bases in DNA samples, which were sequenced by the UC Berkeley DNA Sequencing Facility.

Primer design

The complete coding sequence (CDS) of the gene of interest was analyzed using A Plasmid Editor (APE). Sequencing primers were designed to be between 18 and 22 bases in length, to end with either G or C, and to have an annealing temperature ranging from 51°C to 57°C. Oligonucleotides (50 nmol) were purchased from Thermo Fisher Scientific.

Sequencing protocol

To sequence the plasmid DNA, 1 µg of DNA was combined with 8 pmols of primer, and nuclease-free H_2O was added to achieve a total volume of 13 µL. Sequences of interest were verified using the NCBI Nucleotide BLAST tool (https://blast.ncbi.nlm.nih.gov/Blast.cgi). Additionally, a diagnostic restriction digest was performed to confirm the presence of the insert by analyzing its size.

Immunofluorescence

293T or HeLa cells were cultured on glass cover slips, fixed, and permeabilized with 0.1% Triton X-100 for 5 minutes. They were then stained with specific antibodies and visualized using fluorescence microscopy. The following primary antibodies were used: Rabbit-anti-FLAG (1:2000) and mouse-anti-HA (1:2000). The following secondary antibodies were obtained from Invitrogen and used at a concentration of 5 µg/mL: goat-anti-rabbit Alexa Fluor 546 and goat-anti-mouse Alexa Fluor 488. Cell nuclei were identified using 4,6-diamidino-2-phenylindole (DAPI) counterstaining.

RESULTS

The role of NDR in the SCRIB-dependent regulation of the Hippo Pathway

LATS is part of the NDR/LATS family of serine/threonine kinases, which are components of the Hippo pathway. Like LATS, NDR kinases are activated through phosphorylation by MST and interact with various components of signaling pathways that regulate cell proliferation. Research shows that NDR1 represses TGF-β-dependent cell cycle arrest by preventing the phosphorylation of Smad2. (Pot et al., 2013). Notably, NDR1 has also been reported to form a complex with SnoN (Pot et al., 2013). Our group demonstrated that SnoN interacts strongly with all members of the NDR/LATS family. We also found that NDR1 and NDR2 are not necessary for the stabilization of TAZ by SnoN in the context of cancer (Zhu et al., 2016). The aim of this work was to investigate whether, under normal polarity conditions, NDR1 and NDR2 behave like LATS in promoting the degradation of SnoN and TAZ upon activation by SCRIB.

Verification of gene inserts

The experiments began with identifying the genes of interest within expression vectors using Sanger sequencing. The NDR1, NDR2, and Smad3 genes were sequenced from the plasmid pCMV5b-FLAG using the primer 5'-CGCAAATGGGCGGTAGGCGTG-3'. The SCRIB gene was sequenced from the pTagBFP-N-SCRIB plasmid with the primer 5'-ATGCTCAAGTGCATCCCGSCRIB-3'.

The resulting sequences were compared to those in the NCBI database using the Nucleotide BLAST tool to identify sequences with nearly 100% identity. Each sequence of interest consistently aligned with its expected top match. The NDR1 and NDR2 sequences (**Figs. S3.1A** and **S3.1B**) aligned with Homo sapiens serine/threonine kinase 38 (STK38) (Sequence ID: NM_007271.4) and Homo sapiens serine/threonine kinase 38 like (STK38L) (Sequence ID: NM_015000.4), respectively. The SCRIB sequence (**Fig. S3.1C**) matched the Homo sapiens scribble (SCRIB) mRNA, complete CDS (Sequence ID: AY062238.1). A top hit for the Smad3 sequence (**Fig.S3.1D**) was Homo sapiens SMAD family member 3 (SMAD3), transcript variant 1, mRNA (Sequence ID: NM_005902.4).

The presence of the target genes in the vectors was confirmed by analyzing the sizes of

the DNA fragments. Virtual digests, conducted using APE, demonstrated the expected fragment sizes following digestion with selected enzymes. The vector pTagBFP-N-SCRIB produced a fragment measuring 4897 bp for SCRIB after digestion with EcoRI and BamHI. After digestion with SalI and XbaI, the vectors pCMV5b-FLAG-NDR1 and pCMV5b-FLAG-NDR2 yielded fragments measuring 1398 bp and 1395 bp, for NDR1 and NDR2, respectively. Actual double restriction digests further validated that the expression vectors contained the desired sequences (**Fig. 3.1**). These vectors were subsequently used in transfection experiments.

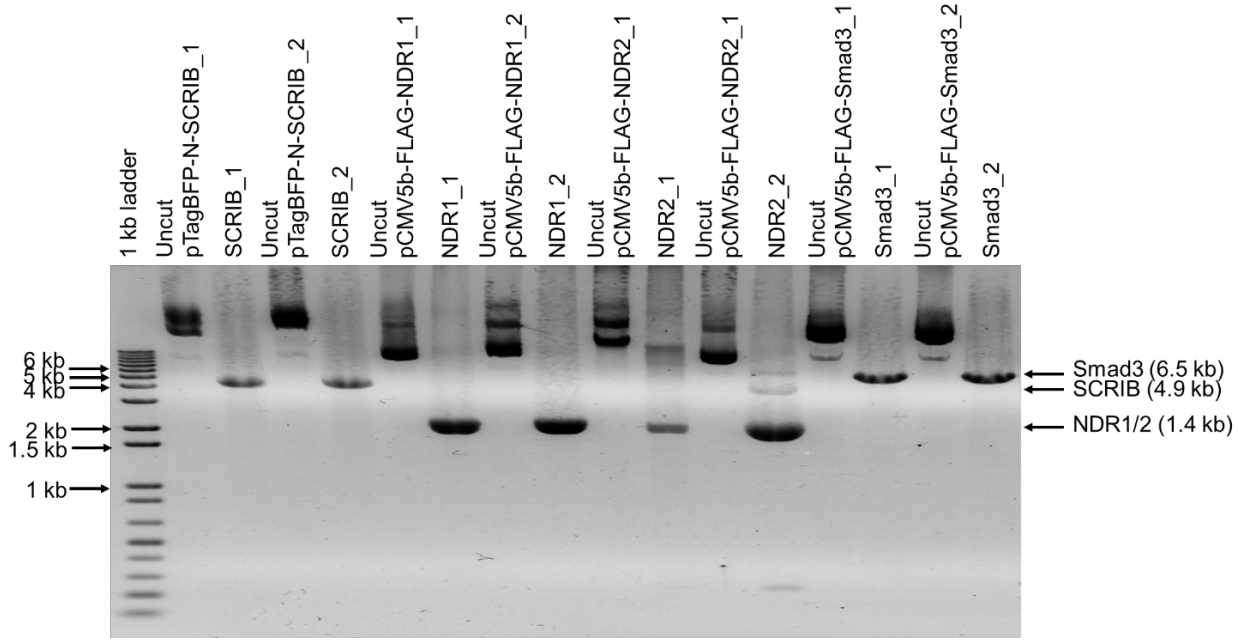

Figure 3.1. Verification of the sizes of NDR1/2 and Smad3 in pCMV5b-FLAG as well as SCRIB in the pTagBFP-N-SCRIB vector.
Gel electrophoresis of restriction digest products validating that expression vectors contained the correct gene sequences. Double digest of pTagBFP-N-SCRIB with EcoRI and BamHI confirmed the expected fragment size of SCRIB = 4897 bp. Double digest of pCMV5b-FLAG-NDR1, pCMV5b-FLAG-NDR2 with SalI and XbaI confirmed expected fragment sizes of NDR1 = 1398 bp, NDR2 = 1395 bp, and Smad3 = 6464 bp. (1 kb Plus DNA Ladder from New England Biolabs).

The impact of NDR1/2 on the stability of SnoN

To evaluate the stability of SnoN in response to NDR1 and NDR2, a Western blot analysis was conducted using 293T cells that were co-transfected with F-SnoN and either NDR1, NDR2, LATS1, LATS2, or an empty pCMV5b vector. LATS1 and LATS2 served as positive controls for SnoN degradation. As expected, the results showed a decrease in SnoN levels in the presence of LATS2. However, the findings regarding the effects of NDR1 and NDR2 on SnoN degradation were inconclusive (**Fig. 3.2**). Notably, the expression level of LATS1 was found to be nearly absent. For subsequent experiments, only LATS2 was used as the positive control. Additionally, to better visualize any degradation of SnoN, a cycloheximide chase assay was performed.

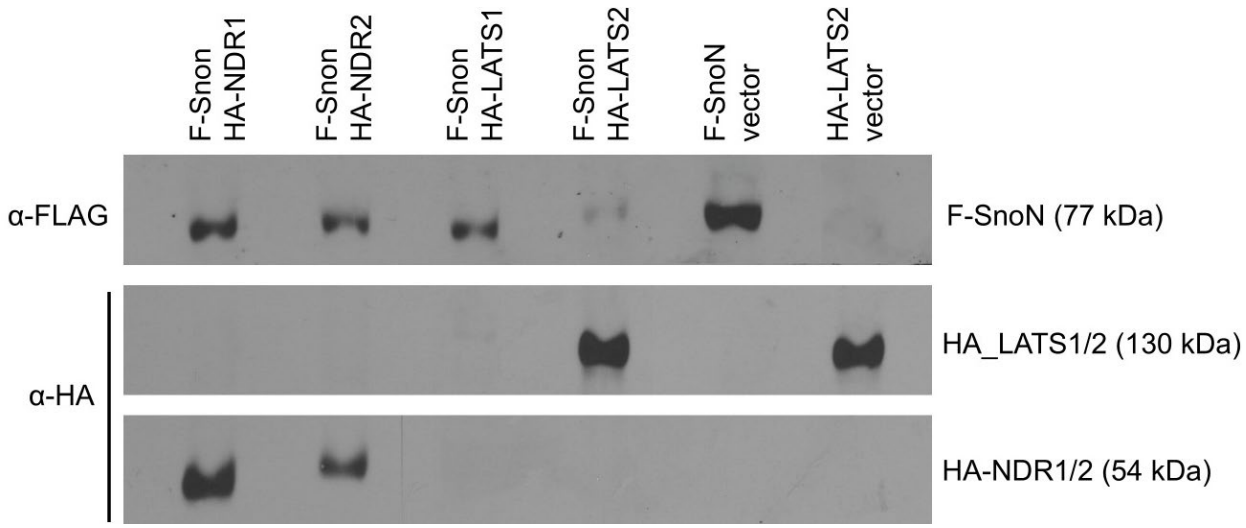

Figure 3.2. The effect of NDR1/2 on the stability of SnoN
To evaluate the stability of SnoN in response to NDR1/2, a Western blot analysis was performed using 293T cells that were co-transfected with F-SnoN and either NDR1, NDR2, LATS1, or LATS2. LATS1 and LATS2 served as positive controls for SnoN degradation. There was an expected decrease in the amount of SnoN in the presence of LATS2, but the results on whether NDR1/2 caused SnoN degradation were inconclusive. The expression level of LATS1 was minimal.

Measurement of SnoN protein degradation in response to NDR1/2

Cycloheximide chase assays are utilized to inhibit translation, which facilitates a more straightforward evaluation of protein degradation. This specific assay was performed to determine whether SnoN is degraded by NDR1 and NDR2 as it is by LATS1/2. After co-transfecting 293T cells with F-SnoN and either HA-tagged NDR1, NDR2, LATS2, or an empty pCMV5b vector, the cells were treated with cycloheximide. Reactions were terminated at the 4-hour and 8-hour marks. The proteins were then purified and analyzed using Western blotting. The results revealed that under normal polarity conditions and outside the context of cancer, NDR1, and NDR2 do not induce the degradation of SnoN (**Figs. 3.3** and **S3.2**). This finding contrasts with the activity of LATS.

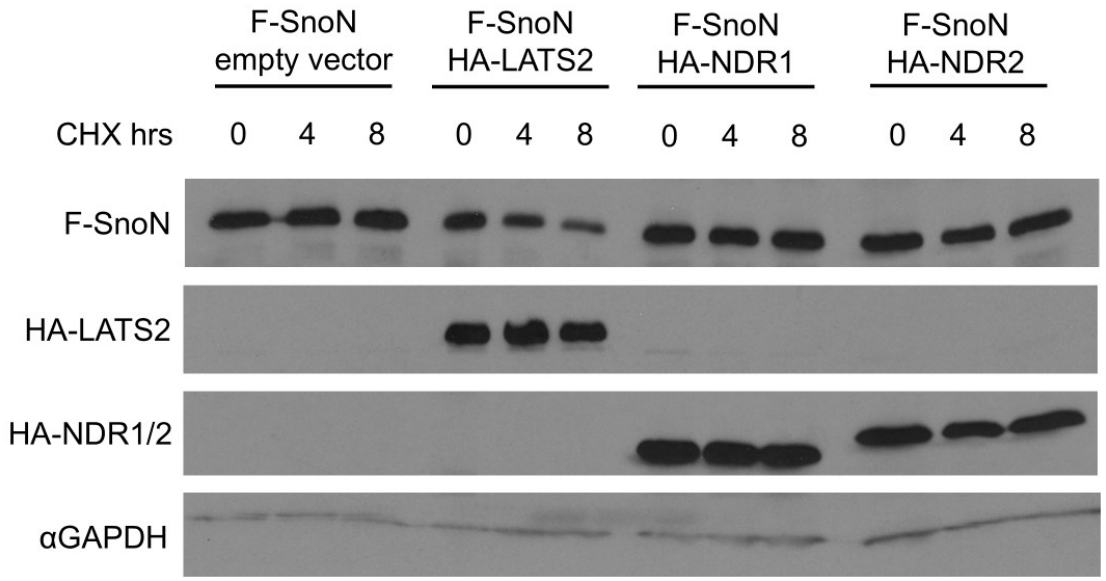

Figure 3.3. NDR1/2 does not degrade SnoN under normal polarity conditions.
293T cells were co-transfected with F- SnoN and HA-NDR1, HA-NDR2, HA-LATS2, or an empty pCMV5b vector. Cells were subsequently treated with cycloheximide for 4 hours and 8 hours. The proteins were then purified and analyzed using Western blotting. The results indicated that, unlike LATS, NDR1/2 does not lead to the degradation of SnoN outside the context of cancer.

Measurement of TAZ protein degradation in response to NDR1/2

A cycloheximide chase assay was conducted to investigate whether TAZ is degraded by NDR1 and NDR2 as it is by LATS1/2. 293T cells were co-transfected with F-TAZ and either HA-tagged NDR1, NDR2, LATS2, or an empty pCMV5b vector. Following this, the cells were treated with cycloheximide, and the reactions were terminated at the 4-hour and 8-hour marks. The proteins were then purified and analyzed using Western blotting. The results indicated that under normal polarity conditions and outside the context of cancer, neither NDR1 nor NDR2 promotes the degradation of TAZ (**Fig. 3.4**). This finding stands in contrast to the activity of LATS.

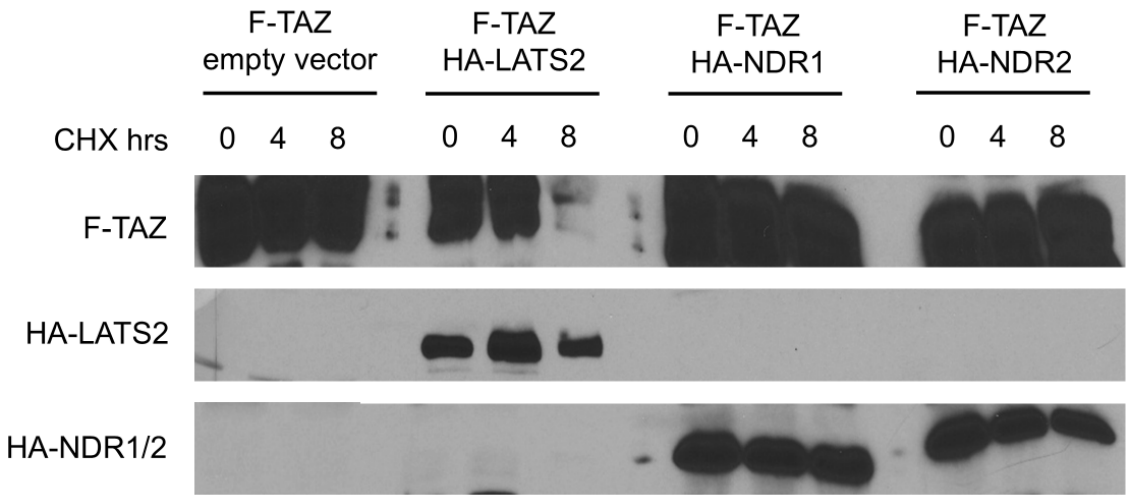

Figure 3.4. NDR1/2 does not degrade TAZ under normal polarity conditions.
293T cells were co-transfected with F-TAZ and HA-NDR1, HA-NDR2, HA-LATS2, or an empty pCMV5b vector. Cells were subsequently treated with cycloheximide for 4 hours and 8 hours. The proteins were then purified and analyzed using Western blotting. The results indicated that, unlike LATS, NDR1/2 does not lead to the degradation of TAZ outside the context of cancer.

The role of DLG and LLGL in the SCRIB-dependent regulation of the Hippo Pathway

DLG and LLGL collaborate with SCRIB in a polarity complex, indicating that they may play a role in regulating SnoN and facilitating its interaction with activated LATS to mediate TAZ signaling. The interdependence of SCRIB, DLG, and LLGL suggests that the entire SCRIB complex may be involved in recruiting SnoN to the plasma membrane. To explore this further, co-immunoprecipitation experiments were conducted to investigate the interactions between SnoN and the components of the SCRIB polarity complex.

Co-immunoprecipitation of SCRIB/DLG/LLGL and SnoN

Co-transfections were conducted to overexpress SnoN in conjunction with SCRIB, DLG, or LLGL in 293T cells. This was accomplished using the vectors pCMV5b-HA-SnoN and pcDNA3.1+/C-(K)DYK (which contains a C-terminal FLAG tag) for SCRIB, DLG1, LLGL1, or LLGL2. To validate the binding of SnoN, Smad3 (cloned into the vector pCMV5b-FLAG) was co-transfected as a positive control. LATS2 served as a positive control for the binding of SCRIB and LLGL. The pCMV5b-FLAG vector was used as a negative control. The objective was to pull down HA-SnoN using FLAG-tagged members of the SCRIB polarity complex.

Western blot analysis confirmed the immunoprecipitation of SCRIB-F (175 kDa), LLGL1-F (115 kDa), LLGL2-F (113 kDa), and F-Smad3 (48 kDa); however, it did not detect DLG1-F (100 kDa) (**Fig. 3.5A**). Furthermore, F-SnoN was not co-immunoprecipitated with any of these proteins, including Smad3. None of the positive controls for binding were effective. For example, LATS2, which is known to colocalize with SCRIB at the plasma membrane, did not show the expected interaction. **Figure 3.5B** illustrates the colocalization of SCRIB and LATS2 in a HeLa cell.

The lack of interactions involving DLG1 and the positive controls makes it challenging to draw conclusions about the relationships between SnoN, DLG, and LLGL. One possible reason

for the failure to detect interactions involving SnoN, DLG1, or LATS2 could be unsuccessful co-transfection experiments with these genes. The low transfection efficiency observed in both 293T and HeLa cells is evident through immunofluorescence, which shows that very few cells were co-transfected with both genes of interest (**Fig. 3.6**). In contrast, larger populations of cells were found to be either transfected with only one gene or not transfected at all.

A.

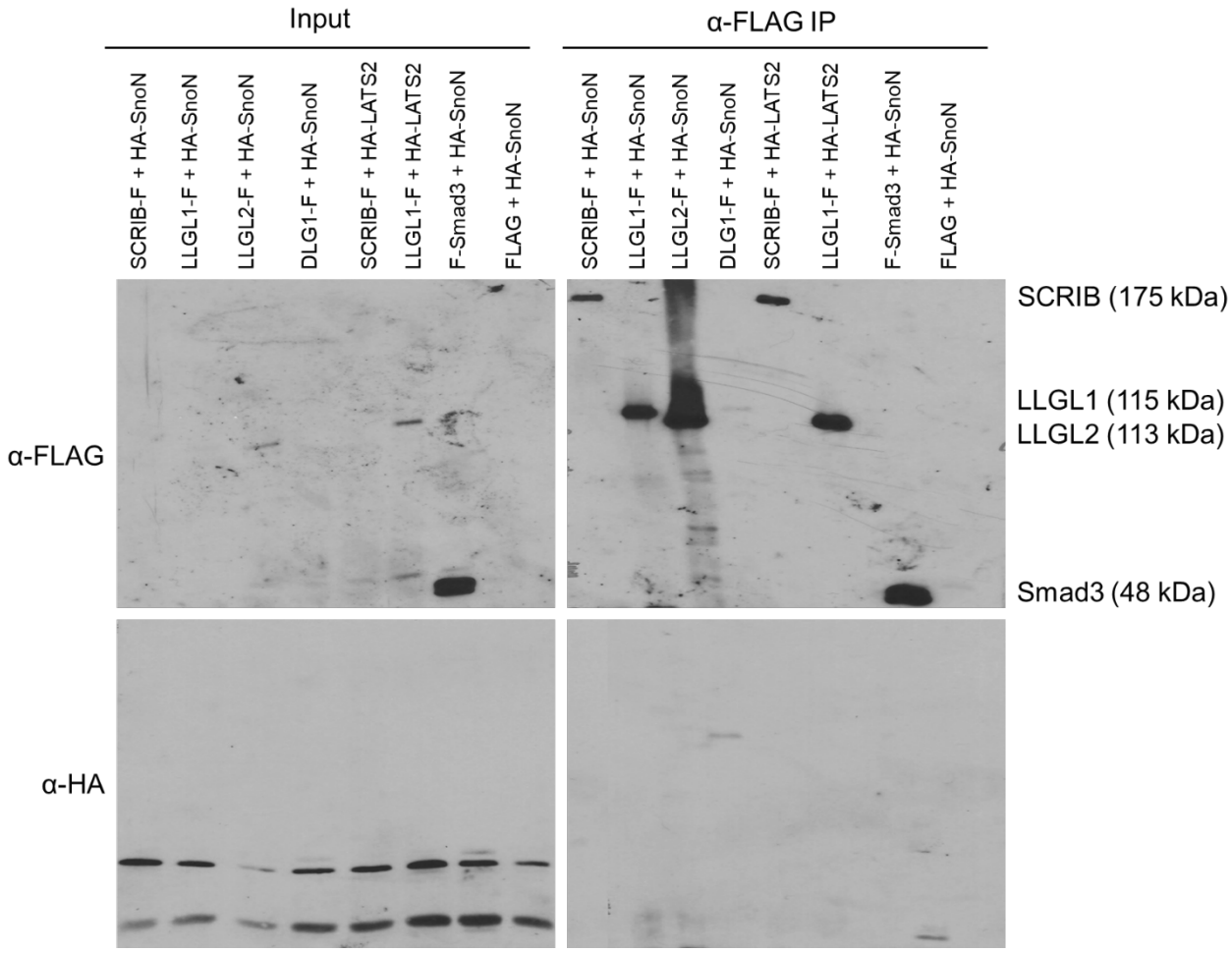

B.

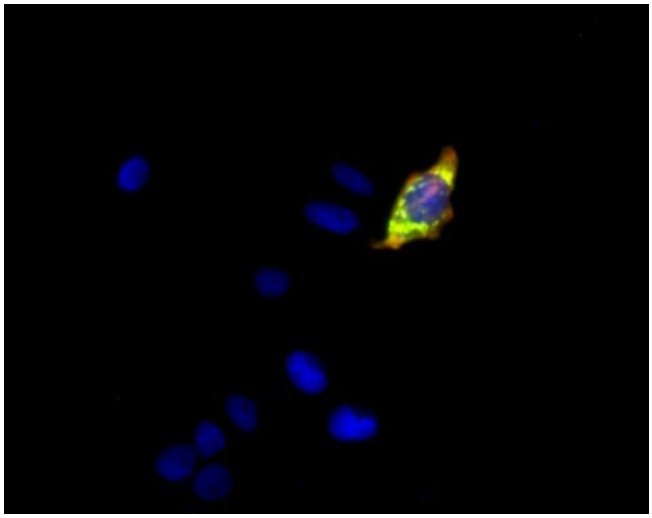

Figure 3.5. Efforts to co-immunoprecipitate SnoN with SCRIB/DLG/LLGL after co-transfection. (A) Western blot analysis confirmed the immunoprecipitation of SCRIB-F (175 kDa), LLGL1-F (115 kDa), LLGL2-F (113 kDa), and F-Smad3 (48 kDa), but did not detect DLG1-F (100 kDa. Positive controls for SnoN, LLGL, and SCRIB binding failed. HA-SnoN was not co-immunoprecipitated. (B) Immunofluorescence image for colocalization (yellow) of SCRIB (orange) and LATS2 (green) in the plasma membrane of a HeLa cell. Nuclei are counterstained blue.

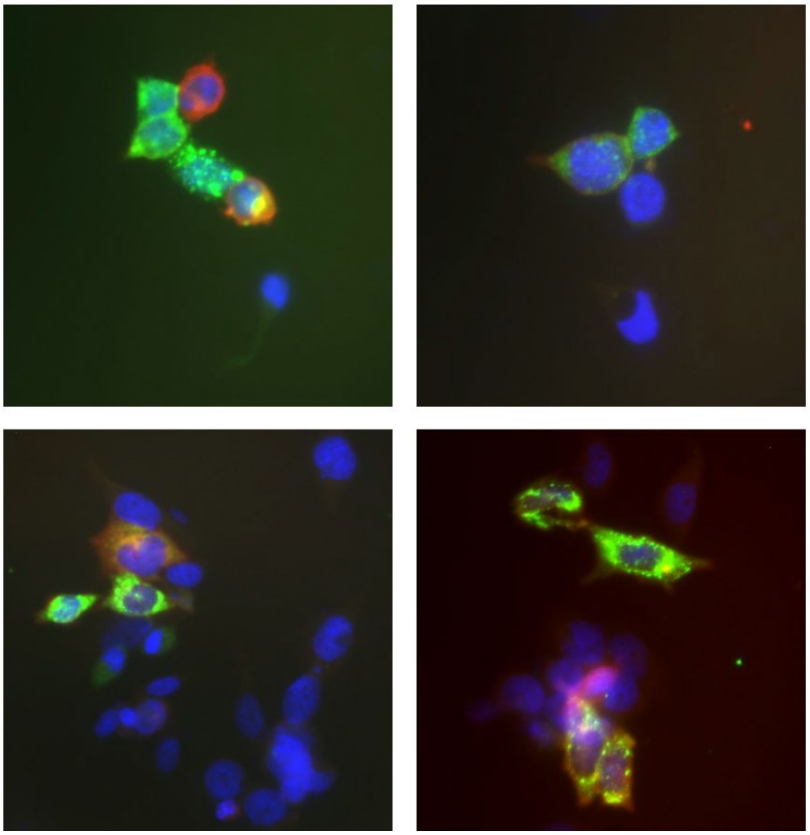

Figure 3.6. Low-efficiency co-transfection was observed in 293T and HeLa cells.
Co-transfection of SCRIB and LATS2 was performed in 293T cells (top panels) and HeLa cells (bottom panels). The colocalization of SCRIB (orange) and LATS2 (green) appears yellow.

DISCUSSION

At the basolateral membrane, SCRIB regulates the stability of SnoN and TAZ. Dysregulation can lead to the development of cancer stem cell traits in breast tumor cells. The aim of this research was to identify proteins that may be directly or indirectly involved in the SCRIB-dependent regulation of the Hippo pathway, particularly in relation to SnoN. NDR1 and NDR2 are noteworthy candidates to consider, as they may influence the SCRIB-dependent regulation of SnoN and TAZ stability due to their relation to the Hippo kinase, LATS. Additionally, it is important to consider DLG and LLGL as participants in this process, as they have been shown to work in conjunction with SCRIB.

The findings suggest that NDR1 and NDR2 do not promote the degradation of SnoN or TAZ. However, given the relationship between NDR and LATS, this result is questionable and indicates the need for further investigation, particularly concerning the phosphorylated forms of NDR1 and NDR2. It is possible that NDR1/2 did not downregulate SnoN or TAZ because they remained inactivated. Future experiments should include *in vitro* phosphorylation of NDR1 and NDR2.

NDR1/2 contains two phosphorylation sites, Ser281/282 and Thr444/442, which are essential for kinase activation *in vitro*. NDR1/2 has been demonstrated to be activated by the Hippo kinases, MST1/2, specifically at the Thr444/442 sites (Stegert et al., 2005). Additionally, the coactivator MOB1 binds to the N-terminus of NDR1/2, facilitating autophosphorylation at Ser281/282 (Bichsel et al., 2004). To achieve robust *in vitro* activation of NDR1/2, cells should be stimulated simultaneously with both MOB1 and MST1/2.

The unsuccessful co-transfection experiments involving DLG and LLGL raise questions about their role in binding to SnoN. To improve the outcomes of co-transfection, it is important to consider several factors: the health and viability of the cell line, the number of passages, the level of confluence, and the quality and quantity of the nucleic acids used. For achieving long-term and consistent gene expression in mammalian cells, stable transfection is generally more effective than transient transfection. The most reliable method for achieving stable gene expression in mammalian cells is through viral transduction, which is particularly effective for cells that are challenging to transfect using non-viral techniques. Moreover, exploring other gene variants for co-transfection experiments, such as DLG5, could lead to more favorable results.

To achieve more conclusive results overall, it may be advantageous to conduct experiments in three-dimensional (3D) cell culture environments that more accurately replicate the natural *in vivo* conditions of living cells (Duval et al., 2017). Utilizing 3D systems could help overcome technical challenges, as characterizing the activity of polarity proteins in epithelial cells can be complex. The organization of cell culture systems significantly impacts gene expression and cellular behavior. For example, 3D culture systems like Matrigel allow epithelial cells to display classical apical-basal polarity. This positively influences the localization and function of proteins involved in signaling pathways, ultimately leading to improved accuracy and reproducibility in experimental results (McCaffrey & Macara, 2011).

SUPPLEMENTAL FIGURES

Figure S3.1

A.

NNNNNNNNNNNNNNAGCNNAGCTCTCTGGCTANCTAGAGAACCCACTGCTTACTG
GCTTATCGAAATTAATACGACTCACTATAGGGAGACCCAAGCTTGGTACCATGGCCT
ACCCCTACGACGTGCCCGACTACGCCTCCCTCGGATCCATGGCAATGACAGGCTCAA
CACCTTGCTCATCCATGAGTAACCACACAAAGGAAAGGGTGACAATGACCAAAGTG
ACACTGGAGAATTTTTATAGCAACCTTATCGCTCAACATGAAGAACGAGAAATGAG
ACAAAAGAAGTTAGAAAAGGTGATGGAAGAAGAAGGCCTAAAAGATGAGGAGAAA
CGACTCCGGAGATCAGCACATGCTCGGAAGGAAACAGAGTTTCTTCGTTTGAAGAG
AACAAGACTTGGATTGGAAGATTTTGAGTCCTTAAAAGTAATAGGCAGAGGAGCAT
TTGGTGAGGTACGGCTTGTTCAGAAGAAAGATACGGGACATGTGTATGCAATGAAA
ATACTCCGTAAAGCAGATATGCTTGAAAAAGAGCAGGTTGGCCACATTCGTGCGGA
GCGTGACATTCTAGTGGAGGCAGACAGTTTGTGGGTTGTGAAAATGTTCTATAGTTT
TCAGGATAAGCTAAACCTCTACCTAATCATGGAGTTCCTGCCTGGAGGGGACATGAT
GACCTTGTTGATGAAAAAAGACACTCTGACAGAAGAGGAGACTCAGTTTTATATAG
CAGAAACAGTATTAGCCATAGACTCTATTCACCAACTTGGATTCATCCACAGAGACA
TCAAACCAGACAACCTTCTTTTGGACAGCAAGGGCCATGTGAAACTTTCTGACTTTG
GTCTTTGCACAGGACTGAAAAAAGCACATAGGACAGAATTTTATAGGAATCTGAAC
CACAGCCTCCCCAGTGATTTCACTTTCCAGAACATGAATTCCAAAAGGAAAGCAGA
AACCTGGAAAAGAAATAGACGTCAGCTAGCCTTCTCCACAGTAGGCACTCCTGACT
ANNTGCTCCTGAGGTGTTCATGCAGACCGGGTACAACAGCTCTGTGATTGGNGGTCG
CTTGGGGTGATCATGTATGANATGCTCATCGGCTACCCNCCTTTNNGTTCTGANANC
CTCAGNNNNNTNTAAGAAGGTGATGAACTGGAAAAANNNTNGNNTTTTCNNCCAAA
ATTCCNNNNNNNNANAGCCNNGGNNNNNNTTTNNNNGTNNNNNNNGAANGGGANN
NNNAATNGNNNNNNGGNNTNNNNAAAAAAANNANNNNTTTTTNANNNGNN

B.

NNNNNNNNNNNNNNNNNNNNNAGCTCTCTGGCTAACTAGAGAACCCACTGCTTAC
TGGCTTATCGAAATTAATACGACTCACTATAGGGAGACCCAAGCTTGGTACCATGGC
CTACCCCTACGACGTGCCCGACTACGCCTCCCTCGGATCCATGGCAATGACGGCAGG
GACTACAACAACCTTTCCTATGAGCAACCATACCCGGGAAAGAGTGACTGTAGCCA
AGCTCACATTGGAGAATTTTTATAGCAACCTAATTTTACAGCATGAAGAGAGAGAA
ACCAGGCAGAAGAAATTAGAAGTGGCCATGGAAGAAGAAGGATTAGCAGATGAAG
AGAAAAAGTTACGTCGATCACAACACGCTCGCAAAGAAACAGAGTTCTTACGGCTC
AAAAGGACCAGACTTGGCTTGGATGACTTTGAGTCTCTGAAAGTTATAGGAAGAGG
AGCTTTTGGAGAGGTGCGGTTGGTCCAGAAGAAAGATACAGGCCATATCTATGCAA
TGAAGATATTGAGAAAGTCTGATATGCTTGAAAAAGAGCAGGTGGCCCATATCCGA
GCAGAAAGAGATATTTTGGTAGAAGCAGATGGTGCCTGGGTGGTGAAGATGTTTTA
CAGTTTTCAGGATAAGAGGAATCTTTATCTAATCATGGAATTTCTCCCTGGAGGTGA
CATGATGACATTGCTAATGAAGAAAGACACCTTGACAGAAGAGGAAACACAGTTCT
ACATTTCAGAGACTGTTCTGGCAATAGATGCGATCCACCAGTTGGGTTTCATCCATC

GGGATATTAAGCCAGACAACCTTTTATTGGATGCCAAGGGTCATGTAAAATTATCTG
ATTTTGGTTTATGTACGGGATTAAAGAAAGCTCACAGGACTGAATTTTATAGAAATC
TCACACACAACCCACCAAGTGACTTCTCATTTCAGAACATGAACTCAAAGAGGAAA
GCAGAAACTTGGAAGAAGAACAGGAGACAACTGGCATATTCCACAGTTGGGACACC
AGATTACATTGCTCCAGAAGTATTCATGCAGACTGGTTACAACAAATTGTGTGACTN
NNNGNCTTTGGNANNGATNTGNNNGAAATGCTATAGGANNTCANCTTTNNGNNNGA
ANNCCNNNNAANNNNNNAGAAANTGATGNNNTGGANNNANNNNNGGAATNNNNCA
AGGNNCNNAANNNNNNNAANCCAGGANTANTTCCGAATTTNNTTTNNNTTNNNNNNG
NATGGNAAANNNNNATGANAAANGAANGNNNNCCTTTTTTAGNNGNNNNNNNTNN
NAA

C.

NNNNNNNNNNNNNNNNNAGCNNAGCTGGTTTAGTGAACCGTCAGATCCGCTAGCGC
TACCGGACTCAGATCTCGAGCTCAAGCTTCGAATTCATGCTCAAGTGCATCCCGCTG
TGGCGCTGCAACCGGCACGTGGAGTCGGTGGACAAGCGGCACTGTTCGCTGCAGGC
CGTGCCGGAGGAGATCTACCGCTACAGCCGCAGCCTGGAGGAGCTGCTGCTCGACG
CCAACCAGCTGCGCGAGCTGCCCAAGCCTTTTTTCCGGCTGCTGAACTTGCGCAAGC
TGGGCCTGAGCGACAACGAGATCCAGCGGTTGCCTCCCGAGGTGGCCAACTTCATG
CAGCTGGTGGAGCTGGACGTGTCCCGGAACGATATCCCTGAGATCCCGGAGAGCAT
CAAGTTCTGCAAGGCTCTGGAGATCGCGGACTTCAGTGGGAACCCCCTCTCCAGGCT
CCCTGATGGCTTCACTCAGCTGCGCAGCCTGGCTCACCTGGCCCTGAATGATGTGTC
TCTGCAGGCACTGCCCGGGGACGTGGGCAACCTCGCCAACCTGGTGACCCTGGAGC
TCCGGGAGAACCTGCTCAAGTCCCTGCCAGCGTCCCTGTCATTTCTGGTCAAGCTGG
AACAGCTGGATCTGGGAGGCAACGATCTGGAAGTGCTGCCAGACACTCTGGGGGCT
CTGCCCAATCTTCGGGAGCTGTGGCTTGACCGGAACCAGCTGTCAGCACTGCCCCCG
GAGCTCGGGAACCTGCGGCGCCTGGTGTGCCTGGACGTGTCGGAAAACCGGCTGGA
GGAGCTGCCTGCTGAGCTCGGCGGGCTGGTGCTGCTCACTGACCTGCTGCTGTCCCA
GAACCTGCTGCGGAGGCTGCCCGACGGCATCGGTCAGCTGAAGCAGCTATCCATCC
TAAAGGTAGACCAGAATCGGCTGTGCGAGGTGACTGAGGCCATCGGGGACTGTGAG
AACCTCTCTGAGCTGATCCTCNCGGANAACCTGCTGATGGCCCTGCCCCGCTCCCTG
GGAAAGCTGACTAAGCTGACCAACCTCAACGTGGACCGGAACCNCCTCGAGGCGCT
GCCGCCCGANATCGGGGGCTGTGTGGCNCTCNNCGTCCTCNCCTTGAGGGANANCC
NCCTGGCCGTCCTGCCNCCANAGCTGGCCNNNCGANAAANCTGCNCNNGCTGGANN
NGGNNGGGAANNCNCTGCANATNNGCCGTTCC

D.

NNNNNNNNNNNNNNNNNNNNNNNNNNNNNGTGACCGTCAGANTTGNNNCTGGTAC
CACGCGTATCGATACCATGGACTACAAGGACGACGATGACAAGGGTCGACAATCGT
CCATCCTGCCTTTCACTCCCCCGATCGTGAAGCGCCTGCTGGGCTGGAAGAAGGGCG
AGCAGAACGGGCAGGAGGAGAAATGGTGCGAGAAGGCGGTCAAGAGCCTGGTCAA
GAAACTCAAGAAGACGGGGCAGCTGGACGAGCTGGAGAAGGCCATCACCACGCAG
AACGTCAACACCAAGTGCATCACCATCCCCAGGTCCCTGGATGGCCGGTTGCAGGT
GTCCCATCGGAAGGGGCTCCCTCATGTCATCTACTGCCGCCTGTGGCGATGGCCAGA
CCTGCACAGCCACCACGAGCTGCGGGCCATGGAGCTGTGTGAGTTCGCCTTCAATAT

GAAGAAGGACGAGGTCTGCGTGAATCCCTACCACTACCAGAGAGTAGAGACACCAG
TTCTACCTCCTGTGTTGGTGCCACGCCACACAGAGATCCCGGCCGAGTTCCCCCCAC
TGGACGACTACAGCCATTCCATCCCCGAAAACACTAACTTCCCCGCAGGCATCGAGC
CCCAGAGCAATATTCCAGANACCCCACCCCCTGGCTACCTGANTGAAAATGGANAA
ACCAGTGACCACCAGATGAACCNCAGCATGGACGCAGGTTCTCCAAACCTATCCCC
GAATCCGATGTCCCCAGNANNTAANAACTTGNNCCTGCNNNCAGTTACCTACTGNN
NNNCGGCCTTNNGGGTGCNCCATNNNCTACTACGNGCTGAACCANNNNNTCGGGGA
AAANATTTCCNNNNCCTNNNNNNCCATCCNNGNACNNGNGGATGGCCTTCCCCNNN
CCCCNNCCAATTTCGNNNNNNNTTNNNNGCCTAAGGGNNNNNNNNNCCAANNNNC
ANNNNNAAATGNNCCCNNNTGGAACNNGAANCCGGGAAAANNNNNNGGAAAANN
NGNNNNGGGGNNNNNNNNNNNNNNGNNNGGGGNNNNGNNNNNCCNAAAANNNNC
CCNNAAANGANNNNNNCCNNTTTTTTNNNCCNNNTNNNNCCCNNNNNNNNAAANN
NNNNNNNNNNNGNNNNGGGNNCCCCNNGCCNNNCCNNNNNNNNNAAAANNNNN

Figure. S3.1, related to Figure 3.1. Verification of the sequences for the NDR1/2, SCRIB, and Smad3 gene inserts.
(A) Sequence of the NDR1 gene fragment. (B) Sequence of the NDR2 gene fragment. (C) Sequence of the SCRIB gene fragment. (D) Sequence of the Smad3 gene fragment. Unidentified bases designated as "N."

Figure S3.2

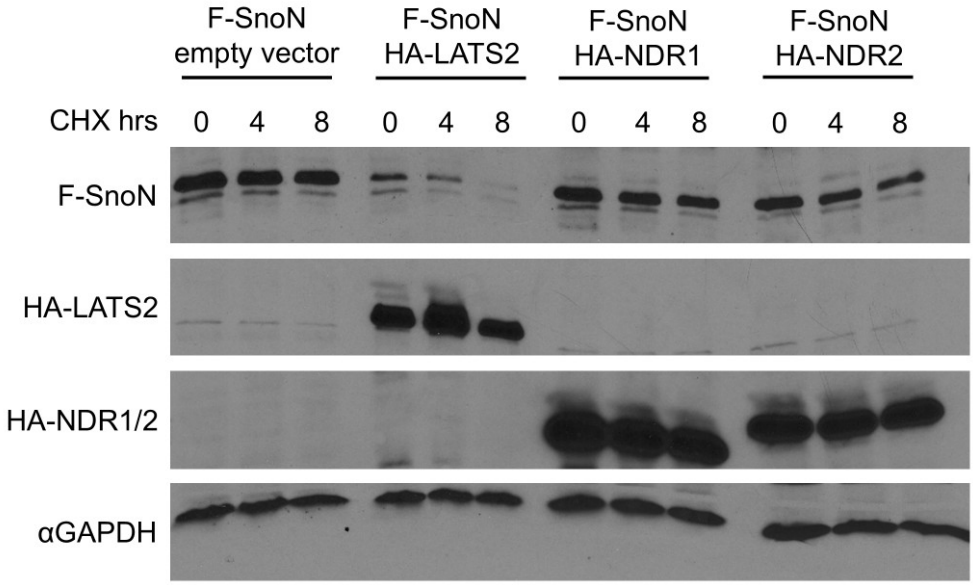

Figure S3.2, related to Figure 3.3. NDR1/2 does not degrade SnoN under normal polarity conditions.
293T cells were co-transfected with F- SnoN and HA-NDR1, HA-NDR2, HA-LATS2, or an empty pCMV5b vector. Cells were subsequently treated with cycloheximide for 4 hours and 8 hours. The proteins were then purified and analyzed using Western blotting. The results indicated that NDR1/2 does not lead to the degradation of SnoN outside the context of cancer.

Chapter 4

Future Directions

SUMMARY

Ongoing troubleshooting and optimization of techniques are essential to address the questions raised in this research. To enhance experimental outcomes involving SnoN, a derivative of the MCF10A cell line (MCF10A-m) will be utilized because it contains a mutation in the Smad binding site. This mutation prevents the degradation of SnoN, which is typically facilitated by Smad3. Once the specific amino acid residues in SnoN crucial for binding to SCRIB are identified, a reciprocal experiment will be conducted to determine which domain of SCRIB is necessary for interacting with SnoN. In this co-immunoprecipitation experiment, β-PIX, a well-characterized binding partner of SCRIB, will serve as a positive control.

After identifying the sequences necessary for the SCRIB and SnoN interaction, the next step involves conducting a series of experiments, as detailed below. The data gathered from these experiments will provide further insights into the interaction, identify additional protein-protein interactions, and help elucidate the function of the SCRIB-SnoN interaction. This data can also contribute to refining the existing model of SCRIB's role in the mutual regulation of SnoN and the Hippo pathway. Most importantly, these experiments may establish a mechanism for therapeutically controlling the stemness of breast cancer cells, which could have significant clinical implications.

The structure motifs mediating the SCRIB-SnoN interaction

PDZ domains are known to recognize specific amino acid motifs located at the C-termini of target proteins, although they can also bind to internal sequences (Bonello & Peifer, 2018a; Chen et al., 2016; Lee & Zheng, 2010). The PDZ domains of SCRIB exhibit distinct yet overlapping binding preferences and are also targeted by oncoviral proteins (Stephens et al., 2018; Humbert et al., 2008, 2003). For instance, the E6 oncoprotein from human papillomavirus binds to a motif at its C-terminus, allowing it to interact with a PDZ domain of SCRIB, which leads to the ubiquitination and degradation of SCRIB. Additionally, SnoN, another oncoprotein, may interact with a SCRIB PDZ domain through its C-terminus (Stephens et al., 2018; Humbert et al., 2008, 2003). Once the amino acid sequences responsible for the interaction between SCRIB and SnoN are identified, online prediction tools can be utilized to determine the secondary structural motifs involved.

The binding affinity of the SCRIB-SnoN interaction

Currently, there are no quantitative measurements of how strongly the SCRIB PDZ domain interacts with SnoN. If one or more of the four SCRIB PDZ domains are found necessary for this interaction, quantitative pull-down assays can be performed to obtain values for the equilibrium dissociation constant (K_d). The K_d represents the binding affinity between the two proteins and is calculated based on the concentrations of the reactants and products at equilibrium ($K_d = (A_{eq})(B_{eq})/(AB_{eq})$). To determine the K_d, the concentration of the prey protein required for half the maximal binding at equilibrium in the pull-down assay can be extrapolated. The lower the K_d value, the higher the binding affinity and the stronger the interaction. Gathering this binding affinity data will help to understand the specific contributions of individual SCRIB PDZ domains to interactions with SnoN and determine if they have different affinities (Lapetina, S. and Gil-Henn, H., J Biol Methods., 2017; Lim, K.Y.B., J. Biol., 2017).

To determine K_d values, SCRIB PDZ domain amino acid sequences can be obtained via PCR cloning of DNA sequences into vectors for stable expression in 293T cells, followed by

purification of the HA-tagged peptides from cell lysates. A cell-free pull-down assay can be conducted by incubating a constant concentration of the bait (F-SnoN bound to beads) with increasing concentrations of the prey (HA-Scribble PDZ) in solution to generate data points. After SDS-PAGE, gels can be stained with Coomassie blue and analyzed using ImageJ software to measure the mean density of each band minus the background. Use graphing software to plot concentrations of the prey protein against mean densities of bands, K_d values for each SCRIB PDZ domain for binding SnoN can be calculated.

The biological function of the SCRIB-SnoN interaction

An important objective is to investigate how changing the interaction between SCRIB and SnoN affects the development of specific characteristics in breast tumor cells, which are caused by TAZ stabilization by SnoN. Evidence supporting the idea that TAZ connects cell polarity to the stemness of breast cancer cells includes TAZ being significantly over-represented in breast cancer gene expression data sets, as well as the SCRIB-dependent regulation of TAZ activity mediated by SnoN (Cordenonsi et al., 2011; Butti et al., 2019).

The stability of TAZ not only helps CSCs grow but also maintains their stem cell properties—self-renewal, initiating tumors, expressing CSC markers, and resisting chemotherapy. It is important to determine if TAZ's activity, which depends on cell polarity, is affected by the interaction between SCRIB and SnoN. If it is discovered that SCRIB-SnoN binding is necessary to inhibit TAZ, it would identify the protein binding motifs as potential targets for therapy to stop the growth of BCSCs and the spread of breast cancer. The following experiments can be used to assess the function of the SCRIB-SnoN interaction.

Dysregulation of the SCRIB-SnoN interaction

The mislocalization of SCRIB has been shown to increase the activity of TAZ and promote CSC characteristics. Notably, SnoN levels correlate with TAZ, and reducing SnoN expression decreases CSC traits (Cordenonsi et al., 2011; Zhu et al., 2016). Future experiments should investigate whether TAZ's modulation of CSC-related characteristics depends on the interaction between SCRIB and SnoN.

Non-transformed MCF10A cells express low levels of TAZ, exhibit reduced TAZ activity, and show fewer CSC-related traits. In contrast, MCF10A-T1k cells (M-II), which are Ras-transformed derivatives of MCF10A, display elevated TAZ levels. It is possible to introduce point mutations in M-II cells using a CRISPR/Cas9 knock-in approach to disrupt the SCRIB DNA sequence responsible for encoding the amino acid motif needed for binding SnoN. Silencing the SCRIB gene will allow an analysis of CSC traits in the CRISPR knock-in M-II cells compared to those of wild-type M-II cells.

A mammosphere formation assay can be performed to evaluate self-renewal by generating both primary and secondary mammospheres *in vitro* to assess CSC traits in M-II knock-ins relative to M-II cells. To determine tumor-initiating potential *in vivo*, the ability to form tumors can be tested using a limiting dilution assay, followed by serial tumor transplantation into the fat pads of immunocompromised nude mice. Additionally, the expression levels of CSC markers, such as Twist, Oct4, and Sox2, can be quantified using quantitative PCR (qPCR).

Reciprocal experiments should focus on identifying the specific SnoN sequence required for binding to SCRIB. Disrupting the SCRIB-SnoN interaction in M-II knock-in cells is anticipated to stabilize downstream TAZ activity, which in turn may enhance CSC

characteristics. This enhancement would be evident through an increase in both the number and size of mammospheres, higher expression levels of CSC markers, and a significantly reduced need for transplanted cells to form tumors, indicating an increased tumor-initiating potential.

The SCRIB-SnoN interaction in modulating chemosensitivity

CSCs exhibit resistance to chemotherapy, leading to their increased presence in tumors. This resistance contributes to cancer relapse and metastasis (Dean et al., 2005; Yu et al., 2012; Butti et al., 2019). The overexpression of TAZ enhances the activity of multidrug resistance proteins (MRPs), which expel anticancer drugs from cancer cells, further increasing resistance to chemotherapy (Cordenonsi et al., 2011; Sodani et al., 2012). If SCRIB-dependent polarity is already disrupted, it may be possible to induce the SCRIB-SnoN interaction, resulting in TAZ degradation. This action could suppress the stemness of CSCs, overcome drug resistance, and restore breast cancer cell sensitivity to cytotoxic agents.

Although TAZ overexpression can be achieved with a constitutively active form of TAZ, known as TAZS89A, this mutant form is not inhibited by LATS phosphorylation. As a result, it is not an effective strategy for upregulating TAZ if the goal is to eventually induce its LATS-dependent degradation. The most effective way to increase TAZ levels is by disrupting polarity through transduction with the SCRIB mutant, ScribP305L. This mutant is characterized by a disruption in the LRR13 membrane binding domain, leading to its mislocalization in the cytoplasm. This mislocalization interferes with E-cadherin expression at cell-cell junctions, ultimately causing the mislocalization of endogenous SCRIB (Elsum et al., 2012; Feigin et al., 2014; Chen et al., 2016). M-II cells can be transduced with ScribP305L and FACS-sorted based on their CD44+/CD24-/low and ALDH1+ phenotype, which is associated with drug resistance.

To facilitate the interaction between SCRIB and SnoN, which results in the degradation of TAZ, a membrane-bound version of the specific SCRIB amino acid sequence can be overexpressed in cells where SCRIB is mislocalized. This process specifically involves overexpressing the SCRIB PDZ domain with the highest binding affinity for SnoN. A tethered version of the SCRIB sequence can be created as a fusion protein through PCR cloning. This fusion protein will consist of the specific SCRIB PDZ amino acid sequence that binds to SnoN, along with a CAAX prenylation motif that anchors proteins to the plasma membrane. The CAAX motif is derived from the Ras membrane-targeting sequence, where "C" represents cysteine, the two "A" residues are aliphatic amino acids, and "X" is variable.

The impact of drug resistance can be studied using Western blot analysis to measure the levels of multidrug resistance proteins (MRPs) and through chemosensitivity assays. In M-II cells, where endogenous SCRIB is mislocalized and TAZ is upregulated, it is hypothesized that overexpressing the specific SCRIB sequence that binds SnoN will recruit cytosolic SnoN to the membrane. This recruitment is expected to trigger the degradation of TAZ by LATS, which would, in turn, lead to a decrease in the expression of MRP1 through MRP9. These proteins are the primary transporters responsible for expelling anticancer drugs among the 13 members of the MRP family (Sodani et al., 2012). Western blot analysis can detect any decreases in MRP levels, which would correlate with increased chemosensitivity.

After transducing M-II cells with the CAAX-tethered SnoN-binding SCRIB PDX sequence, various anticancer drugs such as tamoxifen, etoposide, doxorubicin, cisplatin, and paclitaxel can be tested for their effects. A colorimetric method can be used to evaluate the cytotoxicity of these drugs by measuring cell density through spectrophotometric readings of absorbance. Additionally, to assess the chemosensitivity of breast cancer stem cells (BCSCs),

MTT cell viability assays and flow cytometric analyses can be performed to determine the percentage of apoptotic cells.

The reversal of cancer cell stemness

To gather more evidence supporting the function of the SCRIB-SnoN interaction, it can be used to reverse abnormal TAZ activity, which contributes to CSC-like traits in breast cancer cells (**Fig. 4.1A**). The MCF10A-CA1a cell line (also known as M-IV) is a malignant derivative of MCF10A that expresses higher levels of TAZ and SnoN compared to M-II cells. These cells have been confirmed as a model with significant CSC traits during breast cancer progression (Cordenonsi et al., 2011). Several characteristics defining CSC have been identified in M-IV cells, and data suggests that TAZ expression directly influences these CSC-related properties. Additional data reported significantly more upregulated SnoN levels that mirrored that of TAZ in M-IV cells compared to M-II cells (Zhu et al., 2016). To reduce TAZ levels, diminish TAZ activity, and weaken TAZ-dependent CSC traits in M-IV cells, the specific SCRIB PDX motif that binds SnoN can be fused to the CAAX plasma membrane tether and then overexpressed in cells. When anchored to the plasma membrane, SCRIB is expected to recruit SnoN to the basolateral membrane. At the membrane, the SCRIB-SnoN interaction should facilitate the Hippo kinase-mediated degradation of TAZ and SnoN and reduce CSC-related traits in breast cancer cells (**Fig. 4.1B**).

DLG and LLGL participation in the SCRIB-SnoN interaction

DLG and LLGL collaborate with SCRIB in a polarity complex, indicating that they may play a role in regulating SnoN and forming a complex that facilitates the interaction between SnoN and activated LATS, thereby mediating TAZ signaling. The interdependence of SCRIB, DLG, and LLGL suggests that the entire SCRIB complex may be involved in recruiting SnoN to the plasma membrane (**Fig. 4.2**).

To investigate whether DLG and/or LLGL contribute to the recruitment of SnoN, the BioID (proximity-dependent biotin identification) method can be employed to screen for relevant protein interactions. This involves expressing SnoN fused to a mutant form of the *E. coli* biotin protein ligase BirA (BioID). Experiments in MCF10A cells would allow endogenous proteins in proximity to SnoN to become biotinylated. After isolating the biotinylated proteins through immunoprecipitation with streptavidin beads, mass spectrometry can be utilized to identify the interactors of SnoN.

A BioID screening does not specifically indicate direct or indirect protein interactions; instead, it reflects proximity within a range of 10 to 20 nanometers (Roux et al., 2013). To validate the results from the BioID screen, a cell-free pull-down assay can be performed to determine whether SnoN interacts directly or indirectly with either DLG or LLGL. Since BioID screens are typically conducted in two-dimensional cell cultures, it is important to confirm the findings from these 2D experiments with three-dimensional (3D) culture studies, as 3D cultures better replicate the epithelial organization necessary for proper protein interactions and signal transduction (Debnath et al., 2003; Muthuswamy, 2011). Utilizing fluorescence resonance energy transfer (FRET) in cells within a 3D hydrogel environment would allow for the detection of close spatial overlaps, within a distance of 1 to 10 nanometers, between SnoN and DLG or LLGL. This level of proximity would provide strong evidence of molecular interaction (Donius et al., 2016).

The necessity of DLG and LLGL for the SCRIB-SnoN interaction

To determine whether DLG and/or LLGL are necessary for SnoN-Hippo regulation of TAZ, siRNA gene silencing experiments can be utilized to assess their effects on the co-localization of SCRIB and SnoN at the basolateral membrane, the LATS-dependent phosphorylation of TAZ, and the subsequent degradation of both SnoN and TAZ.

CRISPR-Cas9 technology can be utilized to target and silence the DLG and LLGL genes at once by engineering and delivering guide RNAs specific to each gene in a ribonucleoprotein complex with a Cas9 enzyme. In addition to knocking down DLG and LLGL simultaneously, individual knockdowns can provide insight into whether DLG is essential in an LLGL-deficient background, or whether LLGL is necessary in a DLG-deficient background. The outcomes of these experiments can be analyzed using fluorescent microscopy for co-localization, Western blotting for the detection of protein phosphorylation, and cycloheximide assays for protein degradation.

It is important to consider the DLG5 isoforms and LLGL2 isoforms, as they may introduce redundancies that could affect the results of the knockdown experiments. Current data indicates that DLG1, DLG5, and LLGL1 are mapped to domains of SCRIB. If redundancy becomes a concern, specific gene variants can be targeted for knockdown to better understand the roles of the individual isoforms (Bonello & Peifer, 2018).

FIGURES

A.

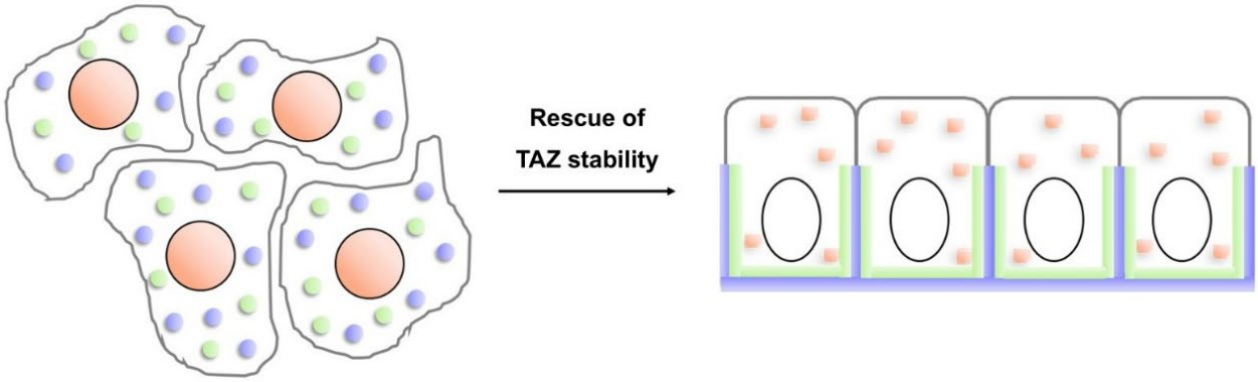

B.

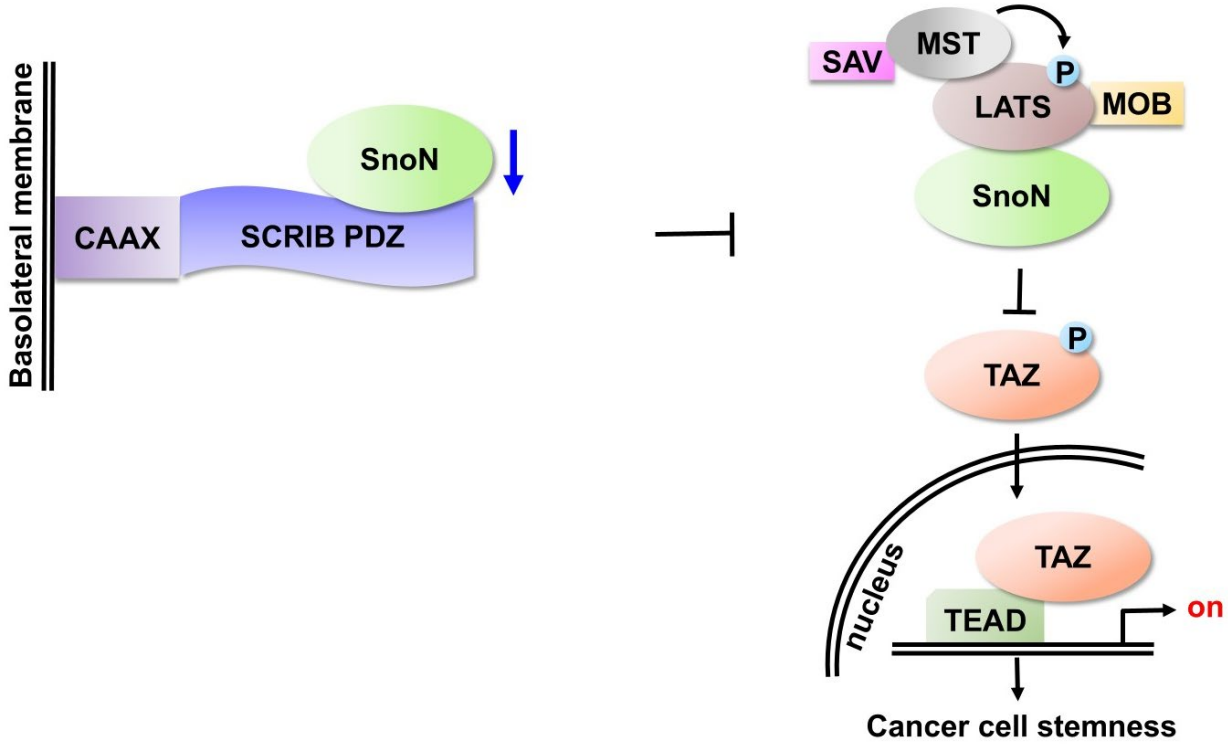

Figure 4.1. A possible model for the rescue of TAZ stability and the reversal of cancer cell stemness.
(A) Rescue of normal TAZ (orange) localization and activity in the cytosol achieved by SCRIB (blue) and SnoN (green) localization to the basolateral membrane. (B) The SCRIB-SnoN interaction is anchored to the plasma membrane by the CAAX protein tether. The blue arrow indicates downregulated protein. The circled Ps indicate phosphorylation.

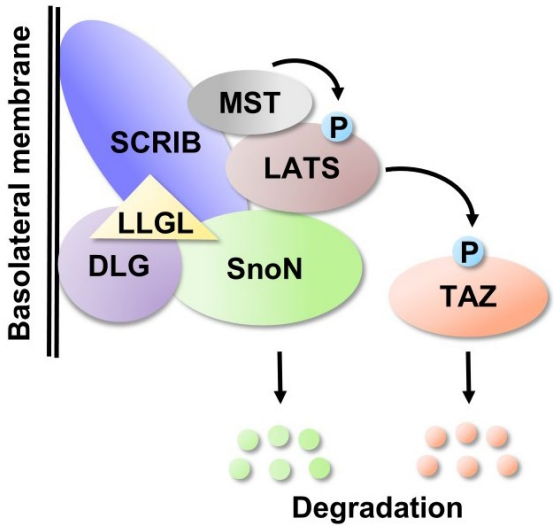

Figure 4.2. **A model depicting a possible mechanism for DLG and LLGL participation in the SCRIB-dependent SnoN and TAZ degradation.**
The circled Ps indicate phosphorylation.

Chapter 5

Teaching Portfolio

INTRODUCTION

The phrase “Those who can, do; those who can’t, teach.” comes from the 1905 play "Man and Superman" by George Bernard Shaw. Even though this phrase has been misused, it has become a way to imply that teachers are incapable because they failed in their discipline. The assumption is that teaching is not a discipline and is inferior to the field in which a teacher is knowledgeable (Free, 2016). However, teaching is a chosen discipline in which one has a deep and true understanding of a field, along with the added ability to convey the nature of that field to others properly (Strontium, 2020). A teacher extracts the building blocks of the skills and knowledge necessary for success in a discipline and instills them into students using effective teaching methods (Free, 2016).

As a result, teaching can be considered greater than one’s field because it requires even more knowledge and skill. Having a strong mastery of a subject area is important for being a good teacher. Studies show that students perform better when the teacher holds a degree in a specific subject area rather than in general education (Wingert, 2012). Furthermore, because teaching is the best way to learn, a teacher becomes more and more adept in their field. This is reflected in Aristotle's statement, “Those who know, do. Those that understand, teach.”

To improve science education, it is crucial to have better teachers at the K-12 levels. Studies indicate that the current approach to teaching science is not beneficial for students. Students in grades K-5 do not receive quality science instruction, as the focus is more on math and language arts (Hatch, 2018; Sharma, 2021). By high school, student interest in science wanes (Hatch, 2018). Despite the high demand for STEM graduates, many students are underprepared by the time they reach college, contributing to an ill-trained STEM workforce (Hatch, 2018).

The focus should be on changing how teachers teach to enhance science education. Science is commonly taught by having students sit and listen to the teacher as they monotonously explain concepts only to have students regurgitate information on tests (David Page, 2017). Instead of the traditional method of lecturing from textbooks, students should have opportunities to work through concepts, conduct experiments, and be creative. Teachers should use strategies that allow students to explore and give them space to figure things out through investigation. Furthermore, it is important for topics to be connected to real-world events, occurrences, and experiences to keep students engaged.

Teaching Inspiration

I am dedicated to breaking down the historical barriers that people of color face in STEM and medicine. My goal is to increase the representation of underrepresented groups in these fields by preparing a diverse student body for academic programs and careers. I pursued a PhD in molecular cell biology not only to gain research skills but also to be a mentor and educator for aspiring scientists in my community. As an adjunct faculty member in a diverse community college system, I take pride in contributing to the education of emerging scientists and healthcare workers of color. My outreach extends into the community to provide representation and mentorship to those who may not have had role models in STEM. With a PhD, I aim to create a laboratory research technician program that prepares community college students for careers in academia and industry and provides them with opportunities to conduct publishable research.

Teaching Experience

I have extensive experience in teaching, ranging from being a private tutor to instructing undergraduate courses. As a private tutor, I offered academic support across various subjects to students of all levels, including adults preparing for professional exams. Additionally, I served as the lead tutor in an afterschool program for Aspire Public Schools, where I assisted elementary students in improving their California State Standardized Test scores by 20%. Furthermore, I managed a community homework and learning center for the Oakland Public Libraries, where I not only facilitated the academic success of youth of color but also provided mentorship to high school students. I also taught at Oakland Technical High School in the Biotech Academy, and at a workforce development agency where I redesigned and taught the biotechnology curriculum for a California state-approved training certificate program.

I have worked as an adjunct faculty member in the Peralta Community College District for 15 years, teaching at both Laney College and Merritt College. At Laney College, I taught in the Biomanufacturing Program, and at Merritt College, I taught anatomy and physiology in the Biology Department. Currently, I teach career and technical education courses in the Merritt College Bioscience Department, covering topics such as fluorescence and confocal microscopy, genomics, mammalian cell culture, bioethics, and lab safety. I am also an adjunct faculty member at Mills College at Northeastern University, where I teach undergraduate chemistry and biology courses, including genetics. Recently, I developed and taught a seminar course that exposed undergraduates to current topics in biology through an examination of scientific research articles. In this course, I taught students how to critically evaluate original research presented in primary literature, helping them develop skills in reading and understanding scientific papers.

During my time as a Graduate Student Instructor (GSI) in Molecular Cell Biology at UC Berkeley, I exceeded the teaching requirements needed for graduation. I instructed a Physiology and Cell Biology Lab, guiding students through experiments aimed at strengthening their understanding of the fundamental mechanisms governing human life processes. As a GSI for the Biology of Human Cancer course, I conducted virtual discussion sections during the pandemic, covering the molecular and cell biology of cancer and its applications in prevention, diagnosis, and treatment. In the Human Physiology Laboratory for senior undergraduates, I taught students about manipulating nucleic acids, proteins, cells, and organisms, and introduced them to key techniques and strategies used in modern cell biology and physiology research. These included DNA gel electrophoresis, bacterial transformation, mammalian cell transfection, PCR, immunoblotting, and fluorescence microscopy. My experience as a GSI allowed me to develop effective teaching methods and ways to motivate students in virtual learning environments. This role also contributed to my growth as an educator and a scientist, as I not only taught but also actively engaged in professional development workshops to enhance my instructional skills in higher education.

Teaching Philosophy

My passion is teaching biological sciences, which covers a variety of subjects. As an instructor, my goal is to keep my students as excited about learning as I am about teaching. At the same time, I focus on fulfilling learning outcomes so that students complete my courses with the knowledge and tools they require to advance academically and prepare for future careers. To maintain an optimal level of excitement while ensuring optimal learning, I fuse my passion with my academic authority. For example, when teaching the fundamentals of fluorescence

microscopy, I convey to my students the excitement of manipulating the energy levels of electrons in samples to produce wavelengths of light, which they visualize as different colors in the images they produce. Overall, I strive to foster an appreciation for science in my students and to enhance their understanding of how science connects to them and the world.

Motivating students and providing solid theoretical knowledge are key characteristics of an effective teacher. I have maintained academic expertise in the subjects I teach through personal growth and improvement. My ongoing education has given me a deep understanding of biological sciences, particularly through my research in cancer biology and my extensive graduate-level education. Moreover, to stay updated with new teaching methods and best serve my students, I regularly attend workshops and seminars to enhance my skills and continue growing as an instructor. I also rely on self-assessment and welcome feedback from both students and colleagues to identify areas for improvement.

As a teacher, I understand that my responsibility extends beyond just providing instruction. It also includes offering emotional support and mentorship to my students. Ensuring that my students have the best learning experience and maintaining their well-being is important to me. I commit to being approachable and available to my students, and I make sure they know that I am there to not simply listen to them, but to truly hear them because what they have to say matters to me. I make it a priority to create a comfortable atmosphere for sharing and communicating, where asking questions is encouraged and never feels uncomfortable. Respect is crucial in my classroom, and I expect my students to respect themselves and each other. I also ask that they prioritize everyone's ability to learn. I strive to treat my students with patience, understanding, concern, and commitment. As a role model, I guide and mentor my students, encouraging them to aim for their highest academic aspirations and pursue their career goals.

Teaching Methods

Because my science classes are bridges between introductory and advanced courses, I utilize Bloom's taxonomy of learning when developing a curriculum. This is a framework for categorizing educational goals that represent progressive levels of mastering content. I reiterate to my students that the objective is for them to climb up these levels of mastery from just remembering information to understanding the content well enough to apply it to questions, analyze data, evaluate situations, and develop the skills to create new situations such as designing an experiment. To apply this tool to course content, I create lessons to deliver appropriate activities, assessments, questioning, objectives, and outcomes.

In my science classes, I use Bloom's taxonomy of learning to help students progress from basic to advanced concepts. This framework sets educational goals at different levels of understanding, from simply remembering information to being able to apply, analyze, evaluate, and create new ideas based on the knowledge. I ensure that my lessons include activities, assessments, questions, objectives, and outcomes that align with this approach. For example, in my research practicum course, students learn to apply the scientific method to design and execute research projects.

To enhance student experiences, I utilize active learning methods to engage them in opportunities to think, practice, discuss, and apply what they learn in class. By providing these opportunities, students can tackle complex questions, propose solutions to problems, and explain their ideas. I incorporate group work as a strategy, which helps students reinforce their understanding of the material. I extend my active learning methods to online classes by using breakout rooms for group work and poll questions to keep students engaged. Another technique

that serves students well is hands-on active learning. For example, in my anatomy class, I incorporate hands-on activities with lectures to allow students to work with anatomical models, preserved organs, or even cadavers to enhance their understanding and connect theories with real-life structures.

I understand that students have different learning styles, such as auditory, tactile, and visual. To accommodate these differences, I provide a variety of learning experiences to engage students and help them succeed academically. For example, I use more images than text in my lectures to cater to visual learners, offer hands-on activities for tactile learners, and reinforce key concepts to aid auditory learners. I provide repetitive exposure to concepts, theories, and take-home messages to facilitate learning. I also relate course material to real-life situations to keep students engaged and encourage them to do the same for better retention.

Diversity, Equity, and Inclusion

As an African American woman in the field of science, I have encountered microaggressions and imposter syndrome, which have been worsened by the lack of diversity in higher education. Today, I am dedicated to promoting and nurturing diversity, equity, and inclusion. I emphasize to my students the significance of these principles in fostering talent and excellence across all social strata. I teach my students that diverse backgrounds bring about new perspectives essential for innovation. Furthermore, I emphasize that there is no evidence to support the notion that success in science or any STEM field is contingent on socially constructed identity markers such as race.

As an educator, I am devoted to creating a safe and fair learning environment for all students, regardless of their ethnicity, gender, or background. I make an effort to integrate inclusive and diverse course materials while acknowledging the historical exclusion of various groups from the field of science. I take pride in making my courses an integral part of advancing diversity, equity, inclusion, and a sense of belonging in STEM. I am honored to be part of a much-needed transformation in the field of science.

To empower minority students and educate well-represented students in the field of science, I design curricula that highlight the significant contributions of underrepresented individuals to science and medicine. This includes discussing the HeLa cell line, which was unethically acquired from Henrietta Lacks, as well as the accomplishments of pioneering embryologist Ernest Everett Just, who recognized the importance of the cell surface in mammalian development. Each class begins with an introduction to a lesser-known figure in STEM, such as Ben Barres, the first openly transgender scientist in the National Academy of Sciences, and Katalin Karikó, who laid the groundwork for mRNA vaccines to combat the COVID-19 pandemic. Additionally, I ensure that my students learn about melanin, the protein responsible for pigmentation, to help them understand that all human beings have brown skin due to the expression of the melanin gene and that differences in expression levels result in varying shades of brown. Through this, I aim to instill in my students the understanding that skin color does not equate to black or white and that prejudices based on skin color are nonsensical. At the end of each course, I remind my students that as future scientists, doctors, dentists, entrepreneurs, inventors, innovators, and educators, they have a responsibility to open doors for those whose opportunities have historically been limited. They may serve on admissions boards and hiring committees, and it is important for them to create opportunities for others.

CURRICULUM VITAE

Summary

- Enthused to teach college-level science
- Resolute to increase diversity in STEM
- Determined to expose youth to science
- Extensive research laboratory experience
- Focused on inhibiting cancer cell growth
- Knowledgeable in cell and molecular biology
- Adept in mammalian cell culture
- Expertise in research grade microscopy

Education

Ph.D., Molecular and Cell Biology, Expected Dec 2024
University of California, Berkeley, CA
Dissertation: Mechanism of SCRIB-Dependent Regulation of the Hippo Pathway.
Advisor: Kunxin Luo

M.S., Biological Science, Completed 73 credit hours, Sep 2014 – Jun 2017
California State University East Bay, Hayward, CA
Thesis: The role of transmembrane protein 55B in tumor cell proliferation and apoptosis.
Advisors: Kenneth Curr and Fred Bauzon

M.S., Medical Health Sciences, Jun 2012
Touro University California, Vallejo, CA
Thesis: The role of p21 and the senescence program in modulating chemosensitivity in human breast carcinoma cells. Advisor: Athena Lin

B.S., Cell and Molecular Biology, Aug 1997
University of Washington, *Seattle*, *WA*
Senior Thesis: Ectopic expression of *pointed* suggests its role in tissue specification and/or appendage formation during *Drosophila* oogenesis. Advisor: Hannele Ruohola-Baker

Certification

Certificate in Biotechnology, Jun 2015
California State University East Bay, Hayward, CA

Certificate in Immunohistochemistry for Research, Jun 2011
Innovex Biosciences, Oakland, CA

Certificate in Advanced Bioscience Microscopy, Jul 2010
Merritt College, *Oakland*, *CA*

Certificate in Polymerase Chain Reaction, Jan 2010
Bay Area Biotechnology Education Consortium, Morgan Hill, CA

Certificate in Optical Microscopy, Dec 2009
Merritt College, *Oakland*, *CA*

Certificate in Biomanufacturing, May 2009
Laney College, *Oakland*, *CA*

Teaching Experience

Adjunct Faculty, Sep 2022 – Present
STEM and Health Science Department, Mills College at Northeastern University, Oakland, CA
BIOL 2301: Genetics and Molecular Biology Lecture, Sp23
BIOL 2302: Genetics and Molecular Biology Laboratory, Sp23
BIOL 3409: Current Topics in Biology Lecture, Sp23
CHEM 1162: General Chemistry Laboratory, F24, Sp24, F23, F22
CHEM 2312: Organic Chemistry Laboratory, Sp24

Graduate Student Instructor, Aug 2018 – May 2022
Molecular and Cell Biology Department, University of California, Berkeley, CA
MCELLBI 32L: Introduction to Human Physiology Laboratory, F18
MCELLBI 132: Biology of Human Cancer Lecture, F20
MCELLBI 133L: Physiology and Cell Biology Laboratory, Sp22

Adjunct Faculty, Aug 2012 – Present
Bioscience Department, Merritt College, Oakland, CA
BIOSC 7: Practical Mammalian Cell Culture Lecture and Laboratory, Sp17, Su16, Su15, F13
BIOSC 11: Lab Safety and Ethics Lecture, Su15
BIOSC 16: Advanced Confocal Microscopy Laboratory, Sp14
BIOSC 20: Emerging Technologies in Microscopy Lecture, Sp13
BIOSC 30: Genomics Theory Lecture, F24, Sp24
BIOSC 101: Theory and Practice of Microscopy Laboratory, F23
BIOSC 102: Fluorescence Microscopy and Specimen Prep Lecture, F24, Sp24, Sp21, F21
BIOSC 102: Fluorescence Microscopy and Specimen Prep Laboratory, F23, Sp23, F22
BIOSC 103: Confocal Microscopy and Research Lecture, F24
BIOSC 103: Confocal Microscopy and Research Laboratory, F21
BIOSC 104: Bioscience Practicum Research Lecture, F24
BIOSC 104: Bioscience Practicum Research Laboratory, F23

Biology Department, Merritt College, Oakland, CA
BIOL 2: Human Anatomy Lecture and Laboratory, F16, F15, Su15, F14, Su14, Sp14, Su13, Sp13
BIOL 20A: Human Anatomy and Physiology Lecture and Laboratory, Sp17, Sp16, Sp15, Sp13
BIOL 20B: Human Anatomy and Physiology Lecture and Laboratory, F13, F12

Research Experience

Doctoral Research, Aug 2017 – Present
University of California, Berkeley, CA
Examining crosstalk between epithelial cell polarity and Hippo signaling to identify genetic targets for controlling the stemness of breast cancer cells and inhibiting tumorigenesis.
Advisor: Kunxin Luo

Pre-Doctoral Scholar, Jun 2016 – Apr 2017
University of California, Berkeley, CA
Cancer immunotherapy-based project using genetic manipulation to prime the immune system and mount a defense against cancer cells in mice. Advisors: David Raulet and Assaf Marcus

Master's Research, Sep 2014 – Aug 2017
California State University East Bay, Hayward, CA
Explored the role of a transmembrane protein in tumorigenesis via gene overexpression and CRISPR-Cas9 knockout experiments. Advisors: Kenneth Curr and Fred Bauzon

Master's Research, Sep 2011 – Jun 2012
Touro University California, Vallejo, CA
Increased the chemosensitivity of breast cancer cells using shRNA knockdown to genetically force them into apoptosis in response to chemotherapeutic drugs. Advisor: Athena Lin

Basic Science Research Intern, Mar 2011 – Aug 2011
Touro University California, Vallejo, CA
Conducted knockdown experiments to determine the genetic regulation of optic axon pathfinding during development in Xenopus as visualized using fluorescence microscopy.
Advisor: Tamira Elul

Microscopy Research Intern, Jul 2010, Jul 2011
Tirimbina Biological Reserve, Sara Paqui, Costa Rica
Merged fluorescence microscopy and cell biology with field biology to investigate rainforest flora, fauna, and fungi for speciation. Advisors: Gisele Giorgi and Hank Fabian

Research Intern, Jul 2010 – Mar 2011
University of California, Berkeley, CA
Constructed injectable bio-nanofibers to create artificial ECM and assessed its effects on neural stem cell proliferation and migration via time-lapsed confocal microscopy. Advisor: Won Suh

Biological Science Technician, Jan 2004 – Jan 2005
U.S. Army Corps of Engineers, Honolulu District, Honolulu, HI
Environmental restoration and the removal of unexploded ordnance from formerly used defense sites throughout the Pacific Islands.

Howard Hughes Medical Institute Undergraduate Research Intern, Jan 1995 – Jan 1996
University of Washington, Seattle, WA
Investigated the genetic regulation of tissue specification during *Drosophila* oogenesis.
Advisor: Hannele Ruohola-Baker

Research Apprentice, Jun 1991 – Sep 1991
Fred Hutchinson Cancer Research Center, Seattle, WA
Classified strains of *E. coli* for recombinant DNA technology in cancer studies.

Managerial & Additional Experience

Laboratory Manager, Jul 2010 – Present
Henrietta Lacks Cell Culture Laboratory, Merritt College, Oakland, CA
Oversee all aspects of lab operation including scientific and administrative tasks.

Program Assistant, Jul 2010 – Jul 2011
Merritt Microscopy Program, Merritt College, Oakland, CA
Provided instruction in compound, fluorescence, and confocal microscopy. Trained students in mammalian cell culture. Assisted with program administration and organization. Led community outreach.

Instructional Assistant, Jun 2009 – Jul 2010
Biomanufacturing Program, Laney College, *Oakland*, *CA*
Conducted an adjunct class to assist students in biomanufacturing, lab math, inorganic chemistry, and scientific writing courses. Prepared weekly biotech labs and assisted students during labs.

Program Coordinator, Jun 2009 – Jul 2010
Biotechnology Workforce Development, Regional Technical Training Center, Oakland, CA
Provided instruction and training for state-approved vocational certification in biotechnology. Organized curriculum and performed workforce development.

Instructional Assistant and Laboratory Manager, Sep 2009 – Jun 2010
Biotechnology, Biotech Academy at Oakland Technical High School, Oakland, CA
Developed biotech lab curriculum and instructed students in theories and techniques. Oversaw all aspects of lab operation.

Lead Tutor, Sep 2008 – Dec 2008
Aspire Public Schools, Oakland, CA
Academically assisted elementary students in an after-school education program. Provided intervention, enrichment, and acceleration, increasing state test scores by 20%.

Private Tutor, Sep 2002 – Present
Tutoring By Tobey, Kaneohe Bay, HI; San Diego, CA; Oakland, CA
Provide tutoring for students of all ages, including adults, in various subject areas and test prep.

Program Director, Sep 2000 – Jun 2002
PASS! Homework and Learning Center, Oakland Public Library, Oakland, CA
Coordinated and conducted a community-based homework and learning center. Tutored elementary and middle school students, mentored high school students, and conducted outreach.

Publications & Presentations

Steele, D.; Kraetzer, S.; **Colston, T.**; Snyder, N.; Cassano, J. (2024, December 30). ***Unlocking Lab Safety: An Escape Room Experience Enhances Lab Safety Awareness.*** Submitted for publication.

Colston, T. (2023, August 11). **Scribble Me This: The Basolateral Polarity Complex Regulates Hippo Signaling.** https://doi.org/10.31219/osf.io/ejfr3

Specimen preparation for fluorescence microscopy.
Advanced Microscopy and Bioimaging Conference, University of Ghana, May 2023

Community college pipelines and the Merritt Microscopy Program.
Advanced Imaging Methods Workshop, University of California, Berkeley, CA, Jan 2021

Localization of transmembrane protein 55B in cancer cell lines.
Student Research Symposium, CSU East Bay, Hayward, CA, Apr 2016

Racial disparities in susceptibility for *BRCA1*-related triple-negative breast cancer.
PCR, DNA Sequencing and Fragment Analysis Presentation, CSU East Bay, Hayward, CA, Dec 2014

The role of p21 and the senescence program in modulating chemosensitivity in human breast carcinoma cells.
11th Annual Research Day, Touro University California, Vallejo, CA, Apr 2012

Teaching the art and science of microscopy: Educational projects from the Merritt Microscopy Program.
1. *8th Advanced Imaging Methods Workshop, UC Berkeley, Berkeley, CA*, Jan 2011
2. *7th Advanced Imaging Methods Workshop, UC Berkeley, Berkeley, CA*, Jan 2010
3. *American Society for Cell Biology, 49th Annual Meeting, San Diego, CA*, Dec 2009

Awards & Fellowships

- Center for Student Research Fellowship, *California State University East Bay*, 2015, 2016
- Graduate Equity Fellowship, *California State University East Bay*, 2015, 2016
- Sally Casanova California Pre-Doctoral Scholar, *California State University East Bay*, 2015
- John and Deborah Tunis Scholarship, *Merritt College*, 2010
- The Charles and Connie Meng Scholarship, *Merritt College*, 2010
- The Wanda Garcia Memorial Scholarship, *Laney College*, 2009
- Undergraduate Art Exhibition, *Wayne State University*, 1999
- Howard Hughes Medical Institute Research Internship, *University of Washington*, 1995
- Academic Achievement: Certificate of Merit, *University of Washington*, 1992
- National Action Council for Minorities in Engineering and Science Scholarship, *University of Washington*, 1991 – 1995
- Women in Science and Engineering, *University of Washington*, 1991

COURSE DESIGN

Sample syllabus

BIOL 3409: Current Topics in Biology
Mills College at Northeastern University
Spring 2023

Course Description
Students in this course will critically examine modern methods of biological investigations. Relevant literature will be used to present biological concepts that address aspects of topics in the biological sciences including cancer biology, neuroscience, development, and virology. Through an examination of selected topics, students will learn how to strategically read and understand scientific articles. A major goal of this course is to critically evaluate original research as presented in primary literature. Presentations of relevant literature and student-led discussions of current research will be stressed.

Instructor
Tobey Colston
Email: t.colston@northeastern.edu
Office: NSB 127
Office Hours: F, 1 - 2 PM or by appointment (subject to change)

Class Meetings
Day & Time: M, Th 8:45 - 10:25 AM
Location: NSB 215

Course Materials
We will NOT be using a textbook. Instead, see the class schedule (below) for assigned readings of original research papers. Most papers are freely available in electronic form on Scholar OneSearch at NU Library Oakland Campus. You will need to perform title searches to find the PDF files of articles indicated in the course schedule. Additional reading materials will be provided by the instructor.

Course Canvas
The course has a Canvas site that can be found using the following link: http://canvas.northeastern.edu. This is where most of our materials will be stored and where assignments and quizzes will be submitted. Please inform me if you are having difficulty accessing Canvas or any of the folders and materials. If necessary contact Canvas Technical support using the Help icon at the lower left corner of the Canvas screen. NU Technical support can be contacted at help@northeastern.edu. Each student is responsible for their access to the internet and Canvas for purposes of this course.

Course Expectations
A major goal of this course is to critically evaluate original research in biological sciences. To do this effectively, it is imperative for you to actively participate, share your point of view, and listen to each other's perspectives. Active participation by everyone makes for a lively and

interesting discussion. Your opinion is important, and you are encouraged to express it.

Grading

Assignments	50 points (5 x 10 points each)
Take-Home Tests	100 points (2 x 50 points each)
Journal Club Presentation	50 points
Engagement	25 points
Attendance	25 points
Total	**250 points**

Late work will receive a penalty of 10% per class period.

Your final grade is determined by % of the total points possible. Please note that decimal points are NOT rounded up. Therefore, the absolute minimum required for an A is 93. A score of 92.99 is an A- so please plan accordingly.

	B+ 87%	C+ 77%	D+ 67%	
A 93%	B 83%	C 73%	D 63%	F Below 60%
A– 90%	B– 80%	C– 70%	D– 60%	

Assignments and Tests

Students will complete assignments to practice the skills learned throughout the course. The instructor will use assignments and tests as tools for assessing student knowledge and skills.

Journal Club Presentation

You will lead a discussion on a peer-reviewed journal article of your choice that is related to a topic of your interest in biological sciences. Please send the article to the instructor at least 2 weeks before you will lead the discussion so that it can be approved and shared with your peers. During the 2 weeks before your presentation, you are encouraged to attend office hours for assistance as you prepare. For students who are not leading the journal discussion, your assignment will be to read the paper thoroughly, answer prompts, and annotate the figure(s) in the paper. You will be graded on your assignment submission and participation during the discussion.

Attendance and Engagement

This is an in-person course and students are expected to make an effort to attend each class meeting unless there is an emergency, unforeseen circumstances, or unavoidable conflict. If a student must miss a class due to an emergency, unforeseen circumstances, or unavoidable conflict, it is the student's responsibility to communicate with the instructor via email as soon as possible. For an absence to be excused, documentation that does not divulge private information, such as a doctor’s note stating dates that a student should not attend class, is required. Remember that there are points that can only be earned by attending class.

Engagement points consist of preparation and participation. Engagement will be evaluated by student contribution to discussions which will depend on carefully reading materials and researching background information ahead of class. Attendance is not enough, but speaking and

advancing the conversation by presenting evidence to support ideas is also necessary.

Diversity, Equity, Inclusion, Belonging, and Respect
As your instructor, I am committed to promoting a safe and equitable learning environment for all students no matter their ethnicity, gender, or background. Diversity enriches the academic environment and I strive to incorporate inclusive, more representative course materials while noting that science has historically excluded a variety of people. I am proud to make this course an integral part of promoting diversity, equity, inclusion, and belonging in biology.

The atmosphere in this course should be non-competitive. Please respect and be supportive of the academic efforts of all students in the class. We should all make an effort to use every individual's form of address (name, pronoun). Please do not hesitate to contact me (anonymously is fine) if you have any questions or concerns.

Academic Integrity
A commitment to the principles of academic integrity is essential to the mission of the university. Academic dishonesty violates the most fundamental values of an intellectual community and undermines the achievements of the entire university. Northeastern expects students to complete all examinations, tests, papers, creative projects, and assignments of any kind according to the highest ethical standards. To safeguard the integrity of assignments, your course may potentially use systems such as TurnItIn, which checks written work. Work that contains academic integrity violations may potentially earn a failing grade, a zero, or may potentially result in a failing grade for the class. Please refer to the university's academic integrity policy at http://www.northeastern.edu/osccr/academic-integrity-policy.

Plagiarism or copying anything that is not your work is academic dishonesty. Make certain to always cite sources and use quotation marks for direct quotes. Plagiarism is a serious breach of academic trust and will result in a 0 and be reported.

Accommodations
If you have any concerns regarding your particular circumstances or learning style and any impact this may have on your academic progress in this course, please meet with the instructor early in the semester. Students requiring formal accommodations should contact the office of Student Access and Support Services (SASS, https://oakland.northeastern.edu/student-services/access-services/, (510) 430-3307) so that accommodations may be arranged. SASS can offer information and assistance to help manage any challenges that may affect your performance in coursework. Note that accommodations must be arranged in advance.

Schedule
The course schedule is tentative and may be subject to change.

Date	Topics	Assignment Due
M Jan 9	Syllabus, Course Introduction	
Th Jan 12	Schedule, The Anatomy of a Research Article	
M Jan 16	Martin Luther King, Jr. Day – **No class**	

Th Jan 19	What Critical Review Means	
M Jan 23	Analyzing Titles and Abstracts	Assignment #1
Th Jan 26	Reviewing the Results	
M Jan 30	Coming to Conclusions	Assignment #2
Th Feb 2	Taking and Organizing Notes	
M Feb 6	Dissecting the Senescence-like Program in Tumor Cells Activated by Ras Signaling (Bihani, et al., 2007)	
Th Feb 9	Dissecting the Senescence-like Program in Tumor Cells Activated by Ras Signaling (Bihani, et al., 2007)	
M Feb 13	DLG5 Suppresses Breast Cancer Stem Cell-like Characteristics to Restore Tamoxifen Sensitivity by Inhibiting TAZ Expression (Liu et al,. 2018)	Submit Journal Paper #1
Th Feb16	DLG5 Suppresses Breast Cancer Stem Cell-like Characteristics to Restore Tamoxifen Sensitivity by Inhibiting TAZ expression (Liu et al,. 2018)	Assignment #3
M Feb 20	Presidents Day – **No class**	
Th Feb 23	Enhancement of Antitumor Immunity by CTLA-4 Blockade (Leach et al., 1996) (Historical)	Take-Home Test I
M Feb 27	Journal Club Presentation #1	Journal Club Assignment
Th Mar 2	Physical Exercise and Gene p53 – A MiniReview (Cabral et al., 2020) (Review)	
M Mar 6	**SPRING BREAK**	
Th Mar 9	**SPRING BREAK**	
M Mar 13	TGF-β-induced DACT1 Biomolecular Condensates Repress Wnt Signaling to Promote Bone Metastasis (Esposito et al., 2021)	Submit Journal Paper #2
Th Mar16	TGF-β-induced DACT1 Biomolecular Condensates Repress Wnt Signaling to Promote Bone Metastasis (Esposito et al., 2021)	Assignment #4
M Mar 20	A Sarcoma of the Fowl Transmissible by an Agent Separable from the Tumor Cells (Rous et al., 2011) (Historical)	
Th Mar 23	**Journal Club Presentation #2**	Journal Club Assignment
M Mar 27	miR-16 Targets the Serotonin Transporter a New Facet for Adaptive Responses to Antidepressants (Baudry et al., 2010)	
Th Mar 30	miR-16 Targets the Serotonin Transporter a New Facet for Adaptive Responses to Antidepressants (Baudry et al., 2010)	Take-Home Test II

M Apr 3	The Genetic Basis of Tail-Loss Evolution in Humans and Apes (Xia et al., 2021)	Submit Journal Paper #3
Th Apr 6	The Genetic Basis of Tail-Loss Evolution in Humans and Apes (Xia et al., 2021)	
M Apr 10	Programmable Dual-RNA–Guided DNA Endonuclease in Adaptive Bacterial Immunity (Jinek et al., 2012)	Assignment #5
Th Apr 13	Programmable Dual-RNA–Guided DNA Endonuclease in Adaptive Bacterial Immunity (Jinek et al., 2012)	
M Apr 17	**Journal Club Presentation #3 – Last Class**	Journal Club Assignment

Sample assignment

BIOSC 102: Fluorescence Microscopy and Specimen Prep
Merritt College
Spring 2024

Cell Culture Media Preparation
View the ATCC webinar that discusses cell culture media and additives (from 25:12 to 29:32).
https://www.atcc.org/en/Form_Confirmations/Webinars/2017/Cell_Culture_101.aspx

Read pgs. 13-19 about Complete Growth Media in the ATCC Cell Culture Handbook.
https://www.atcc.org/resources/culture-guides/animal-cell-culture-guide#Complete

View the ABCAM video that explains sterile handling and aseptic technique while preparing complete media.
https://www.abcam.com/protocols/aseptic-technique-video-protocol

Making Dilutions of Concentrated Solutions
The homework questions involve math calculations and explaining how to prepare media. Refer to the lecture Tissue Culture II_SLIDES as well as the following information:

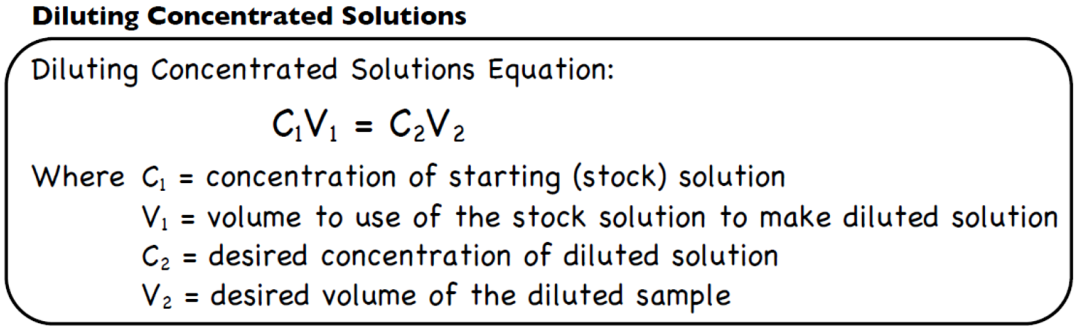

Answer the following questions. Answers can be found in the previous videos, reading, and in the lecture, Tissue Culture II_SLIDES. Where appropriate, your answers should include math calculations and explain how to prepare media (must be included for full points).

Make sure to keep all units when doing calculations:
INCORRECT volume = 5, CORRECT volume = 5 mL

Information required for calculations can be found in the Materials and Reagents table below:

No.	Name	Stock Concentration	Final Concentration	Storage Location
1.0	Cell Media	RPMI or DMEM	N/A	4°C walk-in (026-380C)
2.0	Penicillin-Streptamycin	10,000 units/ml pen. And 10,000 units/ml strep. (100X)	1% (final)	Freezer #2 (026-328S-A)
3.0	L-Glutamine	200mM (100X)	1% (final)	4°C refrig/ -20°C freezer (026-326W-F)
4.0	HEPES	1M	1% (final)	Fridge #5 (026-320S-A)
5.0	Non-essential amino acids	10mM (100X)	1% (final)	4°C refrigerator
6.0	MEM Sodium Pyruvate	100mM	1% (final)	4°C refrigerator
7.0	2-Mercaptoethanol	14.3 M stock	0.05mM (final)	Chemical supply (026-314S)
8.0	FBS	Heat Inactivated Serum	5% or 10% (final)	Freezer #2 (026-328S-A)
9.0	Filter Flasks	Millipore 0.22um filter apparatus	N/A	Supply area

100X indicates the 100% concentrated solution. 1 M (molar) = 1000 mM (millimolar).

1. Why is important to filter sterilized complete media? Can media also be autoclave? Why or why not?

2. What supplements does fetal bovine serum (FBS) add to media? What is the benefit of serum?

3. Why is penicillin-streptomycin (P-S) added to media? What is the disadvantage of adding P-S?

4. Why is L-glutamine (L-glut) an important additive in cell media? What are its many functions?

5. What is HEPES and what is its function in media?

6. Why is complete media used to stop the trypsin reaction when passaging cells?

7. How do you prepare 500 mL of complete DMEM with 15% FBS, 1% P-S, and 2% L-glut?

8. 2-mercaptoethanol (2-ME) serves as an antioxidant, protecting cells and proteins from oxidative harm. How do you prepare 1 L of complete RPMI with 20% FBS, 1% P-S, 1% L-glut and 2-ME at a final concentration of 0.05 mM? Refer to the table and $C_1V_1 = C_2V_2$. Remember: 1 M (molar) = 1000 mM (millimolar).

9. Sodium pyruvate (SP) is commonly added to media as a carbon source in addition to glucose. Since cells make SP, it is not a required supplement for all cell cultures. However, because your cells have been grown in medium that is supplemented with SP, it is recommended to continue use of the supplement as cell growth may lag without it. How much SP would you add to 500 mL of medium for a final concentration of 1 mM which is equal to the 1% SP that is commonly used? Refer to the table and $C_1V_1 = C_2V_2$.

10. You return to your lab after the weekend and observe your cells. You see that the media has turned yellow and cloudy. What does this indicate? What is the standard lab procedure for disposing of cells?

STUDENT EVALUATIONS

MCELLBI 133L: Physiology and Cell Biology Laboratory
University of California, Berkeley
Spring 2022

UNIVERSITY WIDE QUESTIONS (QUANTITATIVE/RATING):
The items in this section are asked across all courses at Berkeley.

Considering both the limitations and possibilities of the subject matter and the course, how would yourate the overall effectiveness of this graduate student instructor?

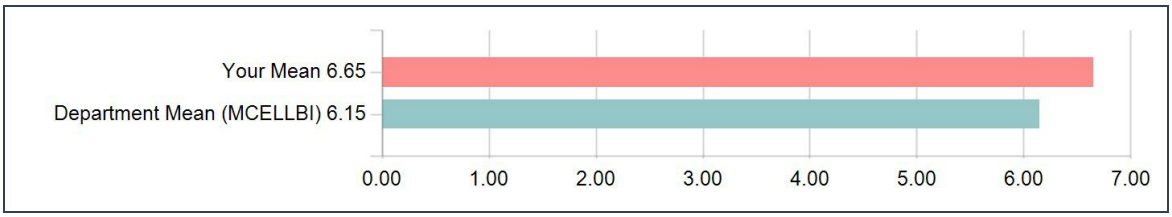

Considering both the limitations and possibilities of the subject matter and the course, how would yourate the overall effectiveness of this course?

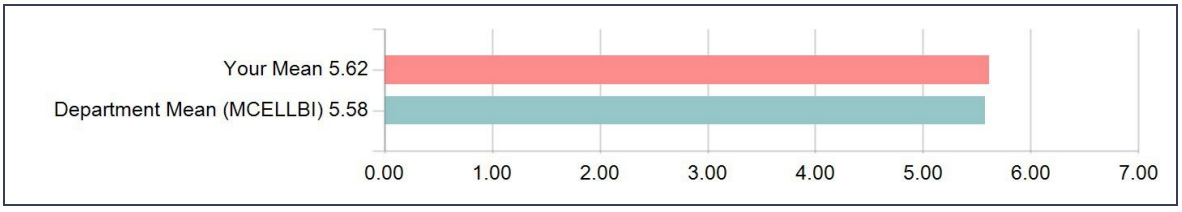

DEPARTMENT PROVIDED INSTRUCTOR QUESTIONS:

Items in this section were selected by MCELLBI for inclusion on this evaluation.

The instructor presented content in an organized manner.

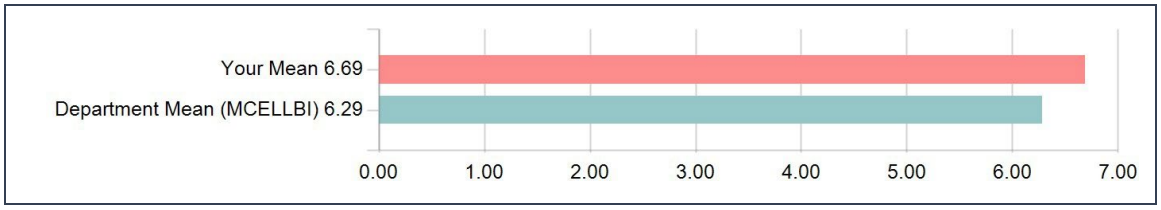

The instructor explained concepts clearly.

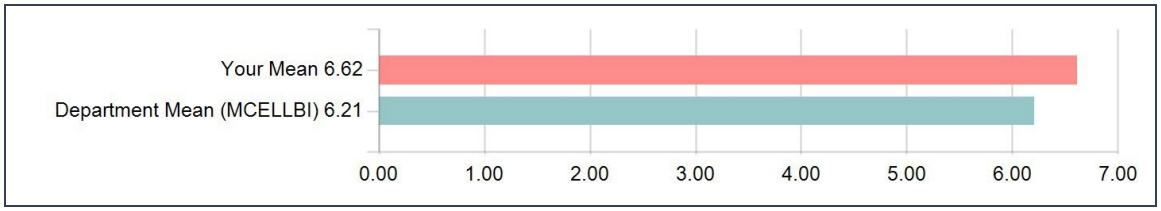

The instructor was helpful when I had difficulties or questions.

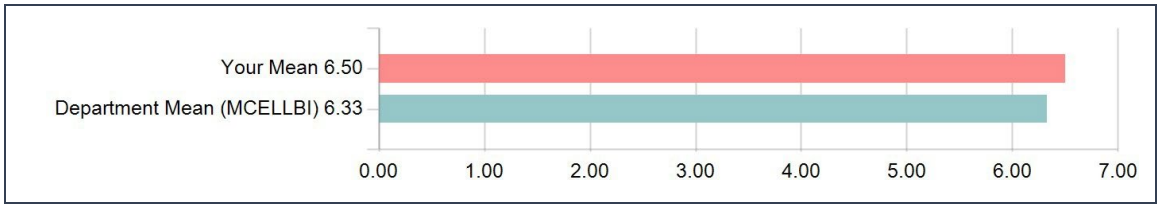

The instructor encouraged student questions and participation.

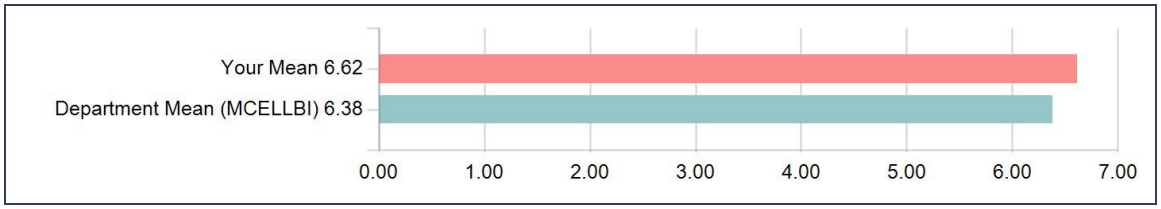

The instructor motivated students to think critically and explore the subject further.

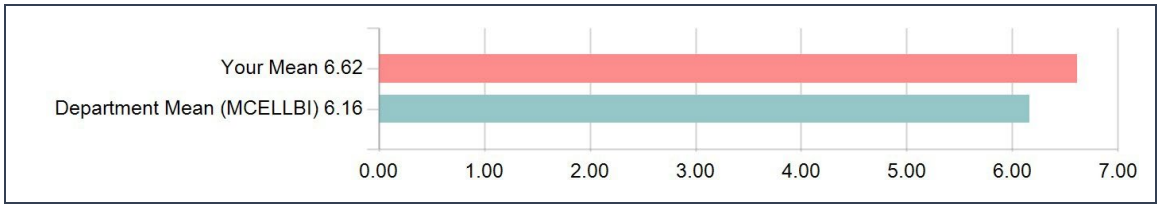

Please use this space to identify what you perceive as the real strengths and weaknesses of theinstructor's teaching.

Comments
I enjoyed starting the lab lectures with some science history and having it follow a theme for promoting underrepresented groups in STEM of the month.
She really made sure all of us were very prepared going into our experiments and spent time answering our questions always. She was always very patient and kind with us.
Tobey was a great GSI, explained concepts clearly and efficiently. The only real weakness is in the structure of the class, which has so many deadlines and assignments in the last few weeks, causing a bit of a delay on getting our grades back.
Tobey did a great job of encouraging students to do their best work always. I would be excited to ask her questions, and she was always kind in giving her answers.
Tobey is really good at answering questions and giving feedback on work, she doesn't leave any student behind and makes sure everyone understands the concepts before moving on.
Strengths: explains concepts well, very kind and compassionate Weakness: NA
Strengths: thoroughly explained concepts, often gave more background information than necessary, organized Weaknesses: lectures were a bit long so the experiments and labs felt very rushed to finish in time
the instructor is great at having organized slides and presenting information
Enthusiastic to teach & makes concepts easy to understand.
Tibet is very good at helping students reach their maximum potential
Tobey was extremely organized, explained concepts clearly, and overall was a very calm and knowledgable instructor in what can be a hectic class! I appreciate everything she brought to the course.
Tobey was very perceptive to student questions and help during our lab period. She was very knowledgeable about the course topics but did not always give us straightforward answers about the content when asked. I often found that we were not getting information about grading or how to improve on our assignments until the first ones were not successful.
Real strengths: very detailed and thorough explanations of the lecture material and lab procedures, very good a lecturing and explaining complex concepts in a way that I was able to understand, PowerPoint slides were very detailed and easy to follow and actually prepared for for lab and the quizzes, very good at engaging students to participate and and encouraging. Real weaknesses: organizing the structure of presenting lecture and doing the actual lab could be improved so that we would not have to stay longer than needed for labs.
Strength: explaining in depth difficult concepts Weakness: sometimes expected too much for assignments
Tobey is really amazing. Not only does she come to class well prepared but she is also very knowledgeable of questions asked in class. She knows the lab methods really well and is really helpful when we ask her for help. She also likes encouraging students
Tobey was always open to us asking as many questions and we needed and made sure we had a deep understanding of all the context presented
Tobey is probably one of the best GSI's I've had at my time at Berkeley. She explains things slowly and allows me to process what she's saying and makes sure I understand the concept before moving on to help the next person. Also if there's something she can't help with, she always makes sure that she can get someone else who can help or is going through something similar so that we can troubleshoot together. Her strength is her compassion as an instructor. Also absolutely love how at the beginning of each lecture she presented a scientist from various identities and backgrounds. I think this is really important. Weaknesses, sometimes things ran a little slow in class but hoenstly sometimes that's how it be.
Very engaging, well structured, organized, and presents material in an easy–to–understand manner. Very helpful and open to answering questions and providing explanations
I really appreciated Tobey's ability to explain material in detail in order to be able to understand the material better. However, a weakness would probably be that Tobey's lectures at the beginning of class are pretty long and take up most of lab class time.
Tobey was one of the best GSIs I've ever had! She was patient and informative, and helped us through whatever concerns we had with lab.
Overall I thought that Tobey was an excellent GSI. For weaknesses, I felt that there was a significant difference in grading between GSIs. It's hard to feel like somehow you just got unlucky with GSI which is a tougher grader when you hear of other classmates receiving full marks for simply turning in an assignment and making a strong effort. The other thing that I felt was not super great was how tough some of the gradings were for early projects. For example, the first lab report should be graded easier as most of us haven't written a lab report in months to years! For strengths, Tobey was also willing to answer questions, explain the experiments, and really made an effort to be there for us as a class.

Suggestions for improvement?

Comments
Time organization was hectic for a few labs, maybe having more microscopes or staggering sections would be beneficial to alleviate 2 lab sections utilizing limited number of microscopes. Microscope practical could have been done over multiple periods of days instead of having people stay over an hour longer than the lab period to just take a microscope practical
I think this class should be worth at least 5 credits, or should be reduced in the number of class meetings.
Tobey’s lectures were very thorough and detailed, but maybe sometimes they were too long
NA I loved Tobey. There's really nothing I can think of
Shorten lectures and make more concise so there is more time to do the experiments without feeling rushed
Lectures can be long
this is NOT a suggestion for Tobey. Overall, the class was structured poorly. The labs are already 2–530pm, and at least 7 times throughout the semester we had to stay over an hour later. It is unreasonable that procedures longer than the allotted time are required, and that there can only be 1/4 of the class using microscopes and computers at one time.
Provide information necessary to do well on the course and assignments prior to completion. We are all smart student and should not be told after the fact that we did something wrong. I would suggest also answering all student questions in a more straightforward manner.
Planning out the lab period so that we can finish the experiments on time and not need to stay longer than needed which happened for many labs.
Maybe we could have more time to ask questions at the end of lab.
No suggestions, she’s really perfect
none
none
Maybe make lab lectures shorter and answer questions at the end instead of the middle of the lab lecture.
None! She was great.
Take it easy on earlier assignments. We're all learning and our first assignments are probably gonna be worse than our later assignments.

Any other comments?

Comments
More time to discuss lab material after — we spend a lot of time preparing for labs beforehand, but not adequately debriefing labs in my opinion
n/a
NA
No
course needs to be structured better. some procedures requiring use of microscope and computer left some groups staying until 630 or 7p, which is really difficult when a lot of us have class or club meetings after, or things to study for, or we didnt have food with us and were extremely hungry.
I feel like the lab exercises and my time in the lab working was not reflective of the grading in the class. Our grade is largely determined by the quiz and lab reports and I feel that there should be more consideration for the amount of effort and time we put in to the actual lab experiments.
Very grateful for having Tobey as my GSI for this course, I felt like she really wanted us to succeed and is a very good teacher. I definitely feel that I was able to perform well on quizzes because of her lecture slides and how she explained everything. She is also very transparent about her expectations and explains things very clearly.
None
This lab indeed increased my thinking abilities. I acquired many skills.
great instructor!!! one of the best

REFERENCES

Allam, A.H., M. Charnley, and S.M. Russell. 2018. Context-Specific Mechanisms of CellPolarity Regulation. J. Mol. Biol. 430:3457–3471. doi:10.1016/j.jmb.2018.06.003.

Assémat, E., E. Bazellières, E. Pallesi-Pocachard, A. Le Bivic, and D. Massey- Harroche. 2008. Polarity complex proteins. Biochim. Biophys. Acta BBA - Biomembr. 1778:614–630. doi:10.1016/j.bbamem.2007.08.029.

Baas, A.F., L. Smit, and H. Clevers. 2004. LKB1 tumor suppressor protein: PARtaker in cell polarity. Trends Cell Biol. 14:312–319. doi:10.1016/j.tcb.2004.04.001.

Bichsel, S. J., Tamaskovic, R., Stegert, M. R., & Hemmings, B. A. (2004). Mechanism of activation of NDR (nuclear Dbf2-related) protein kinase by the hMOB1 protein. *The Journal of Biological Chemistry*, *279*(34), 35228–35235. https://doi.org/10.1074/jbc.M404542200

Bilder, D., M. Li, and N. Perrimon. 2000. Cooperative Regulation of Cell Polarity and Growthby Drosophila Tumor Suppressors. Science. 289:113–116. doi:10.1126/science.289.5476.113.

Bilder, D., and N. Perrimon. 2000. Localization of apical epithelial determinants by the basolateral PDZ protein Scribble. Nature. 403:676–680. doi:10.1038/35001108.

Bonello, T.T., and M. Peifer. 2018. Scribble: A master scaffold in polarity, adhesion, synaptogenesis, and proliferation. J. Cell Biol. jcb.201810103. doi:10.1083/jcb.201810103.

Campanale, J.P., T.Y. Sun, and D.J. Montell. 2017. Development and dynamics of cell polarity at a glance. J. Cell Sci. 130:1201–1207. doi:10.1242/jcs.188599.

Cariati, M., Naderi, A., Brown, J. P., Smalley, M. J., Pinder, S. E., Caldas, C., & Purushotham, A. D. (2008). Alpha-6 integrin is necessary for the tumourigenicity of a stem cell-like subpopulation within the MCF7 breast cancer cell line. International Journal of Cancer, 122(2), 298–304. https://doi.org/10.1002/ijc.23103

Charafe-Jauffret, E., Ginestier, C., & Birnbaum, D. (2009). Breast cancer stem cells: Tools and models to rely on. *BMC Cancer*, *9*(1), 202. https://doi.org/10.1186/1471-2407-9-202

Chen, B., Zheng, B., DeRan, M., Jarugumilli, G. K., Fu, J., Brooks, Y. S., & Wu, X. (2016). ZDHHC7-mediated S-palmitoylation of Scribble regulates cell polarity. *Nature Chemical Biology*, *12*(9), 686–693. https://doi.org/10.1038/nchembio.2119

Cordenonsi, M., F. Zanconato, L. Azzolin, M. Forcato, A. Rosato, C. Frasson, M. Inui, M. Montagner, A.R. Parenti, A. Poletti, M.G. Daidone, S. Dupont, G. Basso, S. Bicciato, and S. Piccolo. 2011. The Hippo Transducer TAZ Confers Cancer Stem Cell-Related Traits on BreastCancer Cells. Cell. 147:759–772. doi:10.1016/j.cell.2011.09.048.

da Silva-Diz, V., Lorenzo-Sanz, L., Bernat-Peguera, A., Lopez-Cerda, M., & Muñoz, P. (2018). Cancer cell plasticity: Impact on tumor progression and therapy response. *Seminars in Cancer Biology*, *53*, 48–58. https://doi.org/10.1016/j.semcancer.2018.08.009

Dontu, G., Al-Hajj, M., Abdallah, W. M., Clarke, M. F., & Wicha, M. S. (2003). Stem cells in normal breast development and breast cancer. *Cell Proliferation*, *36*(Suppl 1), 59–72. https://doi.org/10.1046/j.1365-2184.36.s.1.6.x

Drubin, D.G., and W.J. Nelson. 1996. Origins of Cell Polarity. Cell. 84:335–344. doi:10.1016/S0092-8674(00)81278-7.

Dupont, S., L. Morsut, M. Aragona, E. Enzo, S. Giulitti, M. Cordenonsi, F. Zanconato, J. Le Digabel, M. Forcato, S. Bicciato, N. Elvassore, and S. Piccolo. 2011. Role of YAP/TAZ in mechanotransduction. Nature. 474:179–183. doi:10.1038/nature10137.

Duval, K., H. Grover, L.-H. Han, Y. Mou, A.F. Pegoraro, J. Fredberg, and Z. Chen. 2017. Modeling Physiological Events in 2D vs. 3D Cell Culture. Physiology. 32:266–277. doi:10.1152/physiol.00036.2016.

Ebnet, K., D. Kummer, T. Steinbacher, A. Singh, M. Nakayama, and M. Matis. 2018. Regulation of cell polarity by cell adhesion receptors. Semin. Cell Dev. Biol. 81:2–12. doi:10.1016/j.semcdb.2017.07.032.

Ellenbroek, S.I.J., S. Iden, and J.G. Collard. 2012. Cell polarity proteins and cancer. Semin. Cancer Biol. 22:208–215. doi:10.1016/j.semcancer.2012.02.012.

Elsum, I.A., and P.O. Humbert. 2013. Localization, Not Important in All Tumor- Suppressing Properties: A Lesson Learnt from Scribble. Cells Tissues Organs. 198:1–11. doi:10.1159/000348423.

Free, L. (2016, September 12). 'Those who can, do; those who can't, teach.' *"Great Leaders Inspire Greatness in Others."* https://lizfree.com/2016/09/12/those-who-can-do-those-who-cant-teach/

Genevet, A., and N. Tapon. 2011. The Hippo pathway and apico-basal cell polarity. Biochem. J. 436:213–224. doi:10.1042/BJ20110217.

Gokhale, R.H., and A.W. Shingleton. 2015. Size control: the developmental physiology of body and organ size regulation. WIREs Dev. Biol. 4:335–356. doi:10.1002/wdev.181.

Halder, G., and R.L. Johnson. 2011. Hippo signaling: growth control and beyond.Dev. Camb. Engl. 138:9–22. doi:10.1242/dev.045500.

Harvey, K.F., and I.K. Hariharan. 2012. The Hippo Pathway. Cold Spring Harb. Perspect. Biol. 4:a011288. doi:10.1101/cshperspect.a011288.

Hatch, J. (2018). Better teachers are needed to improve science education. *Nature*, *562*(7725), S2–S4. https://doi.org/10.1038/d41586-018-06830-2

Humbert, P. O., Grzeschik, N. A., Brumby, A. M., Galea, R., Elsum, I., & Richardson, H. E. (2008). Control of tumourigenesis by the Scribble/Dlg/Lgl polarity module. *Oncogene*, *27*(55), 6888–6907. https://doi.org/10.1038/onc.2008.341

Humbert, P., Russell, S., & Richardson, H. (2003). Dlg, Scribble and Lgl in cell polarity, cell proliferation and cancer. *BioEssays*, *25*(6), 542–553. https://doi.org/10.1002/bies.10286

Jahchan, N.S., and K. Luo. 2010. SnoN in mammalian development, function and diseases. Curr. Opin. Pharmacol. 10:670–675. doi:10.1016/j.coph.2010.08.006.

Jahchan, N.S., G. Ouyang, and K. Luo. 2013. Expression Profiles of SnoN in Normal and Cancerous Human Tissues Support Its Tumor Suppressor Role in Human Cancer. PLoS ONE.8:e55794. doi:10.1371/journal.pone.0055794.

Kallay, L.M., A. McNickle, P.J. Brennwald, A.L. Hubbard, and L.T. Braiterman. 2006. Scribble associates with two polarity proteins, lgl2 and vangl2, via distinct molecular domains. J. Cell. Biochem. 99:647–664. doi:10.1002/jcb.20992.

Katoh, M., and M. Katoh. 2004. Identification and characterization of human GUKH2 gene in silico. Int. J. Oncol. 24:1033–1038.

Kim, W., and E.-H. Jho. 2018. The history and regulatory mechanism of the Hippo pathway. BMB Rep. 51:106–118. doi:10.5483/bmbrep.2018.51.3.022.

Krakowski, A. R., Laboureau, J., Mauviel, A., Bissell, M. J., & Luo, K. (2005). Cytoplasmic SnoN in normal tissues and nonmalignant cells antagonizes TGF-beta signaling by sequestration of the Smad proteins. *Proceedings of the National Academy of Sciences of the United States of America*, *102*(35), 12437–12442. https://doi.org/10.1073

Lapetina S, Gil-Henn H. A guide to simple, direct, and quantitative in vitro binding assays. J Biol Methods. 2017;4(1):e62. doi:10.14440/jbm.2017.161

Lee, S. S., Weiss, R. S., & Javier, R. T. (1997). Binding of human virus oncoproteins to hDlg/SAP97, a mammalian homolog of the Drosophila discs large tumor suppressor protein. *Proceedings of the National Academy of Sciences of the United States of America*, *94*(13), 6670–6675.

Lim, K.Y.B., N.J. Gödde, P.O. Humbert, and M. Kvansakul. 2017. Structural basis for the differential interaction of Scribble PDZ domains with the guanine nucleotide exchange factor β-PIX. J. Biol. Chem. 292:20425–20436. doi:10.1074/jbc.M117.799452.

Lv, X.-B., C.-Y. Liu, Z. Wang, Y.-P. Sun, Y. Xiong, Q.-Y. Lei, and K.-L. Guan. 2015. PARD3 induces TAZ activation and cell growth by promoting LATS1 and PP1 interaction. EMBO Rep.16:975–985. doi:10.15252/embr.201439951.

Ma, S., Z. Meng, R. Chen, and K.-L. Guan. 2019. The Hippo Pathway: Biology and Pathophysiology. Annu. Rev. Biochem. 88:577–604. doi:10.1146/annurev- biochem-013118-111829.

Margolis, B. 2005. Apicobasal polarity complexes. J. Cell Sci. 118:5157–5159. doi:10.1242/jcs.02597.

Mathew, D., L.S. Gramates, M. Packard, U. Thomas, D. Bilder, N. Perrimon, M. Gorczyca, and V. Budnik. 2002. Recruitment of scribble to the synaptic scaffolding complex requires GUK-holder, a novel DLG binding protein. Curr. Biol. CB. 12:531–539.

Maugeri-Saccà, M., and R. De Maria. 2018. The Hippo pathway in normal development and cancer. Pharmacol. Ther. 186:60–72. doi:10.1016/j.pharmthera.2017.12.011.

McCaffrey, L.M., and I.G. Macara. 2011. Epithelial organization, cell polarity and tumorigenesis. Trends Cell Biol. 21:727–735. doi:10.1016/j.tcb.2011.06.005.

Meng, Z., T. Moroishi, and K.-L. Guan. 2016. Mechanisms of Hippo pathway regulation. Genes Dev. 30:1–17. doi:10.1101/gad.274027.115.

Misra, J.R., and K.D. Irvine. 2018. The Hippo signaling network and its biological functions. Annu. Rev. Genet. 52:65–87. doi:10.1146/annurev-genet-120417- 031621.

Mohajan, S., P.K. Jaiswal, M. Vatanmakarian, H. Yousefi, S. Sankaralingam, S.K. Alahari, S. Koul, and H.K. Koul. 2021. Hippo pathway: Regulation, deregulation andpotential therapeutic targets in cancer. Cancer Lett. 507:112– 123. doi:10.1016/j.canlet.2021.03.006.

Mohseni, M., J. Sun, A. Lau, S. Curtis, J. Goldsmith, V.L. Fox, C. Wei, M. Frazier, O. Samson, K.-K. Wong, C. Kim, and F.D. Camargo. 2014. A genetic screen identifies an LKB1/PAR1 signaling axis controlling the Hippo/YAP pathway. Nat. Cell Biol. 16:108–117.doi:10.1038/ncb2884.

Moon, S., S. Yeon Park, and H. Woo Park. 2018. Regulation of the Hippo pathway in cancer biology. Cell. Mol. Life Sci. 75:2303–2319. doi:10.1007/s00018-018-2804-1.

Moreno-Bueno, G., F. Portillo, and A. Cano. 2008. Transcriptional regulation of cell polarity in EMT and cancer. Oncogene. 27:6958–6969. doi:10.1038/onc.2008.346.

Nakagawa, S., and J.M. Huibregtse. 2000. Human Scribble (Vartul) Is Targeted for Ubiquitin-Mediated Degradation by the High-Risk Papillomavirus E6 Proteins and the E6AP Ubiquitin-Protein Ligase. Mol. Cell. Biol. 20:8244–8253.

Navarro, C., S. Nola, S. Audebert, M.-J. Santoni, J.-P. Arsanto, C. Ginestier, S. Marchetto, J. Jacquemier, D. Isnardon, A. Le Bivic, D. Birnbaum, and J.-P. Borg. 2005. Junctional recruitment of mammalian Scribble relies on E-cadherin engagement. Oncogene. 24:4330–4339.doi:10.1038/sj.onc.1208632.

Nelson, W.J. 2003. Adaptation of core mechanisms to generate cell polarity. Nature. 422:766–774. doi:10.1038/nature01602.

Nomura, N., S. Sasamoto, S. Ishii, T. Date, M. Matsui, and R. Ishizaki. 1989. Isolation of human cDNA clones of ski and the ski-related gene, sno. Nucleic Acids Res. 17:5489–5500. doi:10.1093/nar/17.14.5489.

Page, D. (2017). Beyond Education Regurgitation. EMS World. https://www.hmpgloballearningnetwork.com/site/emsworld/article/12319348/beyond-education-regurgitation

Patel, S., F.D. Camargo, and D. Yimlamai. 2017. Hippo Signaling in the Liver Regulates Organ Size, Cell Fate, and Carcinogenesis. Gastroenterology. 152:533–545. doi:10.1053/j.gastro.2016.10.047.

Peitzsch, C., Tyutyunnykova, A., Pantel, K., & Dubrovska, A. (2017). Cancer stem cells: The root of tumor recurrence and metastases. *Seminars in Cancer Biology*, *44*, 10–24. https://doi.org/10.1016/j.semcancer.2017.02.011

Piccolo, S., and M. Cordenonsi. 2013. Regulation of YAP and TAZ by Epithelial Plasticity. In The Hippo Signaling Pathway and Cancer. M. Oren and Y. Aylon, editors. Springer, New York,NY. 89–113.

Piccolo, S., S. Dupont, and M. Cordenonsi. 2014. The Biology of YAP/TAZ: Hippo Signalingand Beyond. Physiol. Rev. 94:1287–1312. doi:10.1152/physrev.00005.2014.

Pickett, M.A., V.F. Naturale, and J.L. Feldman. 2019. A Polarizing Issue: Diversity in the Mechanisms Underlying Apico-Basolateral Polarization In Vivo. Annu. Rev. Cell Dev. Biol.35:285–308. doi:10.1146/annurev-cellbio-100818- 125134.

Pires, H.R., and M. Boxem. 2018. Mapping the Polarity Interactome. J. Mol. Biol. 430:3521–3544. doi:10.1016/j.jmb.2017.12.017.

Schroeder, M.C., and G. Halder. 2012. Regulation of the Hippo pathway by cell architecture and mechanical signals. Semin. Cell Dev. Biol. 23:803–811. doi:10.1016/j.semcdb.2012.06.001.

Sharma, M. (2021, September 15). 5 characteristics of an effective science teacher – from a researcher who trains them. *The Conversation*. http://theconversation.com/5-characteristics-of-an-effective-science-teacher-from-a-researcher-who-trains-them-165211

Shingleton AW. The regulation of organ size in Drosophila: physiology, plasticity, patterning and physical force. Organogenesis. 2010 Apr-Jun;6(2):76-87. doi: 10.4161/org.6.2.10375. PMID: 20885854; PMCID: PMC2901811.

Stegert, M. R., Hergovich, A., Tamaskovic, R., Bichsel, S. J., & Hemmings, B. A. (2005). Regulation of NDR Protein Kinase by Hydrophobic Motif Phosphorylation Mediated by the Mammalian Ste20-Like Kinase MST3. *Molecular and Cellular Biology*, *25*(24), 11019–11029. https://doi.org/10.1128/MCB.25.24.11019-11029.2005

Strontium. (2020, September 9). The 'Those who can't do, teach' fallacy. *Medium*. https://medium.com/@strontiumz38/the-those-who-cant-do-teach-fallacy-8116b0e12de5

Stroschein, S. L., Bonni, S., Wrana, J. L., & Luo, K. (2001). Smad3 recruits the anaphase-promoting complex for ubiquitination and degradation of SnoN. Genes & Development, 15(21), 2822–2836. https://doi.org/10.1101/gad.912901

Su, W.-H., D.D. Mruk, E.W.P. Wong, W.-Y. Lui, and C.Y. Cheng. 2012. Polarity protein complex Scribble/Lgl/Dlg and epithelial cell barriers. Adv. Exp. Med. Biol. 763:149–170.

Stephens, R., Lim, K., Portela, M., Kvansakul, M., Humbert, P. O., & Richardson, H. E. (2018). The Scribble Cell Polarity Module in the Regulation of Cell Signaling in Tissue Development and Tumorigenesis. *Journal of Molecular Biology*, *430*(19), 3585–3612. https://doi.org/10.1016/j.jmb.2018.01.011

Swaroop B, S.S., R. Kanumuri, I. Ezhil, J.K. Naidu Sampangi, J. Kremerskothen, S.K. Rayala, and G. Venkatraman. 2021. KIBRA connects Hippo signaling and cancer. Exp. Cell Res. 403:112613. doi:10.1016/j.yexcr.2021.112613.

Visvader, J. E., & Lindeman, G. J. (2008). Cancer stem cells in solid tumours: Accumulating evidence and unresolved questions. *Nature Reviews Cancer*, *8*(10), 755–768. https://doi.org/10.1038/nrc2499

Wen, W., and M. Zhang. 2018. Protein Complex Assemblies in Epithelial Cell Polarity and Asymmetric Cell Division. J. Mol. Biol. 430:3504–3520. doi:10.1016/j.jmb.2017.09.013.

Wingert, P. (2012, August 1). *Building a Better Science Teacher*. Scientific American. https://www.scientificamerican.com/article/building-a-better-science-teacher/

Yang, C.-C., H.K. Graves, I.M. Moya, C. Tao, F. Hamaratoglu, A.B. Gladden, and G. Halder. 2015. Differential regulation of the Hippo pathway by adherens junctions and apical-basal cell polarity modules. Proc. Natl. Acad. Sci. U. S. A. 112:1785–1790. doi:10.1073/pnas.1420850112.

Yang, X., Wang, H., & Jiao, B. 2016. Mammary gland stem cells and their application in breast cancer. Oncotarget, 8:10675–10691. doi:10.18632/oncotarget.12893

Yoshihama, Y., K. Chida, and S. Ohno. 2012. The KIBRA-aPKC connection. Commun. Integr. Biol. 5:146–151. doi:10.4161/cib.18849.

Yu, F.-X., and K.-L. Guan. 2013. The Hippo pathway: regulators and regulations. Genes Dev. 27:355–371. doi:10.1101/gad.210773.112.

Yu, F.-X., B. Zhao, and K.-L. Guan. 2015. Hippo Pathway in Organ Size Control, Tissue Homeostasis, and Cancer. Cell. 163:811–828. doi:10.1016/j.cell.2015.10.044.

Zanconato, F., M. Cordenonsi, and S. Piccolo. 2016. YAP/TAZ at the Roots of Cancer. Cancer Cell. 29:783–803. doi:10.1016/j.ccell.2016.05.005.

Zeitler, J., C.P. Hsu, H. Dionne, and D. Bilder. 2004. Domains controlling cell polarity and proliferation in the Drosophila tumor suppressor Scribble. J. Cell Biol. 167:1137–1146. doi:10.1083/jcb.200407158.

Zhang, X., Powell, K., & Li, L. (2020). Breast Cancer Stem Cells: Biomarkers, Identification and Isolation Methods, Regulating Mechanisms, Cellular Origin, and Beyond. *Cancers*, *12*(12), 3765. https://doi.org/10.3390/cancers12123765

Zhang, Y., H. Guo, H. Kwan, J.-W. Wang, J. Kosek, and B. Lu. 2007. PAR-1 Kinase Phosphorylates Dlg and Regulates Its Postsynaptic Targeting at the Drosophila NeuromuscularJunction. Neuron. 53:201–215. doi:10.1016/j.neuron.2006.12.016.

Zhu, J., Y. Shang, Q. Wan, Y. Xia, J. Chen, Q. Du, and M. Zhang. 2014. Phosphorylation-dependent interaction between tumor suppressors Dlg and Lgl. Cell Res. 24:451–463. doi:10.1038/cr.2014.16.

Zhu, Q., A.R. Krakowski, E.E. Dunham, L. Wang, A. Bandyopadhyay, R. Berdeaux, G.S. Martin, L. Sun, and K. Luo. 2007. Dual Role of SnoN in Mammalian Tumorigenesis. Mol. Cell. Biol.27:324–339. doi:10.1128/MCB.01394-06.

Zhu, Q., E. Le Scolan, N. Jahchan, X. Ji, A. Xu, and K. Luo. 2016. SnoN Antagonizes the Hippo Kinase Complex to Promote TAZ Signaling during Breast Carcinogenesis. Dev. Cell. 37:399– 412. doi:10.1016/j.devcel.2016.05.002.

Zinatizadeh, M.R., S.R. Miri, P.K. Zarandi, G.M. Chalbatani, C. Rapôso, H.R. Mirzaei, M.E. Akbari, and H. Mahmoodzadeh. 2019. The Hippo Tumor Suppressor Pathway (YAP/TAZ/TEAD/MST/LATS) and EGFR-RAS-RAF-MEK in cancer metastasis. Genes Dis.8:48–60. doi:10.1016/j.gendis.2019.11.003.